DEVELOPMENT OF A FINITE ELEMENT MODEL FOR A PRESSURIZED-WATER-REACTOR CORE
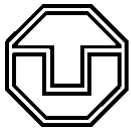
Master Thesis

Sarah Nalewajski

Dresden, 23 July 2018

Master thesis

Topic:	Development of a Finite Elements Model for a Pressurized Water Reactor Core
Author:	Sarah Nalewajski
Matriculation number:	4752588
Processing time:	01.03.2018 bis 23.07.2018
Place, date of delivery:	Dresden, 23.07.2018
Number:	WKET-2017-22
Supervisors:	Dr.-Ing. Carsten Lange
	Dipl.-Phys. Marco Viebach
Resp. University teacher:	Prof. Dr.-Ing. habil. Wolfgang Lippmann

Text pages: 73
Appendix pages: 19
Appendices: 4

WKET

Aufgabenstellung Masterarbeit WKET-2017-22

Name der Studierenden   **Sarah Nalewajski**

Studium   ERASMUS-Studentin der Universitat Politècnica de València

Entwicklung eines Finite-Elemente-Modells für einen Druckwasserreaktor-Kern

Development of a Finite Elements Model for a Pressurized-Water-Reactor Core

In German KWU pressurized water reactors, the neutron flux is measured with in-core and the ex-core detectors. Investigating the signal fluctuations of these detectors at fixed burnup, periods of growing and periods of decreasing fluctuation amplitudes can be found, a phenomenon that is not entirely explained.

In order to understand this neutron flux behavior, several institutions investigate it using different approaches. One idea is that dynamical fuel assembly bow driven by fluid forces acts as a main source of the measured neutron flux fluctuations. The master thesis should contribute to the understanding of the dynamical behavior of the fuel assembly collective.

For this purpose, a simplified model of the reactor core, i. e. fuel assemblies and core barrel, is to be implemented in ANSYS using the Mechanical APDL. The model will be investigated via time-dependent analyses. Time-dependent forces are intended as the input and the time-dependent displacements of appropriate points evaluated will be the output.

Various time-dependencies of the forces will be studied. Correlation function and auto spectral power density can be used to quantify the qualitative results found by inspection of the time-dependent elongations. The results should be compared to the neutron flux fluctuation data available in literature.

The following main points have to be covered:

- Development of an ANSYS model for the time-dependent analysis of the core barrel and the fuel assemblies
    - design of fuel assemblies by beams approximating a given detailed structure,
    - core barrel as a short pipe,
    - core barrel's bending amplitude limited by core stops,
    - fuel assemblies' bending amplitudes limited by distance to respective adjacent fuel assemblies,
- investigation of the influence of forces applied to the structure (sinusoidal and given time-series):

Mitglied von:
DRESDEN
concept

- o at appropriate positions, evaluation of elongations of appropriate components
- o description of the behavior, correlation of the elongations, comparison of the elongations with neutron flux fluctuation data

Betreuer an der TU Dresden:	Dr.-Ing. Carsten Lange
	Dipl.-Phys. Marco Viebach

Ausgehändigt am:	01.04.2018
Einzureichen am:	31.07.2018

Prof. Dr.-Ing. habil. Wolfgang Lippmann
betreuender Hochschullehrer

ABSTRACT

The aim of this project is the creation of a geometrically simplified ANSYS model of the nuclear reactor core. This model is created in order to perform an analysis to contribute to the understanding of the behaviour of the fuel assemblies due to the movement of the mechanical structure of the reactor core caused by the propagation of the coolant. The idea of this analysis arises from the increase in the phenomenon of the neutron flux fluctuations observed in some pressurized water reactors. It is therefore the results obtained in this project are compared with the neutron flux fluctuations data in order to help understanding the neutron flux behaviour mentioned above. These fluctuations present unexplained correlations which may be due to the mechanical behaviour of the fuel assemblies. The results obtained from the analyses show certain similarities with the neutron flux fluctuation data, although this does not occur in all the cases due to the simplifications taken in the mode.

KURZFASSUNG

Das Ziel dieses Projekt ist die Anfertigung eines vereinfachten ANSYS Modells eines Druckwasser-Reaktorkerns. Dieses Modell wurde kreiert, um eine Analyse zu liefern, die dazu dienen soll, das Verhalten von Brennelementen durch die Bewegung der mechanischen Struktur des Reaktorkerns durch die Propagation der Kühlflüssigkeit verständlich zu machen. Die Idee dieser Analyse ist durch das vermehrte Aufkommen von Neutronenfluss-Schwankungen, die in einigen Druckwasserreaktoren beobachtet wurden, entstanden. Daher werden die Resultate dieses Projekts mit den Daten der Neutronenfluss-Schwankungen verglichen, um das oben genannte Phänomen zu verstehen. Diese Fluktuationen zeigen ungeklärte Korrelationen, die eventuell durch das mechanische Verhalten der Brennelemente zu begründen sind. Die Ergebnisse aus den Analysen möglichen weise aufgrund der Vereinfachungen in dem Modell nicht in allen Fällen auftritt.

TABLE OF CONTENTS

1   INTRODUCTION

The present project titled: "Development of a finite element model for a pressurized-water-reactor core", is the Master's Thesis of the student Sarah Nalewajski and represents the last step for the conclusion of the studies of Master's Degree in Industrial and Environmental Safety, specialty in Nuclear Safety, completed at Fakultät Maschinenwesen of the Technische Universität Dresden.

In the recent years, several studies have been conducted on the increase in neutron flux fluctuations observed in some German KWU pressurized water reactors. This type of reactors is located in different countries and among those which have witnessed this problem are Germany, Switzerland and Spain. [1]

The neutron flux has been measured with both in-core and ex-core detectors, and thanks to the data obtained from these detectors, results that show periods of increasing and periods of decreasing fluctuation amplitudes have been obtained. [2] Because of the fact that this phenomenon does not have a clear explanation to the present, studies with different approaches have been performed.

One possible reason for the phenomenon of the neutron flux fluctuations is the movement of the mechanical structure caused by the propagation of the coolant, that is, the movement of the dynamical fuel assembly bow driven by fluid forces.

In order to contribute in the investigation of the phenomenon of the neutron flux fluctuation, a study of the dynamic behavior of the fuel assembly collective has been made.

For this purpose, a simplified model of all the relevant components of the reactor pressure vessel has been generated. This model has been analyzed using a finite element software, ANSYS APDL. [3] The influence of the forces acting on the structure, mainly random white noise time dependent forces on the core barrel, has been investigated on the simplified model. As a result, different displacements of the mechanical structure of the model at the appropriate points are obtained.

Finally, data obtained from this analysis, that is, elongations, have been compared with the neutron flux fluctuation data.

2 GENERALITIES

2.1 Pressurized water reactor

The Pressurized Water Reactors (PWR) are by far the most common type of reactors in nuclear power plants in use today, there are more than 230 reactors in use for power generation. [4] This type of reactors obtains the energy released by the fission of a nucleus of Uranium and uses this energy to heat water that is used to produce steam that at the end will propel a generator that will provide electrical energy. The name expresses that in this type of reactors the water is kept under such high pressure that it does not boil even at the highest temperature in the circuit. Since the maximum operating temperature is about 320ºC, this means an operating pressure of approximately 155 to 160 bar for the entire primary system. The most common types of these reactors: Westinghouse, Kraftwerk Union (KWU), Babcock & Wilcox and VVER. [5]

Among the different types of pressurized power reactors mentioned above, this project focuses on the PWR-KWU design. This type of reactors was designed in the 1980s and 1990s. There are two different types of these reactors. The difference between both is the characteristic of the primary coolant cycle. On the one hand, there are KWU reactors which operates at 1300-1400 MWe with a total of 193 fuel assemblies and a four-loop primary coolant cycle. [6] On the other hand, some plants feature a three-loop primary coolant cycle, operating at 1000 MWe and with a total of 177 fuel assemblies. An example of the second type is Trillo nuclear power plant which is located in Spain. [7]

In the following image (**Figure 2-1**: Reactor of Trillo nuclear power plant [8]) it is possible to see the appearance of the KWU reactor core of the Trillo nuclear power plant. The elements of the reactor that can be seen are the following:

1. Reactor pressure vessel
2. Core barrel
3. Fuel assembly
4. Control rod
5. Upper support plate

6. Lower support plate
7. Flow homogenizer
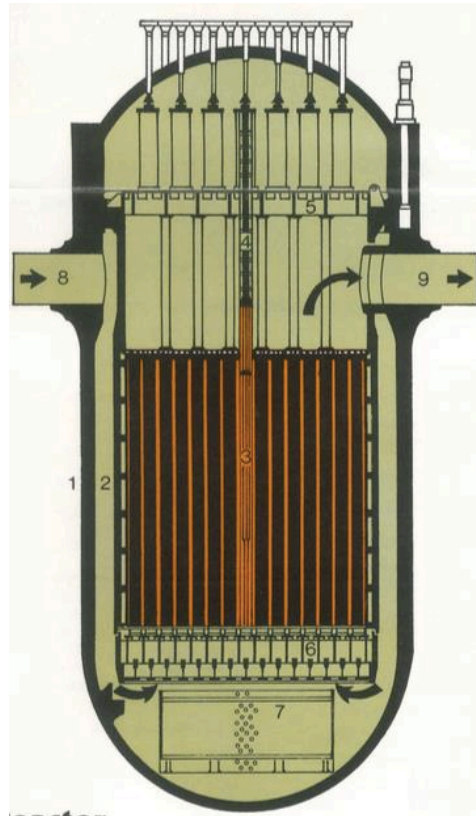8. Coolant inlet nozzle
9. Coolant outlet nozzle

Figure 2-1: Reactor of Trillo nuclear power plant [8]

This work focuses on the nuclear reactor core, more specifically in the reactor pressure vessel that contains the core barrel, the fuel assemblies, the shroud and the core stops among many other elements. This is the part of the reactor that may be contributing to the increasing fluctuations amplitudes while measuring the neutron flux. There are some assumptions that associate this fact to the dynamical fuel assembly bow driven by fluid forces. The forces cause certain vibrations that produce the bending of the core barrel and in turn the displacement of the fuel assemblies. Next, each element of the reactor core considered in this work is explained.

In this case, it will focus on the first element, the core support structure. One of the elements that belongs to this part is the core barrel because it houses a reactor core. The barrel is a long, cylindrical,

one-piece welded structure. Like the most components of the internals, the core barrel is made of low carbon, chromium-nickel stainless steel because it is situated in a corrosive environment and the material should not get oxidized. The core barrel is supported on a ledge machined into the pressure vessel flange and is centered at its upper flange with alignment pins. The barrel transmits the weight of the core to the reactor vessel and inside both elements there are located the fuel assemblies. In addition, this element forces the water to flow downward in the space between the reactor vessel wall and the core barrel, this space is called downcomer. [9]

Respecting the fuel assemblies, these are responsible for storing the reactor fuel, more specifically the uranium dioxide that is pressed into pellets. These pellets are loaded and encapsulated within a fuel rod which is made of zirconium alloys due to its very low absorption cross-section. [10]

The individual fuel rods are placed forming a square matrix, for example 16x16 making a total of 256 rods of almost 4m in length for large pressurized water reactors or 15x15 or 14x14 for smaller reactors. The distance between the centers of adjacent fuel rods when loaded into the assembly is called the pitch. The rod separation is kept as small as possible in order to minimize the size of the assembly, and hence of the core and the reactor pressure vessel.

A PWR fuel assembly comprises a bottom nozzle into which rods are fixed through the lattice and to finish the whole assembly it is ended by a top nozzle. There are spacing grids between the nozzles, which are responsible to ensure an exact guiding of the fuel rods. The bottom and top nozzles are heavily constructed as they provide much of the mechanical support of the fuel assembly structure. [10]

The elements that form part of a fuel assembly are the following:

- Fuel rods: contain the fuel
- Top and bottom nozzle: provides the mechanical support for the fuel assembly structure
- Spacing grid: ensures an exact guiding of the fuel rods
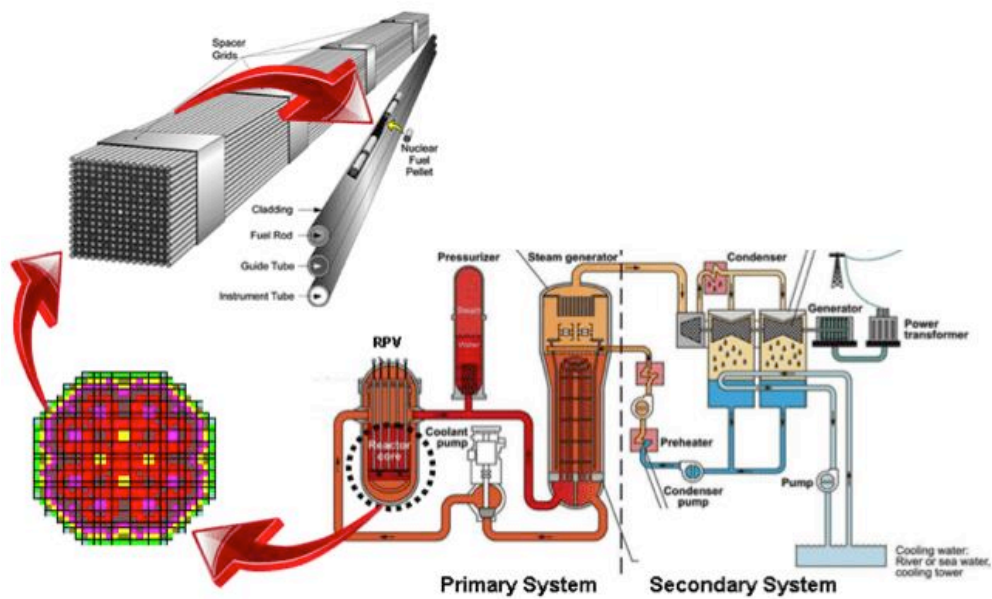- Guide thimble tube: for controlling rods or in-core instrumentation. [10]

Figure 2-2: Scheme of the location of the fuel assemblies [10]

The shape of the head and foot part of the fuel assemblies requires a series of special characteristics to consider depending of the reactor. The part of the head consists of a square frame in which the absorber guide tubes are welded. The tops of the fuel rods are set into indentations in an upper end plate.

At the bottom, the foot part of the fuel assembly is designed to fit firmly into a lower plate made of steel fit and at the same time releases a sufficient cross section for the coolant. Through the plate there are two sets of holes, each with a distinct function: the first set of small holes receives the lower ends of the fuel rods. A second set of holes serves as entries for cooling water into the core region.

The upper and lower end plates are connected by long rods bolted on both ends in order to firmly fix the fuel rods. Bolting together the upper and lower end plates suffices only to hold the ends of the fuel rods.

An additional design element is needed to prevent vibration of and possible damage to the rods during transportation to the reactor site or by the flow of high-velocity cooling water during reactor operation. To stabilize the fuel rod bundle, spacer grids are placed at regular intervals along the

assembly. The vertical spacing of the grids along the fuel bundle is chosen to minimize vibration of the rods produced by the flowing coolant. [5] [11]

The core shroud is a stainless-steel cylinder surrounding a nuclear reactor core whose main function is to direct the cooling water flow. Cold water is pumped into the reactor pressure vessel from an outside water source. The cold water flows down in between the wall of the reactor pressure vessel and the outside wall of the core shroud where it meets the fuel assemblies.

The core shroud is open at the bottom and the top and is composed of multiple cylindrical thermal shields stacked on top of each other. Core shroud walls are relatively thin because the shroud is not under pressure, it only separates the flow directions of reactor cooling water and water at different temperatures. [12] [13]

The core barrel is only fixed in its upper part, in the lower part it is free of any support. To avoid that, in case of an accident that involves lateral deflection of the core barrel, these deflections would be higher there are six supports attached to the lower part of the reactor pressure vessel. These supports are called core stops and they also support the entire weight of the reactor core in case of an accident that involves the fall of the core barrel. [5] [14]

2.2   Neutron flux fluctuations

2.2.1   General definition of noise

In general terms, noise is defined as all anomalous signals or disturbances in a transmission system that cause that the information does not arrive clearly or it is distorted. In other words, it is all the unwanted signal that is mixed with the useful signal that has to be transmitted. [15] [16]

It is the result of various types of disturbances that tend to mask the information when it occurs in the frequency band of the signal spectrum, that is, within its bandwidth.

In the following image (**Figure 2-3**: Representation of sinusoidal signal with and without **noise [17]**), it can be seen a representation of a sinusoidal signal. The black colour represents the signal without noise and the red colour represents the same signal but with some noise.
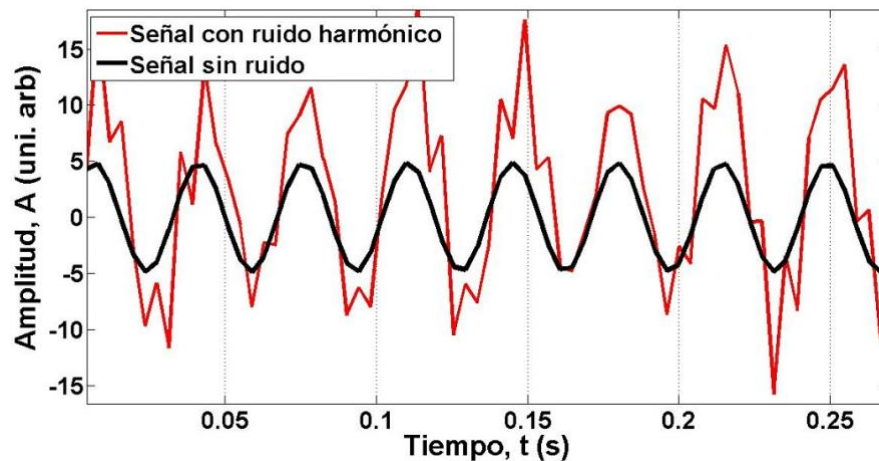
Figure 2-3: Representation of sinusoidal signal with and without noise [17]

2.2.2   Noise inside a reactor

A reactor can show noise in a variety of ways and one of them is the neutron noise. This term can be descriptively defined as neutron flux oscillations from a process of operation or stationary operation regarding to the signal value. [18]

Reactor noise and neutron fluctuations are general terms used to describe the modelling and sampling of higher moments of the neutron population in multiplying systems due to internal and external factors. [19]

The neutron flux noise in the PWR plants is caused by the interactions between the moderator, the fuel, the absorbents and the neutron flux which in turn may be due, among others, to the temperature and fluctuations in the primary coolant. That is the reason of why the origin of the reactor noise can be divided into two different factors of stochasticity:

- Internal noise: due to the stochastic nature of the neutron life cycle and the fission chains.
- External noise: corresponding to the reactivity fluctuations caused by factors such as temperature changes, mechanical vibrations, fluid instabilities, etc. [19] [20]

The neutron flux signals continuously measured by the instrumentation of a PWR inside the core (in-core) and outside the core (ex-core) are processed in the reactor power system, in the reactor power limitation system, and in the lower power range, also in the reactor power control system. [21]

One example of the origin of the neutron fluctuations is the coolant density fluctuations, which influence the change in the moderating properties of the coolant and increase as a result of temperature fluctuations, flow rate, and pressure of the coolant in the reactor. When steam starts to form, the nonlinearity of the dependence of the coolant density on the amplitude of the fluctuations of the coolant parameters at the entrance into a fuel assembly becomes stronger. As a result, the amplitude of the coolant density fluctuations increases, which increases the amplitude of the neutron flux noise in the region of boiling. [20]

2.3 Finite elements analysis

2.3.1 Definition

The finite element method (FEM) can be briefly and concisely defined as a discretization procedure of continuous problems to obtain an approximate solution of them. More widely can be defined as a numerical method for the solution of engineering problems commonly used to solve problems involving a high degree of complexity in applied mathematics as well as physics-mathematics due to the problems that occur in these areas like complex geometries, complex loads and determination of material properties, so it is usually not possible to obtain an analytical solution directly from mathematical expressions. [22] The analytical solution of these problems generally require the solution to boundary value problems for partial differential equations. [23]

Among the areas of physical-mathematics and engineering, in which the finite element method is applied stand out: structure analysis, heat transfer problems, fluid flow, mass transport as well as the calculation of electromagnetic potential.

It is understood as analytical solution those mathematical expressions that throw values for some determined incognito, which is valid throughout the studied body and therefore, it is also valid in any section of the body in an infinite number of locations within the body. These analytical solutions generally require the solution of differential equations which are not possible to solve.

However, the proposed formulation through the use of the finite element method allows the problem to be posed as a series of simultaneous algebraic equations, instead of requiring the resolution of complex differential equations. Since the problem has to be discretized, this numerical method

generates approximate values of the unknowns in a finite number of locations within the body, which depend directly on the number of elements used to calculate the discretization of the piece.

Discretization is the process of modeling a body that consists of the equivalent division of the same in a system conformed by smaller bodies (finite elements) interconnected by common points or nodes, which form surfaces and behave as volumes of independent control that are affected by the border conditions that affect the studied body as a whole. During the application of the finite element method, instead of trying to solve the problem as a whole in a single operation, the body is divided into a finite number of elements, which solve and obtain the result of the whole problem conformed by the results of the finite elements method. [22]

The following section explains in more detail the equations to be used.

2.3.2   Theoretical fundaments

Although it is not necessary to know the mathematical basis of the calculation by finite elements to be able to solve problems though software, it is a complement that should not be ignored. Its compression will help to use the software more intelligently and with greater confidence, making better use of its capabilities while being aware of its limitations

In the field of Solid Mechanics, the objective is to provide a relationship between the forces that are applied to the objects and the displacements caused by them. This is done as follows:

1. The continuous solid is divided into a finite number of elements. Depending on the element, degrees of freedom and form functions are defined, which are valid to approximate the solution.

2. These elements are interconnected by nodes located at their limits and, occasionally, in their interior. The displacements of these nodes will be the unknown parameters that must be found. To find then, in a simplified way, it will be necessary to apply the three fundamental relationships that must be fulfilled in each point:

- Equilibrium equation: $\sigma_{i,j} + X_i = 0$
- Compatibility equations: $\varepsilon_{i,j} = \frac{1}{2} \cdot (u_{ij} + u_{ji})$

- Law of elastic behavior: $\sigma_{i,j} = \lambda \cdot \vartheta \cdot \delta_{ij} + 2 \cdot G \cdot \varepsilon_{ij}$

The resolution of the elastic problem must comply with the previous equations and the boundary conditions to which it is subjected.

In addition, it is important to note that the displacement of each element is a function of the displacements of each of its nodes, and that with the initial deformations and the properties of the materials will be possible to define the tensional state along each element.

Finally, the definition of boundary conditions will also be necessary, in which the displacement of certain nodes in certain directions will be imposed. The boundary conditions must be enough for the system to be compatible and able to reach equilibrium after a certain time, in case it is not a transient analysis.

3.Then the system of equations to find the displacements and reactions is solved:

$$\{F\} = [K] \cdot \{u\}$$

Where F is the vector of forces, u represents the field of displacements in the whole domain and K is the stiffness matrix.

4.Finally the field of deformations ε and of tensions σ is found through the relations above. [24]

2.4 ANSYS APDL

ANSYS, abbreviated form of ANalysis SYStem [25], is a Finite Elements program, which serves for the solution of linear and nonlinear problems of structural mechanics, fluid mechanics, acoustics, thermodynamics and others. There are two different versions, the ANSYS APDL and the ANSYS Workbench. The only difference between both of them is the so-called workflow or work's form. Both have the same solver so the solutions will be the same for the similar problems but it changes the way of defining the problems, the interaction between different disciplines, etc.

In this case it will focus on the first version mentioned above, more specifically the version 15.0 of Ansys APDL. APDL is an acronym for ANSYS Parametric Design Language, which is a powerful feature of ANSYS that can be used to type a model in terms of parameters and allows the automation of common tasks. It is a program designed to be used by commands. Each command is an instruction that is given to the program and there are divided in three types: command that provide input data (e.g.materials), commands that define specifications (e.g. solver type) and commands that lead to perform certain actions (e.g. solve, make a graph, etc.). It also has a GUI (Graphical User Interface) from which commands can be executed through menus, however some of them are not available in that GUI. Due to this parameterization of the model, the user can easily obtain precise information about the influence that the different parameters involved may have in the final solution. Furthermore, any parameter value can be simply modified by only changing the parameter definition once the user has completer control over the model.

This version is chosen because it has a large number of advantages that are needed when designing the model, for example, repetition of commands, do-loops and macros (a file composed of ANSYS commands that can be executed from the model as a normal command). In this project a free text editor, NotePad++, is chosen. [26] The advantages of this text editor it is that it has the option to save the text files in .mac that is the extension for the macros in Ansys. In addition, during the writing it highlights the typical APDL commands.

In general, the evaluation of a finite element solution can be divided into the following three phases, which represents the general pattern that can be used for the creation of any finite element analysis. (see **Figure 2-4**: Workflow in ANSYS)

- The preprocessor serves to produce the necessary data of a problem that after will serve as an input to the next solution menu. It contains all the geometric specifications, the properties of the element materials and also the finite element model generation. The necessary data are:
    - Material properties definition
    - Element type and real constants if are needed
    - Model geometry specification
    - Mesh generation
    - Model constraints specification

- Solution: in this module it is possible to define the type of analysis (static, transient, etc.) and you can also define the loads and the boundary conditions and finally run the solver to solve the load case of the model. The solution phase is completely automatic. Bases on the nodal values and their derivatives, the finite elements analysis generates arrays of elements and saves the results in files.

- Post processing: is used to show the results of the calculation graphically. Its function is to review the results of the model and it is divided into two: General Postprocessor and Timehistory Postprocessor. The first one can, among others, visualize the deformed geometry, tensions, deformations, field flows, safety factors, etc. This is shown on the piece to be studied with a color scale or you can also access to the lists of numerical data. The TimeHistory Postprocessor allows to obtain and graph the evolution of the results according to the time, frequency, etc. In addition, it allows to make accounts with these results and save them in the form of variables that can be used.

Preprocessor
- Geometry
- Constraints
- Materials
- Mesh

Solution
- Analysis type
- Boundary conditions
- Loads

Postprocessor
- Graph solution
- Numerical solution
- Mathematical operations
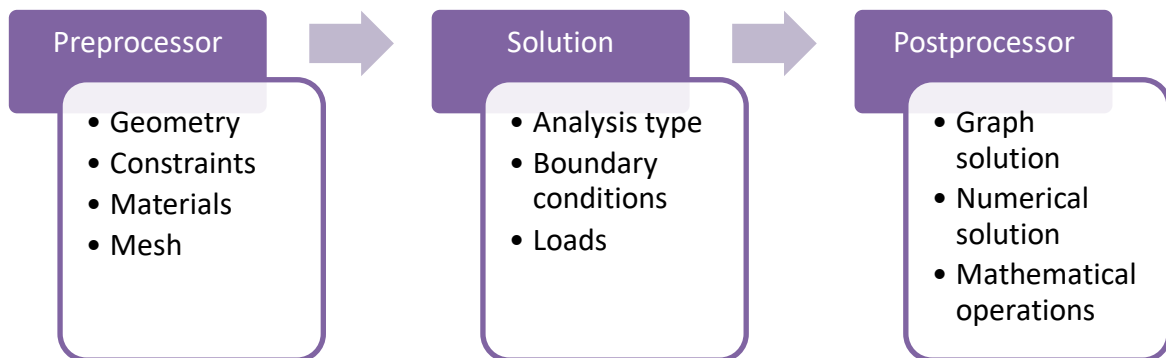
Figure 2-4: Workflow in ANSYS

3 DESCRIPTION OF THE MODEL

As already specified in the previous sections, the fact that certain vibrations can occur in some components of the reactor pressure vessel, is due to the fact that the KWU type of reactors are designed in such a way that a play exists in the lower part of the vessel. This can happen when the coolant flows through the downcomer and, as a result, produce a force on the surface of the core barrel. As a consequence, the most affected parts of the reactor are, among others, the core barrel and the fuel assemblies. One of the possible origins of neutron flux fluctuations is the horizontal movement of the fuel assemblies when approaching or moving away from each other allowing higher or lesser passage of the coolant flow and also possible movements of the core barrel.

The development of the ANSYS model of the selected components of the reactor pressurized vessel is explained in this section. In this design a set of simplifications will be carried out in order to make the model in a simpler way as long as it has enough details to bring it closer to the reality.

In the first place, the set of the fuel assemblies is modeled using the beam element considering all the details from a given detailed model. Secondly, the core barrel is designed as a short pipe. To simulate the shroud the same type of element is used as in the case of the fuel assemblies. The core stops are created with a different beam element that is appropriate for short elements in order to limit the bending amplitude of the core barrel.

Another aspect that is considered in this model is the location of the fuel assemblies, with their respective beams corresponding to the shroud, in the lower grid plate inside the core barrel. This is simulated by the creation of the rigid region between these 3 elements as it is explained in the Rigid region section of this document.

It is also necessary to fix the degrees of freedom of the upper parts of all the elements in order to simulate the fact that they are fixed within a lower grid plate.

As the fuel assemblies are not totally rigid and have a significant length, there is a possibility that when a force is applied, a deformation occurs at some point of the fuel assembly and if the elongation is sufficient a contact between two elements can occur. This can also happen between the shroud beams

and the fuel assemblies from the external part of the whole distribution. In addition, in case the acting force is relatively high, there is a possibility that a contact between core stops and the core barrel will occur. This is considered using the contact elements as explained in the Contact section.

The force applied in each of the analyzes performed, are explained in the section corresponding to each analysis.

4 PROCEDURE TO MODEL IN ANSYS APDL

4.1 Preprocessor

Everything related to the definition of the model is included in the Pre-processor as it is indicated in the ANSYS APDL section. The following subsections describe all the parameters necessary for the study of the simplified reactor core.

4.1.1 Units

The first step is to determinate in which units the model will be created. The program internally only makes calculations without considering in which units have the different parameters have been introduced. That is the reason of why is necessary to use a consistent system of units. The most recommended is the International System since it is well known and with easy access to information about it. The units of the most important parameters that are going to be used can be seen in the table shown below (**Table 4-1**: Measurement units).

Table 4-1: Measurement units

Parameter	Units	Description
L	m	lenght
t	s	time
F	N	force
E	Pa	Young's modulus
ρ	kg/m^3	density

4.1.2 Elements

BEAM189 element is used for modeling of 3D structures. It is a quadratic beam element, 3 node, with six degrees of freedom at each node (translations in x,y and z directions, and rotations about the x,y and z directions. Beam 189 is especially appropriate for modeling slender to moderately thick beams. [3]

This element is used for the 193 fuel assemblies that are part of the model as well as for the simulation of the shroud.
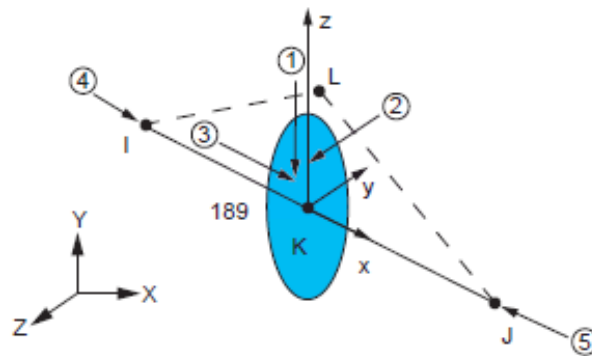
Figure 4-1: Geometry of BEAM189 element [3]

PIPE289 is a 3D quadratic pipe elements connecting three nodes with six degrees of freedom at each node that can be either translations along the three axes and rotations around the x,y and z direction. In the same way that BEAM189, is appropriate for analyzing slender to moderately stubby/thick pipe structures. [3]

The pipe is used to create the core barrel that contains all the fuel elements.
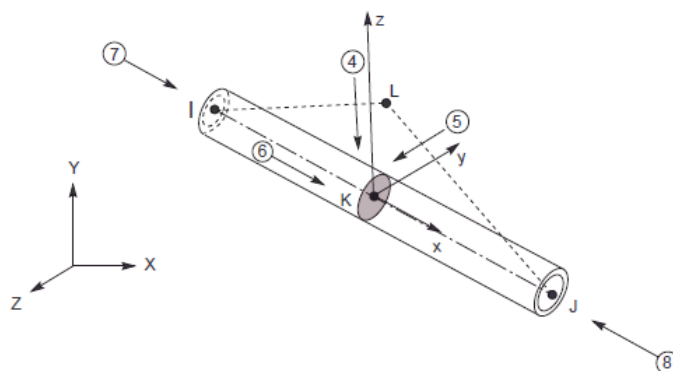
Figure 4-2: Geometry of PIPE289 element [3]

BEAM188 is a 3D linear, quadratic or cubic beam element connecting two nodes with six degrees of freedom each one that can be either translations along the three axes and rotations around the x, y and z directions. It is especially appropriate for modeling slim to moderately thick beams. This element supports nonlinear material models, as well as, elasticity, plasticity and creep. Besides that, the cross-sections are not distorted and remain on plane after deformation. [3]

In this model, BEAM188 is used to model the core-stop beam.

CONTA176 represents contact and sliding between 3-D line segments and a deformable line segment, defined by this element. It consists of two or three nodes with three degrees of freedom at each node, which are the displacements along the three axes UX, UY and UZ respectively. CONTA176 is applicable to beam-beam structural contact analyses and is located on the surfaces of the elements. The contact occurs when the element surface penetrates one of the 3-D straight line on a specified target surface. [3]

TARGE170 is used to represent the target parts with the contact elements (CONTA176 in case of this project). The contact elements are superimposed on the solid elements, the plate or lune that describes the limits of a deformable body and the potential contact with the target surface. In this case line-to-line contact is used. [3]

The two elements specified above are used to generate the possible contact between the fuel assemblies and the shroud.
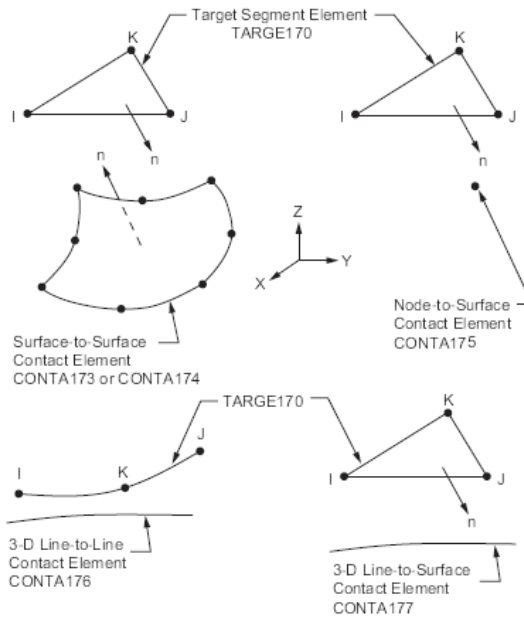
Figure 4-3: Possible geometries of TARGE170 element [3]

CONTA178 represents contact and sliding between two nodes of two different elements, no matter which type of elements they are. It consists of two nodes with three degrees of freedom at each node, which are the displacements along the three axes UX, UY and UZ respectively. CONTA178 can be used not only in 3D models, but also in 2D ones by constraining the UZ degree of freedom. The element can support both compression in the contact normal direction and Coulomb friction in the tangential one. Initially either a gap or a normal preload can be specified. [3]

This element is used to generate the contact between the core stops and the core barrel
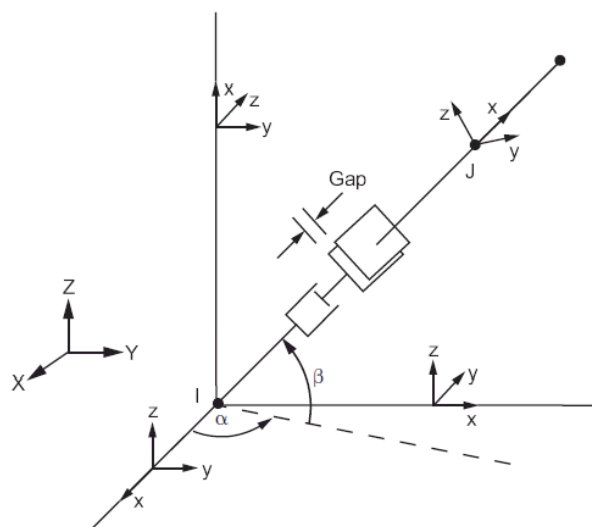
Figure 4-4: Geometries of CONTA178 element [3]

4.1.3 Geometry

The second step consists in defining the geometry of the model. In order to know the real dimensions of the elements that define the ANSYS model, that is, the core barrel, the fuel assemblies, the shroud and the core stops, different books and articles about the type of reactor to be analyze have been consulted. The creation of this model is done by taking some bases from a detailed model available on the disposal of the chair. This available model represents one fuel assembly formed by 16 fuel rods that are represented with all the details.

With the purpose of knowing the geometry of a fuel assembly the cross-sectional area and the height are taken in account.

In the case of the core barrel it is necessary to know the outer diameter and the internal diameter that corresponds to the wall thickness, as well as, the height of this element.

As stated above, the shroud is simulated with beams each of which is located at a defined distance from each external fuel assembly so that each fuel assembly that is on the outside of the whole distribution has its corresponding beam that is simulating the shroud.

To create the core stops, those are created with the appropriate type of beam for its dimensions, as well as in the case of the fuel assemblies and the shroud.

The entire geometric model is created by points (keypoints in ANSYS) and lines that are subsequently assigned to the corresponding type of element. This method is chosen because it is much easier compared to others and faster when solving the model.

The main dimensions for the defined types of elements, which correspond to the heights and some common data, can be found in the following table.

Table 4-2: Main common dimensions

Parameter	Units	Value	Description
pitch	m	0.23	lattice constant
FAs gap	m	0.0016	
zbsuk	m	0.01	lower edge
zbsok	m	4.835	upper edge
zbsazu	m	0.354	lower edge active zone
zbsazo	m	4.254	upper edge active zone

One fuel assembly is defined by a total of 13 points distributed at different distances along their height and 12 lines that join the points defined above. A total of 9 of these defined points correspond to the so-called spacers whose function is to maintain the proper form of the fuel assembly structure and to ensure the safety of reactor core design.

There are 193 fuel assemblies, distributed in a certain way, forming part of the reactor core. Each fuel assembly is separated from its neighboring fuel assembly with a fixed distance which correspond to the nominal value of the water gap between two fuel assemblies in hot condition. The value of this parameter is 1.6 mm. [27] Another necessary parameter to know the exact measurements is the lattice constant that as can be seen in the image (**Figure 4-5**: Sketch of 3 neighboring fuel assemblies) has a value of 230 mm. [5]

To calculate the width and length, that both have the same dimensions, the following scheme is created, which facilitates the visualization of the calculation that has been made.
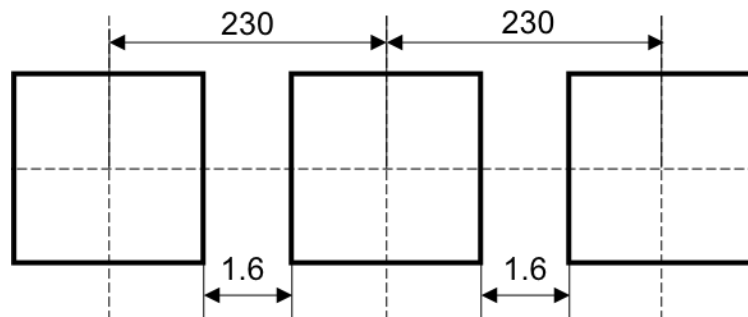
Figure 4-5: Sketch of 3 neighboring fuel assemblies

$$L = W = pitch - gap = 0.23\ m - 0.0016\ m\ \rightarrow L = W = 0{,}2284\ m$$

Table 4-3: Geometrical data fuel assemblies

Parameter	Units	Value
Pitch	m	0.23
FAs gap	m	0.0016
Lenght	m	0.2284
Width	m	0.2284
Height	m	4.835

To crate the entire distribution of these elements, which are defined by points and lines, a total of 7 different positions of rows and columns composed of 4 do-lops, that contain all the characteristics defined before, are used in order to create the 193 fuel assemblies.

The first and second do-loop correspond to the location on the x and y axes where all the points and lines, which are along the z axis, of each fuel assembly are located.

The third do-loop is necessary to create the points corresponding to the seven spacers as defined in the detailed model.

The last do-loop is used to join by lines the 13 points created in the previous step. To do this, it is necessary to go through all the points and join the first with the next one, thus obtaining a total of 12 lines that together form the structure of one fuel assembly.

Regarding the function that defines the position of each element, the following expression is given from the detailed model:

$$x = (i - 0.5) \cdot pitch$$

$$y = (j - 0.5) \cdot pitch$$

Where the variables i and j determinate the desired specific position of each element. These can take values from 1 to 15 since there are up to 15 different positions along the x and y axes that the fuel assemblies can take. This is done, as already mentioned before, by using do-loops.

The way to create the core barrel is exactly the same as the case of the fuel assemblies but with the difference that only one position is needed (the central position of the fuel assembly's distribution). As in the previous case, the first two do-loops correspond to the different positions in the x and y axes, in the case of the core barrel these can be suppressed since, as just pointed out, only one x and y position is necessary, that can be directly defined by the same equation as in the previous case. Therefore, only the last two do-loops are used for the same purpose as in the creation of the fuel assemblies.

Regarding the geometry of the core barrel it is necessary to know its external diameter and thickness. The data in the following table have been taken to implement the model (**Table 4-4**: Geometrical data core barrel). [28]

Table 4-4: Geometrical data core barrel

Parameter	Units	Value
diameter ext	m	4.5
thickness	m	0.08
height	m	4.835

As mentioned above, the shroud is created by beams that are placed around each fuel assembly that is displayed on the outside part of the whole distribution. There are 44 external fuel assemblies in total, as can be seen and counted in the **Figure 4-6**: Scheme configuration fuel assemblies with helper lines for the creation of shroud. However, this does not mean that there will only be 44 beams corresponding to the shroud but there is a total of 60 beams that form part of the shroud because of the external fuel assemblies that are located in the corners and in turn they need two shroud elements instead of one to cover all the geometry of the fuel assembly.

Then to create the shroud a total of 60 different positions are needed since, as specified before, there are 60 shroud elements. To proceed with the definition of the location of this element, this process is carried out with the help of imaginary lines to make easier the definition of the exact position, first in a horizontal direction and then in the vertical direction, as can be seen in the **Figure 4-6:** Scheme configuration fuel assemblies with helper lines for the creation of shroud. That is why in some cases, such as lines L2 and L3, it has not been possible to create a do-loop in order to define all the positions of the same line at once, but it is necessary to enter the position manually. In total there are 28 imaginary lines, 14 in each direction.
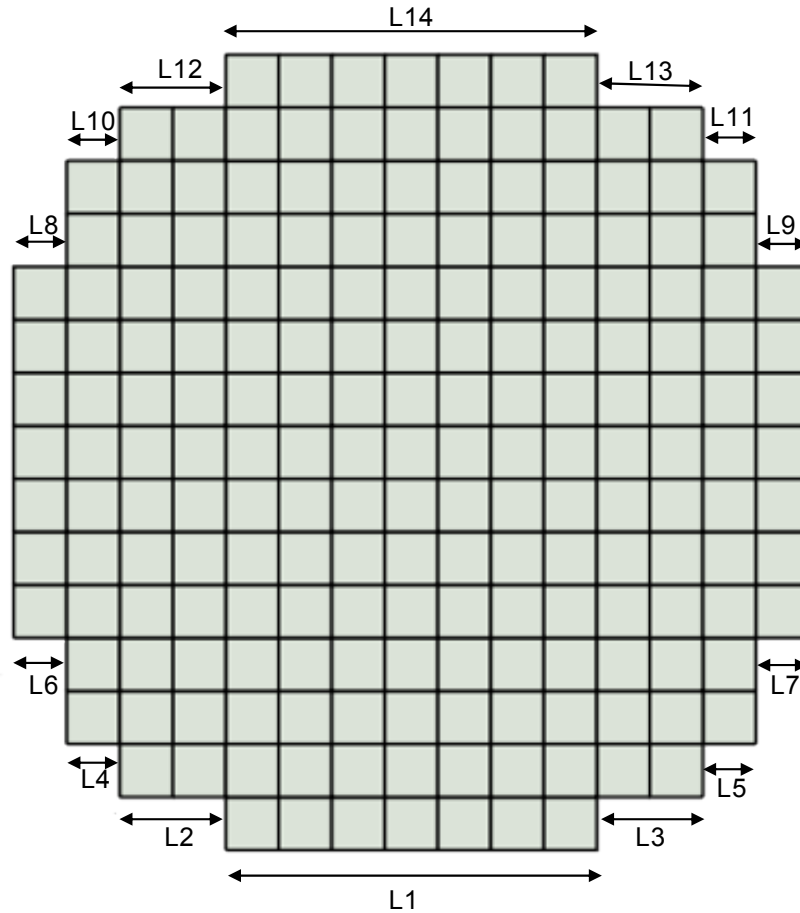
Figure 4-6: Scheme configuration fuel assemblies with helper lines for the creation of shroud

Regarding the separation between the fuel assemblies and the shroud, the same value is taken as in the case of separation of two fuel assemblies.

For the geometric data, as in the case of the fuel assemblies it is necessary to define the width and length of the beam corresponding to the shroud. From the bibliography it is possible to obtain the value corresponding to the thick of the shroud which will be in this case the width of the beam [29]. For the length it is necessary to take a value that prevents the contact of one beam with another, which can take place more easily in the corner fuel assemblies where there are two beams.

Table 4-5: Geometrical data core shroud

Parameter	Units	Value
width	m	0.023
lenght	m	0.15
height	m	4.835

During the creation of this elements, the equation of the position of each one changes with respect to the position function defined for the fuel assemblies and the core barrel. As it can be seen in the following image (**Figure 4-7**: Sketch of one fuel assembly with ist neihgboring shroud beam), it is necessary to add the value corresponding to the gap between both elements, the half part of the width of the fuel assembly as well as the half part of the width of the shroud. Then, the following equation for the new position is obtained:

$$x = (i - 0.5) \cdot pitch + gap_{FA-SH} + \frac{W_{FA}}{2} + \frac{W_{SH}}{2}$$

$$y = (j - 0.5) \cdot pitch$$
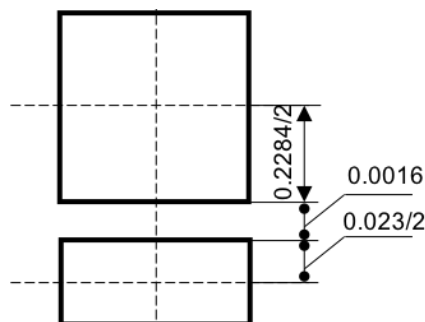
Figure 4-7: Sketch of one fuel assembly with ist neihgboring shroud beam

This is in the case of the horizontal lines, in the case of the vertical lines, in the case of the vertical ones the equation is exactly the same but adding the values, that are added to the x position, to the y position.

The heights of the points that define the three elements discussed above, and therefore the lines that unite them, are distributed with the same geometric data to later be easier to work with two or three of these elements at the same time.

As previously specified in the model explanation, it is necessary to create a total of 6 core stops. The core stops are located around the core barrel and since its shape is circular, the frequency with which an element of this type is placed can be calculated dividing the 360º, that a circle has, between 6 in order to know every how many degrees it is necessary to create the element, in this case every 60º. With this data it is possible to finally calculate the position of each of the core stops, that is shown in the following lines. The separation between each core stop and the core barrel is 5 mm since they are normally not in contact with the core support barrel and have a clearance of approximately 5 mm during the operation as said before. The geometrical parameters of the core stops can be found in the next table [5] [14]:

Table 4-6: Geometrical data core stops

Parameter	Units	Value
width	m	0.1
lenght	m	0.2
height	m	0.1

The positions for each of these 6 elements are calculated individually following the next sketch, **Figure 4-8**: Sketch position core stops. The central point of the model, the origin of the x and y axes, the external radius of the core barrel and the radius of the location of the core stops, are represented with its corresponding distances.
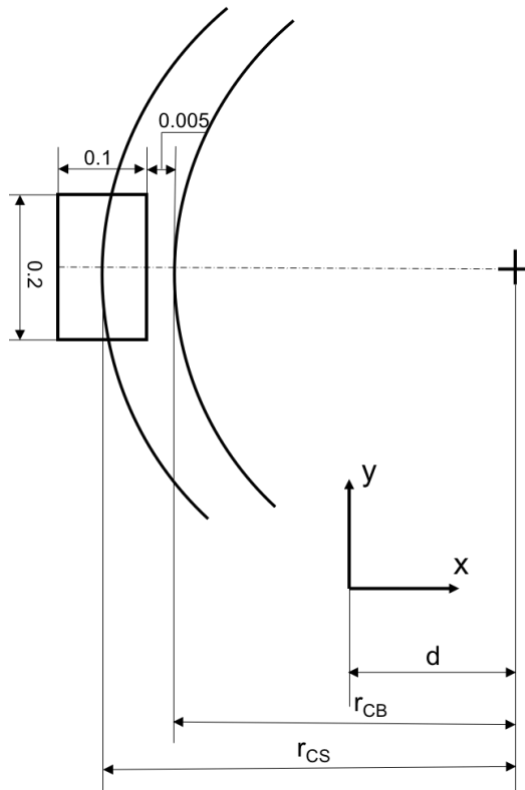
Figure 4-8: Sketch position core stops

From the sketch it is possible to determinate the radius of the imaginary circus that goes though the center of each core stop.

$$r_{CS} = r_{CB} + gap_{CS-CB} + \frac{width_{CS}}{2} = 2.25\ m + 0.005\ m + \frac{0.1\ m}{2} \rightarrow r_{CS} = 2.305\ m$$

Two of the six core stops, the first and fourth one, do not have any inclination with respect to the core barrel since they are in the position corresponding to 0 and 180 degrees. So, the positions of these two core stops are calculated and created using the following equation:

$$x_n = r_{CS} \cdot \cos\theta + d$$

$$y_n = r_{CS} \cdot \sin\theta + d$$

To create the rest of the core stops, the same equation is used, changing the value of the angle. However, to be able to create the element with a certain inclination it is necessary to define a help keypoint that is used later in the command corresponding to the creation of the element. The coordinates of this point are:

$$x_{help-n} = x_n + \cos\theta$$

$$y_{help-n} = y_n + \sin\theta$$

4.2 Materials

To model the different materials, the constants that define their behavior in the area of interest, in this case the structural field, may be known or estimated. In this model, two different materials are defined.

On the one hand, one material for core barrel, shroud and core stops need to be defined. It is considered a single material for these three elements since they are all made of steel. The differences in exact composition of each element are neglected. Steel properties are shown in the next table (**Table 4-7**: Steel properties):

Table 4-7: Steel properties [29]

Parameter	Units	Value	Description
E	Pa	$2.1 \cdot 10^{11}$	Young's modulus
ν	-	0.3	Poisson's ratio
ρ	kg/m^3	7850	density

On the other hand, it is necessary to define a different material for the fuel assemblies. As the properties of this material is not found as public data, the characteristics that define it are obtained from a detailed model available on the disposal of the chair (WKET).

Firstly, the density of this material is calculated. The way to obtain this value is based on calculating the mass of water circulating in one fuel assembly, starting from the detailed model that takes this detail into account, and adding this value to the mass of one fuel assembly and thus known the volume

of one fuel assembly and its mass, it is possible to obtain the value of the density. For this consideration the spacers are neglected. This process is divided into 6 steps:

1. Calculation of the volume of one fuel assembly from this the model:

$$V_{FA-1} = W \cdot L \cdot H = 0.2284 \cdot 0.2284 \cdot 4.835 \rightarrow V_{FA-1} = 0.252 \ m^3$$

2. Calculation of the volume of one fuel assembly from detailed model:

The necessary data are obtained from the detailed model and represented in the following table:

Table 4-8: Geometrical data of a fuel assembly from the detailed model

Parameter	Units	Value	Description
diameter ext	m	0.01075	external diameter of one fuel rod
height	m	4.835	height of the fuel rods
n_{FR}	-	236	number of fuel rods
diameter ext	m	0.01380	external diameter of one guide tube
height	m	4.835	Height of the guide tubes
n_{GT}	-	20	number of guide tubes

Since one fuel assembly from the detailed model is formed by 236 fuel rods and 20 guide tubes, first the volume of a single fuel rod and a single guide tube is calculated. Then, in order to know the total volume of one fuel assembly of this model, the calculated volume of each element is multiplied by the number of fuel rods and guide tubes respectively:

$$V_{FR} = \pi \cdot r^2 \cdot h = \pi \cdot \left(\frac{0.01075 \ m}{2}\right)^2 \cdot 4.835 \ m \rightarrow V_{FR} = 4.388 \cdot 10^{-4} \ m^3$$

$$V_{GT} = \pi \cdot r^2 \cdot h = \pi \cdot \left(\frac{0.01380\ m}{2}\right)^2 \cdot 4.835\ m\ \rightarrow V_{GT} = 7.232 \cdot 10^{-4}\ m^3$$

$$V_{FA-2} = V_{FR} \cdot n_{FR} + V_{GT} \cdot n_{GT} = 4.388 \cdot 10^{-4}\ m^3 \cdot 236 + 7.232 \cdot 10^{-4}\ m^3 \cdot 20\ \rightarrow V_{FA-2}$$
$$= 0.118\ m^3$$

3. Difference between two volumes:

Now the difference in the fuel assembly volume between the two models is calculated, which corresponds to the volume of water inside one fuel assembly:

$$V_{H_2O} = V_{FA-1} - V_{FA-2} = 0.252\ m^3 - 0.118\ m^3 \rightarrow V_{H_2O} = 0{,}134\ m^3$$

4. Mass of water:

To calculate the mass of water inside one fuel assembly the following equation is used:

$$m = V \cdot \rho$$

For this, the value of the water's density is needed. During the operating conditions of a nuclear reactor the temperature and pressure inside the core are very high, which makes the density of water different. In the case of pressurized water reactors, the pressure is 160 bar and the temperature around 300ºC [5]. With these data a water density of 727,46 kg/m³ is obtained [31].

Now the previous formula is applied in order to know the mass of water:

$$m_{H_2O} = 0.134\ m^3 \cdot 727.46\ kg/m^3 \rightarrow m_{H_2O} = 97.48\ kg$$

5. Mass of one fuel assembly with water:

It is easy to obtain the total mass of one fuel assembly together with the water that is inside by adding the values of the masses of one fuel assembly without water, 830 kg [5], and of the water calculated before.

$$m_{T-FA} = m_{FA} + m_{H_2O} = 830 \ kg + 97.48 \ kg \ \rightarrow \ m_{T-FA} = 927.48 \ kg$$

6. Density of the material:

Once the value of the mass of one fuel assembly and its volume are known, it is possible to finally calculate the value of the density using the same equation than in the previous step:

$$\rho = \frac{m_{T-FA}}{V_{FA}} = \frac{927.48 \ kg}{0.252 \ m^3} \ \rightarrow \ \rho = 3680.48 \ kg/m^3$$

To obtain the value of Young's modulus and Poisson's ratio, the procedure that is followed is to apply a force to the detailed model and see the elongation of the fuel assembly that occurs. Then the same force is applied to the designed model from which the geometry of only one fuel assembly is extracted. Once seen the elongation of this second analysis, the aim is to vary the material properties (Young's modulus and Poisson's ratio) until the elongation will be the same as in the detailed model.

To do this, a static analysis is performed where a force of 100 N is applied to the node located at the middle height of the structure. The elongation that is taken into account is the one of the node where the force is applied. In the detailed model the value of this elongation is $0.252114 \cdot 10^{-2}$ m. The first elongation obtained in the designed model is $0.8518 \cdot 10^{-4}$ m. As the difference is quite large, therefore it is decided to reduce the value of the Young's modulus considerably. By varying this data to a value of $3.355 \cdot 10^9$ Pa, a displacement of $0.252104 \cdot 10^{-2}$m is obtained. The value obtained is accepted as the error is lower than 0.01 %.

$$\% \, error = \frac{|exact \, value - approximate \, value|}{exact \, value} \cdot 100 =$$

$$= \frac{|0.252114 \cdot 10^{-2} - 0.252104 \cdot 10^{-2}|}{0.252114 \cdot 10^{-2}} \cdot 100 \; \rightarrow \% \, error = 0.0039\%$$

The following table shows all the data obtained for the material for the fuel assemblies:

Table 4-9: Fuel assemblies material properties

Parameter	Units	Value	Description
E	Pa	$3.355 \cdot 10^9$	Young's modulus
ν	-	0.3	Poisson's ratio
ρ	kg/m³	3680.48	density

4.3 Mesh

Meshing is the phase in which the model is discretized in a finite number of nodes and elements. To generate it, it is necessary to follow the next steps:

- Select the elements
- Control the generation parameters of mesh
- Mesh the model

For the correct mesh definition regular shapes of the elements must be ensured. Those that have either very large or very small angles are not desirable elements. Another important aspect is to ensure that the size and shape control are correct. This means choosing a reasonable mesh size and pretending that all the elements are similar in shape. To do this, it is necessary to specify how many elements have to be created for each already created line. The elements must be assimilated as much as possible to a square.

Since 3 of the 4 components that are part of the model have a similar geometry and size, in terms of height, the part of mesh has been divided into two parts.

The first part corresponds to the core barrel, shroud and fuel assemblies. The size chosen for this part of mesh is 0,001 m, which gives a total of 59 nodes for each of the elements that are meshed in this first step.

The second part of the mesh is the one that corresponds to the core stops. In this case a rather smaller mesh size is chosen since the size of these elements is also smaller in comparison with the three previous components. It is opted for a mesh size of 0,08 m, that is, each core stops consists of 4 nodes.

With the mesh types chosen, it is confirmed that the number of elements is sufficiently high, as required by the correct meshing since the meshed elements have a regular shape and when solving the model, the solution is detailed enough to aim the desired objectives in a reasonable time of solution.

The created geometric model is shown below:
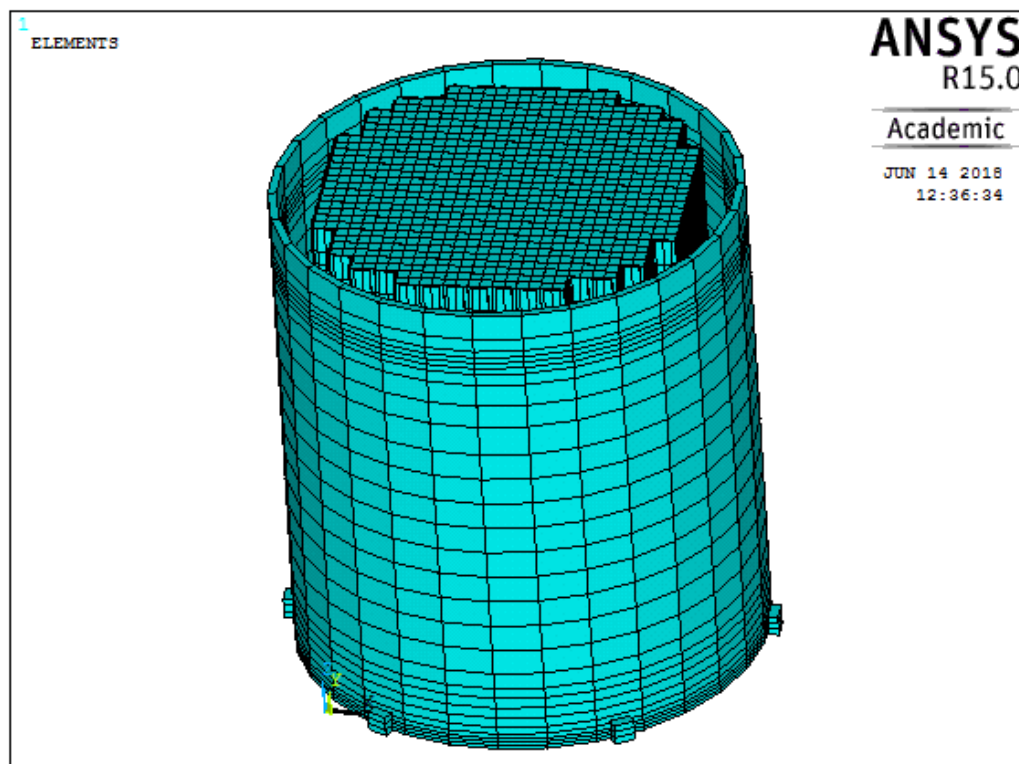
Figure 4-9: Isometric view of the geometrical model
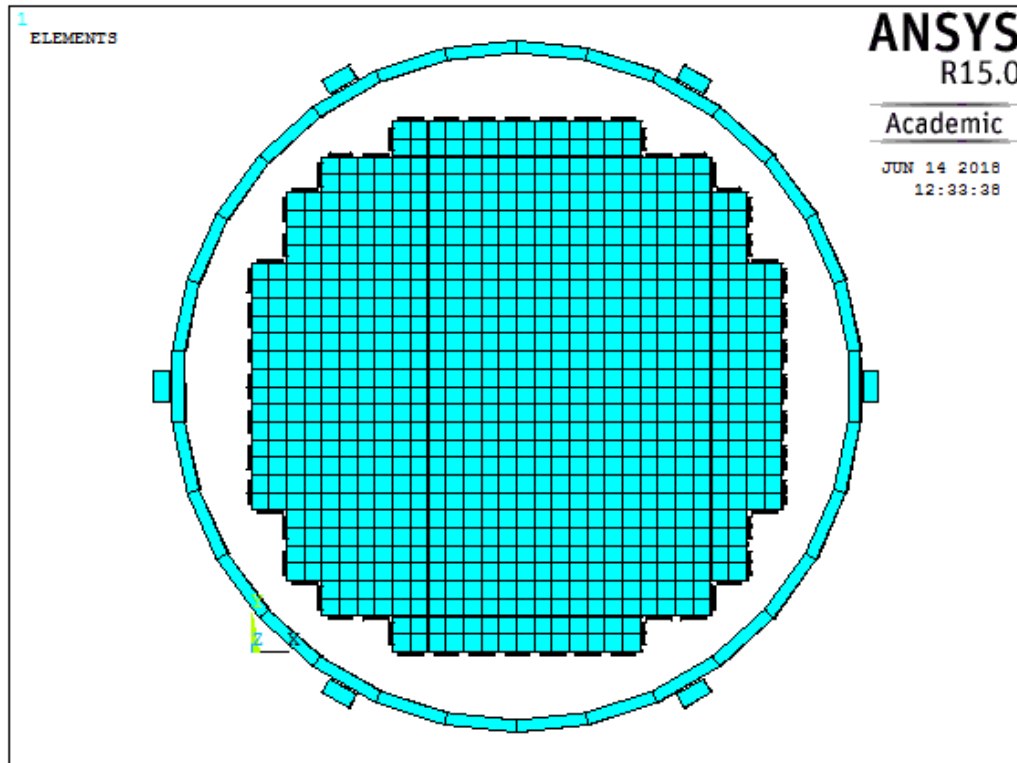
Figure 4-10: Top view of the geometrical model

4.4 Boundary conditions

The boundary conditions are those which impose values to some degrees of freedom of the model. Defining boundary conditions involves identifying the location of the boundaries and supplying information at them. In this section all the boundary conditions that have been defined in the model are explained. To satisfy the need of the model, three different types of conditions have had to be used. Next it is explained how each of them was created.

4.4.1 Rigid region

As well as it is known, the different elements that are part of the core of a nuclear reactor and that have been implemented in this model, are located in fixed positions regarding some elements that are in their surroundings. This is the case of the shroud regarding the core barrel and regarding the fuel assemblies. Then, this condition is simulated with two separated parts.

In the first case, the constant distance between the core barrel and the shroud is considered at the midpoint height of the structure, that is at the height of the 5th spacer.

So, to achieve this restriction in ANSYS, the coupling degrees of freedom is used. The command that does this function is CP which function is specified as defining a set of coupled degrees of freedom. However, in the created model it is not possible to use the command mentioned above because while assigning the nodes to a set, one node can only be part of one defined set, fact that in this case it is not possible due to the need of having the same node in more than one sets.

The solution for this problem is to define a rigid region by writing constraint equation to define rigid lines linking a designated retained node ("master") to a number of removed nodes ("slaves"). This can be achieved by using the CERIG command.

To proceed to apply this command, the "master" node is defined as the node located in the middle height, 5th spacer, of the core barrel and the "slaves" nodes are all the nodes that belong to the shroud and are at the same height as the master. Once located, selected and defined as such, the CERIG command is applied. The movements that are restricted with this command are in x and y direction.

The second case corresponds to the rigid region defined in the lower part of the structure and that affects the fuel assemblies, the core barrel and the shroud. This is because the fuel assemblies that are located inside the core barrel in a certain position are placed inside a grid located in the lower part of them. This fact also affects to the shroud that is supported there.

This step is implemented exactly in the same way as the previous case with the difference that now the lower node of the structure that corresponds to the core barrel is defined as "master" node. The "slave" nodes are the rest of nodes corresponding to the shroud and the fuel assemblies and also located in the lower part of the structure.

As a result of the application of this command the desired restriction is achieved. The result of the application of the rigid region can be seen in the following image where, in both cases, all the lines leave the central node and create the rigid region with its slave nodes.
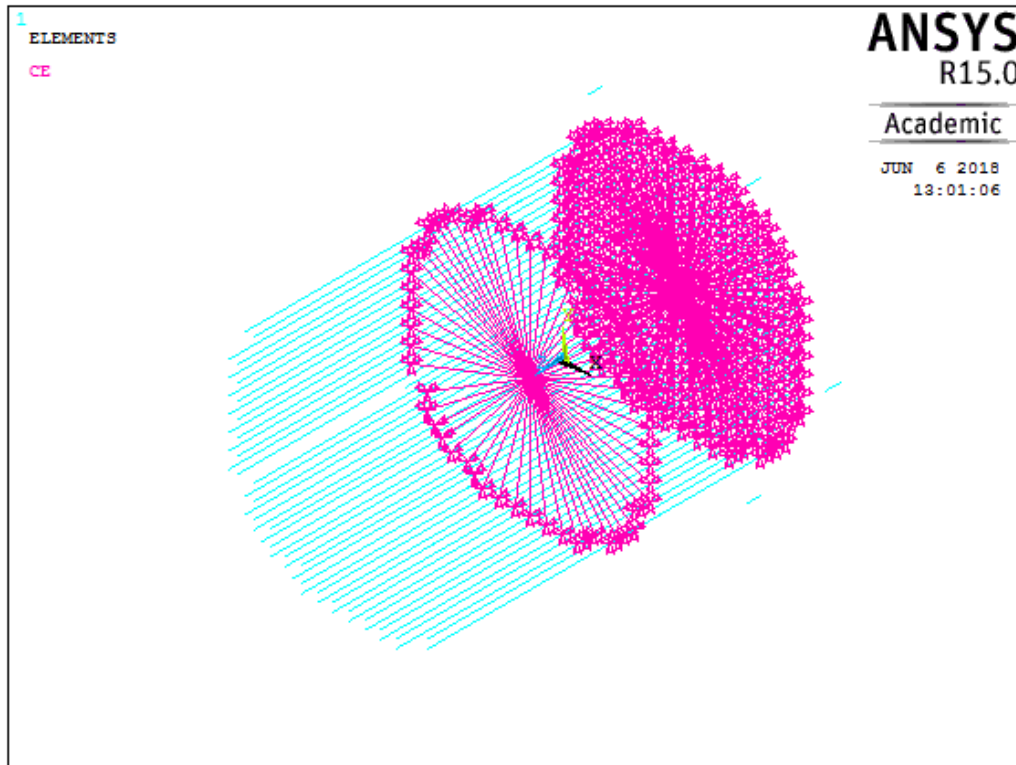
Figure 4-11: Isometric view of the rigid region. The blue lines show the elements that make up the model and the pink lines show the two defined rigid regions where the triangles show the slave and the master nodes.

4.4.2   Degrees of freedom

Regarding the necessary restriction for fixing the whole structure in its upper part, a strong approximation is assumed in order to simplify the model. For this it is considered that both the core barrel and the fuel assemblies together with the shroud cannot sustain any displacement as well as any rotation in x, y and z axes. However, this is not totally for the case of the core barrel since this element is not clamped on its upper part and this assumption may suppose a too rigid structure.

To achieve this goal D command is used. This consists of defining degrees of freedom constrains at nodes. In this case it is necessary to make the restriction in all directions, both displacements and rotations, as it was previously specified.

Firstly, this applies to the core barrel, the fuel assemblies and the shroud. To apply the D command, all the nodes, that interest from the structure, are selected, that is, those belonging to its top part. Then the degrees of freedom that are to be restricted are specified, in this case all of them.

34

Secondly, the same procedure is applied to the core stops. The reason why this is done in two steps is the same as in case of the rigid region. The first restriction of the degrees of freedom, the one corresponding to the core barrel, the fuel assemblies and the shroud, is located at the top height of the structure. In the case of the core stops, those are located at the bottom part of the model so it is necessary to select these elements separately. The application of the D command is exactly the same as in the previous case.

The restriction of the displacement and rotation in all directions in the lower part of the structure can be seen in the following image:
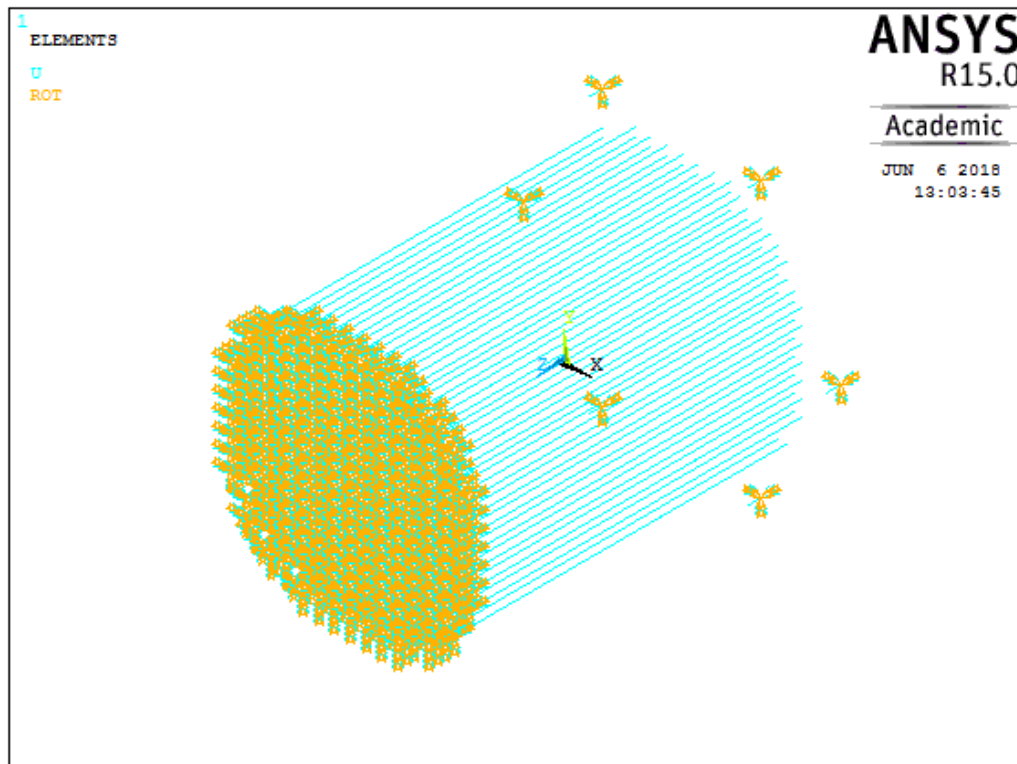
Figure 4-12: Isometric view of the restriction of degrees of freedom. The blue lines show the elements that make up the model and the blue-yellow triangles the restricted degrees of freedom (blue for displacements, yellow for rotations).

All the boundary conditions applied to the model and explained above can be seen in the following image:
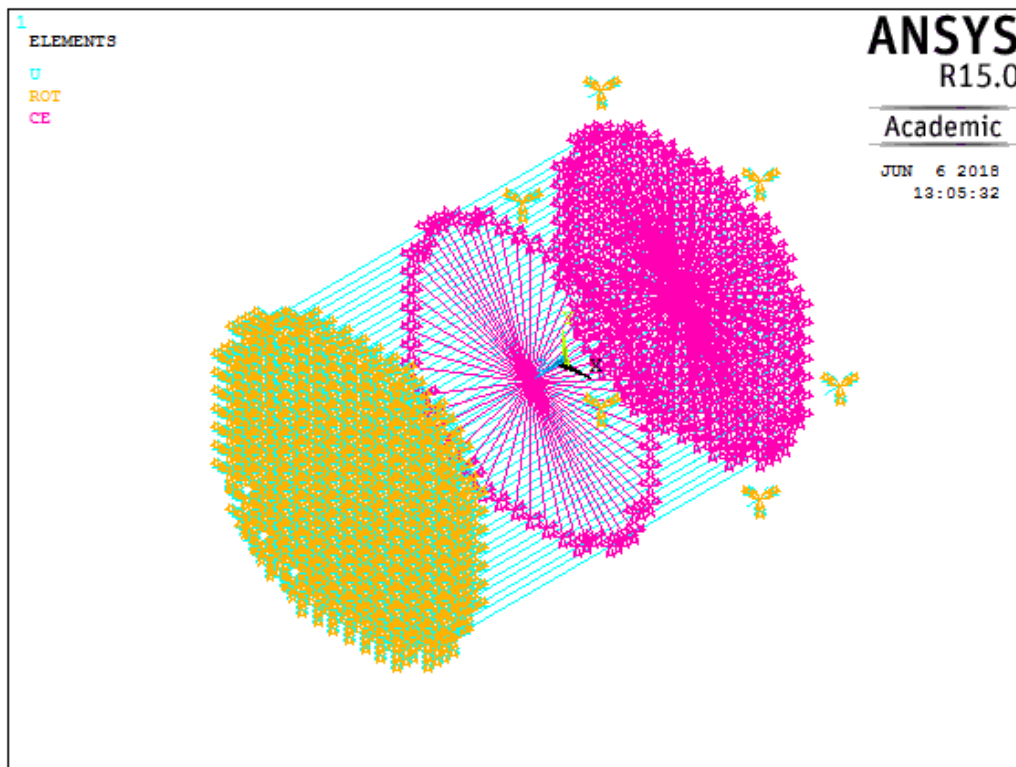
Figure 4-13: Isometric view of the boundary conditions. The blue lines show the elements that make up the model, the pink lines show the two defined rigid regions and the blue-yellow triangles the restricted degrees of freedom.

4.5 Contact

Apart from the previously defined boundary conditions, it is necessary to define the contact between different elements that occurs due to the action of the acting force. The sets of elements that can experience the contact are the following: fuel assemblies and shroud, fuel assemblies among themselves, core stops and core barrel. All these components are defined as beam elements except the core barrel that is defined as a pipe. However, all of them, regardless of the type of element to which they belong, have been created through a set of lines that define each element. The line to line contact is typically used to model 3-D beam to beam contact, crossing beams or beams that are parallel to each other. [32] As in this case the parallel contact between beam is needed, the line to line contact is chosen.

In order to create the contact, two types of new elements will be defined. On the one hand, the contact element is defined by CONTA176 as explained in the Elements section of this document. On the other hand, the previously defined element needs another type of element so that contact is possible. To make it possible, the TARGE170 element is created as explained in the same section of this document.

The first possible contact case is the one that can occur between the shroud beam and the fuel assembly beam to which the shroud beam belongs. As specified in the ANSYS tutorial, in the case of having two elements of different materials, the softer element is defined as the contact and the stiffer as a target. [32] For this, all the lines that form a beam of the shroud are selected and the target element is assigned to them using ESURF command. Then, it is necessary to add as a contact element the lines that are part of the neighboring fuel assembly. This is done using the ESURF command too.

In the case of the possible contact between the fuel assemblies, the procedure to generate it is exactly the same as in the previous case with the difference that one fuel assembly is defined as the contact of its neighboring fuel assembly that is his target but at the same time is the contact of the next one and so on.

It is highlighted that since the contact can only be external, it is necessary to apply some restrictions for each element using the keyopt command.

Regarding the possibility of contact between the core stops and the core barrel, the node to node contact is defined. To do this, a node of each core stops and a node of the core barrel that are at the same height are selected. Then, the contact element, CONTA178 as explained in Elements section, is generated between the two already selected nodes. In addition, the gap between both elements is defined by real constants.

4.6 Solution

Once the model is defined, the implementation of the model solution is described. The final objective of this work is the investigation of the influence of the forces applied to the structure that are mainly time dependent forces on the structure. This implies the need for a transitory analysis. Apart from taking these forces into account, the model is analyzed with a sinusoidal force in order to investigate the influence of the force and evaluate the elongations that may be produced. However, before

proceeding with the main analyzes, three additional analysis are done in order to verify and understand better the model.

First, to verify that the model works correctly, a comparison between a static analysis and a transient analysis is made.

In second place, a modal analysis is also carried out to determinate the natural mode shapes and frequencies of the structure during free vibration.

Finally, a harmonic analysis is performed in order to determinate the value of the stiffness damping parameter.

For the realization of the simulation described above, the following equipment and software was used:

- Technical data:
  - Processor Intel®Core™ i7-5820K CPU
  - 3.30 GHz, 432 Gb RAM
- Operating system:
  - Windows 8.1 Enterprise
- Software:
  - ANSYS Mechanical APDL 15.0

5 VERIFICATION OF THE MODEL

As previously noted, to confirm the validity of the model, the comparison of two types of different analysis is performed. This involves a static analysis and a transient one. Verification is based on the application of the same force at exactly the same point in both analyzes. Once the force is applied, the displacements that occur at a specific point in the structure are studied, as it is logical it has to be the same point for both types of analysis. Below is a brief description of each of the analyses and the obtained results.

5.1 Static analysis

This type of analysis is very easy to apply using the ANSYS APDL commands. It is only necessary to specify the node where the force has to be applied and its direction. The node where the force is applied belongs to the lower node of all the nodes that define the core barrel. As specified in the book [33], for VVER-440 reactor with 6 loops the maximum force that acts on the core barrel due to the

circulation of the coolant is 50,000 N. Since this type of reactor is smaller than the KWU reactor, larger forces are expected for this second case. Making a rough estimation, the force value that is decided to apply is of the order of 100,000 N in the x direction. The point at which the displacement will be analyzed belongs to an exterior fuel assembly chosen randomly. In order to see the displacement of one point of the fuel assembly a node that is located at the middle height of the element is chosen.

The result of the displacement obtained in this analysis is $1.49937 \cdot 10^{-6}$ m.

5.2 Transient analysis

The transient analysis is a bit more complex when implementing the ANSYS macro. In contrast with the previous one, besides applying loads it is necessary to specify the load step options. The first step in applying transient loads is to establish the initial conditions. In this case, both the initial displacement and the initial velocity are zero. The remaining substeps that are applied in this analysis are the points where force is applied. An analysis of a total of 10 s is chosen. Once the analysis is solved, with exactly the same force and points as in the previous analysis, a displacement with a value of $1.49957 \cdot 10^{-6}$ m is obtained in the last substep, that is, after the 10 s of analysis as it can be seen in the following graph (**Figure 5-1**: X elongation transient analysis):
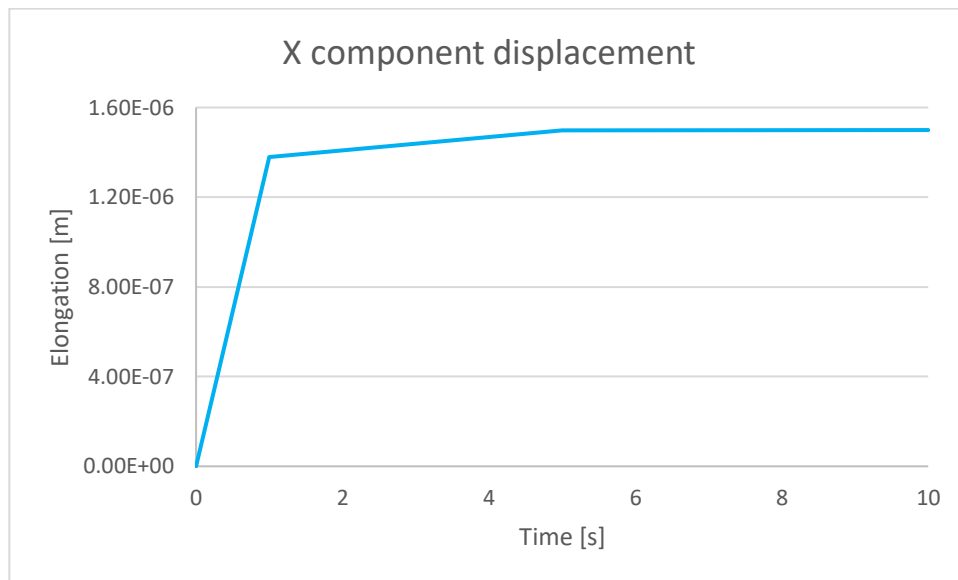
Figure 5-1: X elongation transient analysis

5.3 Results

The following table shows the results obtained from the two previous analyses:

Table 5-1: Elongatios results of static and transient analysis

Analysis	Units	Elongations
Static	m	$1.49937 \cdot 10^{-6}$
Transient	m	$1.49957 \cdot 10^{-6}$

As it can be seen the displacement values obtained in the two types of analysis are similar but not exactly the same. When dealing with very small values, of the order of micrometers, the error rate is very small as can be seen below:

$$\% \, error = \frac{|exact \, value - approximate \, value|}{exact \, value} \cdot 100 =$$

$$= \frac{|1.49937 \cdot 10^{-6} - 1.49957 \cdot 10^{-6}|}{1.49937 \cdot 10^{-6}} \cdot 100 \rightarrow \% \, error = 0.01\%$$

Since the error is much lower than 1%, the validity of the model is confirmed after making the comparison between the static and transient analysis.

6 MODAL ANALYSIS

It is decided to perform a modal analysis to better understand the model as it is an important method for describing the vibration behavior of a linear mechanical system. Modal analysis is based in the determination of natural frequencies and the associated vibration modes of a structure. Natural frequencies are those frequencies with which the linear mechanical system moves when there is no external excitation. At each natural frequency, there is a vibration waveform that indicates how the individual points of the structure move relative to each other, those are called the mode shapes of the structure and with its help it is possible to provide a comprehensive picture of deformations that are occurring. [33]

6.1 Single beam model

6.1.1 Unrestricted

Before proceeding with the modal analysis of the entire complete model, it is decided to perform this type of analysis on the model extracted of a single beam, the same one that was used to calculate the material properties. This is done to check the validity of the analysis since the modes of this analysis are theoretically known. [34]

For this, the beam is assumed with the condition that it is completely fixed at one of its ends and free at the other one, which is called cantilever beam (see **Figure 6-1**: Cantilever beam). The restriction that is imposed to accomplish this condition in ANSYS is to fix all the degrees of freedom of the las node that is at the end. To perform this type of analysis a total of 10 modes are considered with the beginning of the frequency range of interest at 0.01 Hz.
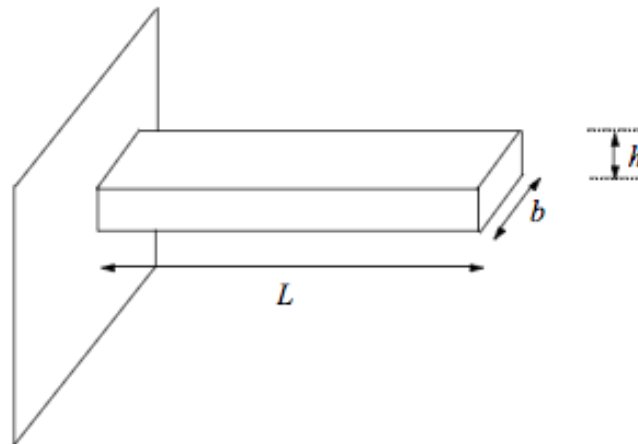
Figure 6-1: Cantilever beam

In the case of this type of beams, the resonance frequencies can be determined by the Euler-Bernoulli equation [34]:

$$f_n = \frac{1}{2 \cdot \pi} \cdot \frac{\mu_n^2}{L^2} \cdot c$$

where

$\mu_1 = 1.875; \; \mu_2 = 4.694; \; \mu_3 = 7.854; \; \mu_n \approx (2 \cdot n - 1) \cdot \frac{\pi}{2} \; for \; n > 3$

$c^2 = \frac{E \cdot I}{\rho \cdot S} \; where \; I = \frac{1}{12} \cdot b \cdot h^3 \; and \; S = b \cdot h$

Substituting the previous values, the following equations are obtained [34]:

$$f_1 = 0.162 \cdot \frac{h}{L^2} \cdot \sqrt{\frac{E}{\rho}}$$

$$f_2 = 6.27 \cdot f_1$$

$$f_3 = 17.55 \cdot f_1$$

$$f_n = 2.81 \cdot \left(n - \frac{1}{2}\right)^2 \cdot f_1$$

6.1.2 Results

As it is a two-dimensional symmetric model, for each frequency two modes are obtained. These two modes correspond to the vibrations produced in two different directions, yz and zx. As expected, the maximum deflection values are exactly the same for both cases. However, there is the 7th mode corresponding to the frequency of 28.381 Hz that shows a little relevant result since the maximum deflection that is observed is of the order of pico meters. Therefore, it is a solution that is considered as not real and maybe due to the numerical issues of the software it may have led to this result.

The different modes obtained in this analysis, without including the 7th mode that can be ignored for the reason stated above, are shown next:
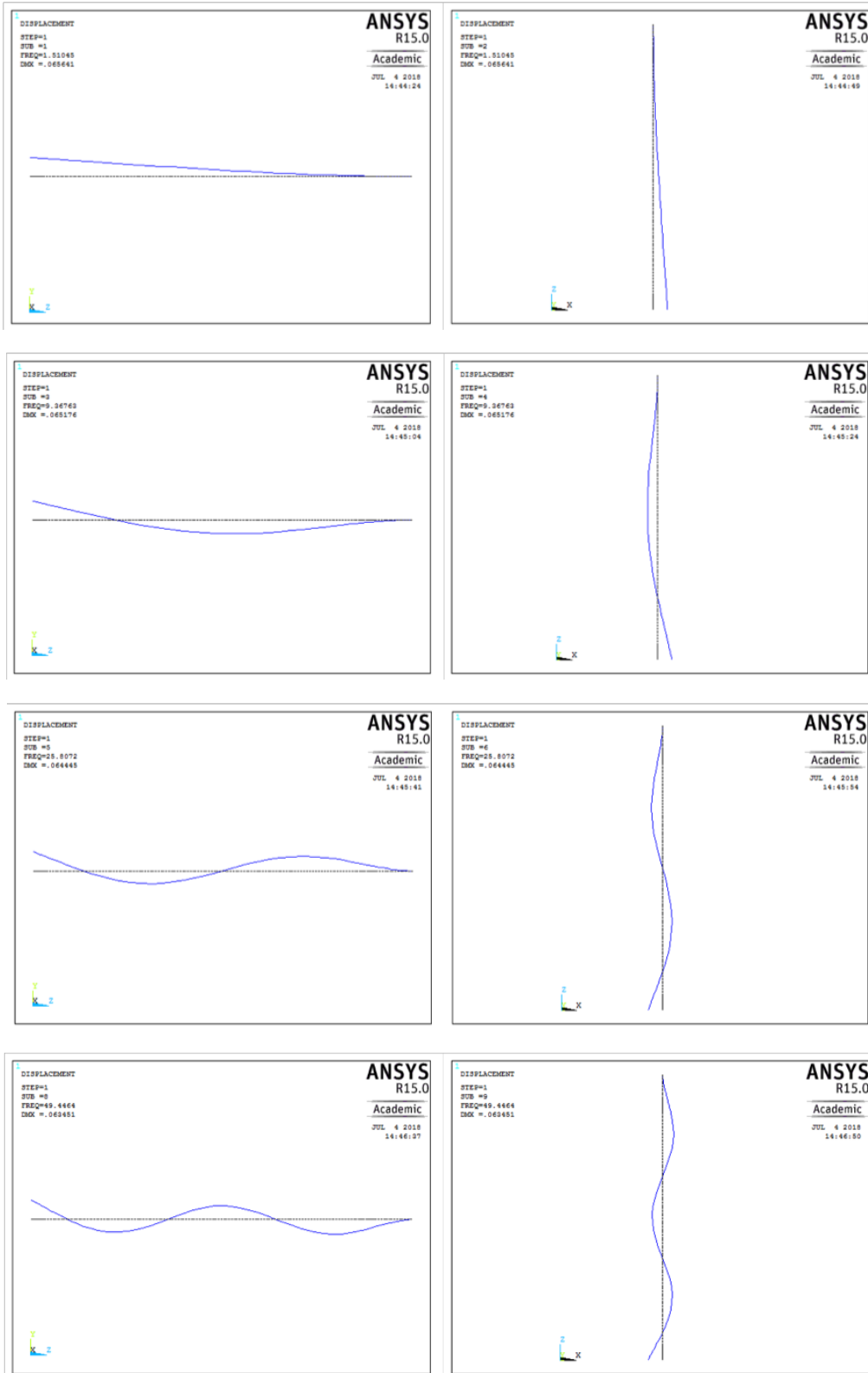
Figure 6-2: Different modes from the simulation, left: YZ deflection, right: ZX deflection

The table shows the natural frequencies corresponding to each of the modes from the analysis performed with ANSYS:

Table 6-1: Values of the simulated natural frequencies

Mode	Units	Natural frequency
1-2	Hz	1.5105
3-4	Hz	9.3676
5-6	Hz	25.807
7-8	Hz	49.446

Now, the results obtained from the modal analysis are compared with the results calculates theoretically. [34]

For the calculation of the theoretical natural frequencies for the first four mode shapes of the cantilever beam, the following expression and the data obtained in the previous sections (**Table 4-3: Geometrical data fuel assemblies**,**Table 4-9**: Fuel assemblies material properties) are used:

$$f_1 = 0{,}162 \cdot \frac{h}{L^2} \cdot \sqrt{\frac{E}{\rho}}$$

$$f_2 = 6.27 \cdot f_1$$

$$f_3 = 17.55 \cdot f_1$$

$$f_n = 2{,}81 \cdot \left(n - \frac{1}{2}\right)^2 \cdot f_1$$

The results obtained from these calculations are listed in the following table:

Table 6-2: Values of the theoretical natural frequencies

Mode	Units	Natural frequency
1-2	Hz	1.5112
3-4	Hz	9.475
5-6	Hz	26.521
7-8	Hz	52.019

Finally, the deviation that exists between the natural frequencies obtained from the simulation and the theoretical values is calculated and shown below:

$$\% \; error = \frac{|exact \; value - approximate \; value|}{exact \; value} \cdot 100$$

Table 6-3: Deviation between simulated and theoretical natural frequencies

Mode	Units	Deviation
1-2	%	0.046
3-4	%	1.15
5-6	%	2.76
7-8	%	4.95

Observing the previous table, it is concluded that the maximum percentage deviation between both methods is 4.95 %. The mode shapes obtained from the simulation agree with the theoretical ones. After comparing both results of the same type of beam, it is possible to affirm the validity of the model.

6.1.3 Restricted

The aim of the following analysis is to get closer to the complete model. The boundary conditions defined in the model, as specified in Boundary conditions section, are:

- Fixed degrees of freedom at the top part of the structure
- Rigid region that restricts movement in x and y directions at the lower part of the structure

To simulate the first condition mentioned above in a simple beam, the same procedure as in the previous section and in the complete model is carried out, that is, to fix all the degrees of freedom of the upper part of the beam. For the second condition, since it is not possible to define a rigid region of an element formed by a single node for each height, it is decided to fix the degrees of freedom in the x and y directions since it is the most similar approach to the defined boundary condition in the complete model.

As well as in the previous case, the modal analysis is performed for a total of 10 modes with the beginning of the frequency range of interest at 0.01 Hz.

6.1.4 Results

It is a symmetric model, so for each value of frequency two modes are obtained with elongations in two different directions, yz and zx, as in the previous case. There is also obtained one mode that is ignored in the analysis since it is due to the numerical issues and does not correspond to any real deformation.

The modes obtained in this analysis are shown next:
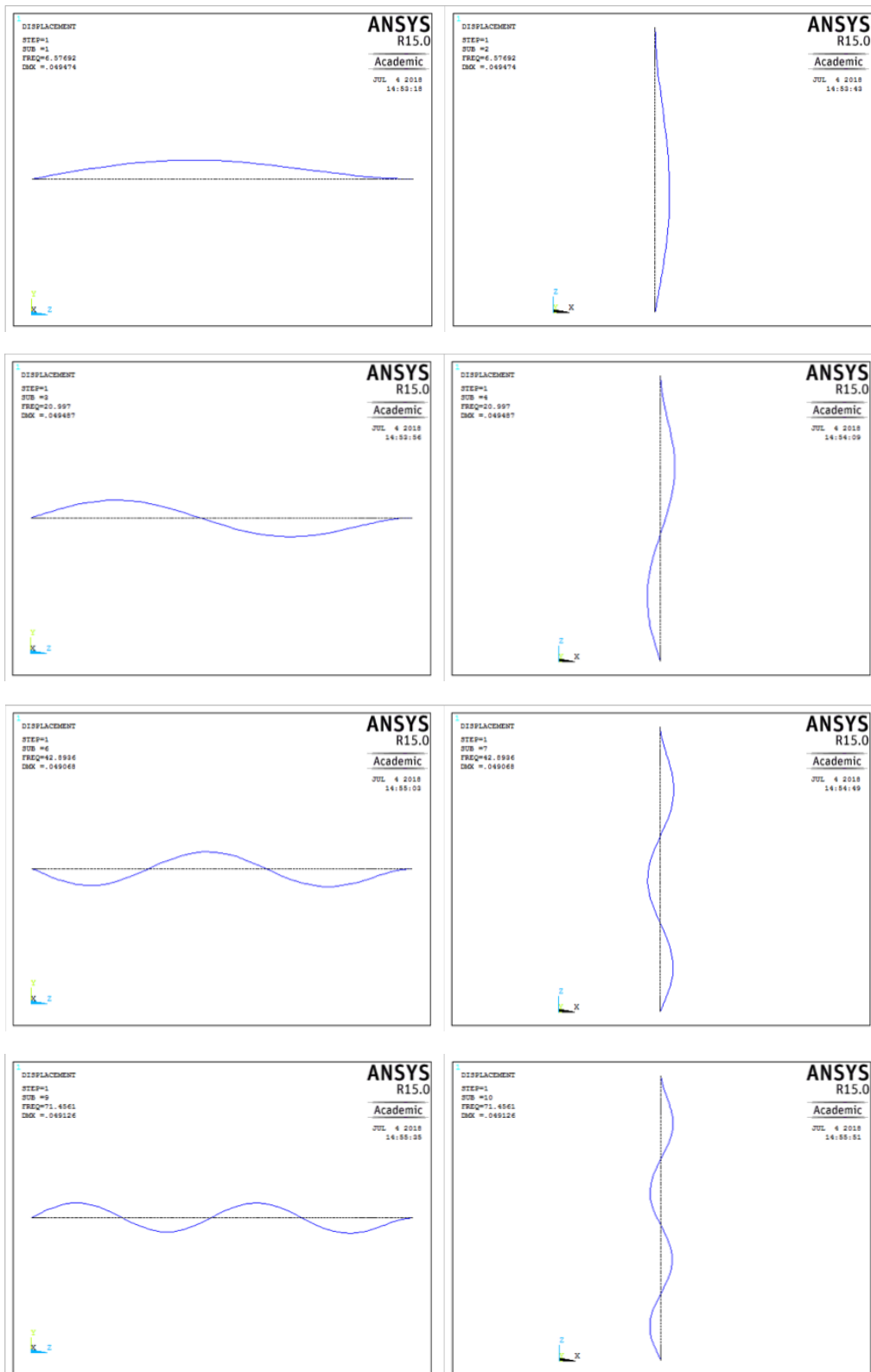
Figure 6-3: Different modes from the simulation, left: YZ deflection, right: ZX deflection

The table shows the natural frequencies corresponding to each of the modes from the analysis performed with ANSYS:

Table 6-4: Values of the simulated natural frequencies

Mode	Units	Natural frequency
1-2	Hz	6.5769
3-4	Hz	20.997
5-6	Hz	42.894
7-8	Hz	71.456

After obtaining the results of this second modal analysis, it is observed that the natural frequencies increase when adding the restriction in the lower part of the beam.

6.2 Full structure model

In this section, the results obtained from the modal analysis of the complete model with all its boundary conditions are discussed. However, the contact condition, as specified in the ANSYS manual, is ignored in this type of analysis.

In this analysis the same number of modes as in the previous one is considered. Once all the modes are analyzed, the first 5 are chosen to analyze the results since they show more significant information.

In the images from the next section, each of the chosen modes are shown and commented. For each mode there are two pictures, one with the side view and one with the top view. The black lines or points (depending on the view) represents the elements without any elongation, that is, in the initial position. In contrast, the blue color represents the possible elongation that occurs in each mode.

6.2.1 Results

In the first mode, it can be seen that the elongation occurs in the middle part of the fuel assemblies which means that both, the upper and the lower end remain in their initial position. This is because in the upper part of the structure the assumption of restricting all the degrees of freedom is taken, that is, there is no movement allowed. On the other hand, in the lower part there is a rigid region that maintains the constant distances in x and y direction between the fuel assemblies, the core barrel and

the shroud. As will be explained below, the last two elements mentioned above do not undergo any deformation and that is why the fuel assemblies do not neither. Finally, it is important to emphasize that the elongation occurs in the positive x direction, as can be seen in the top view.
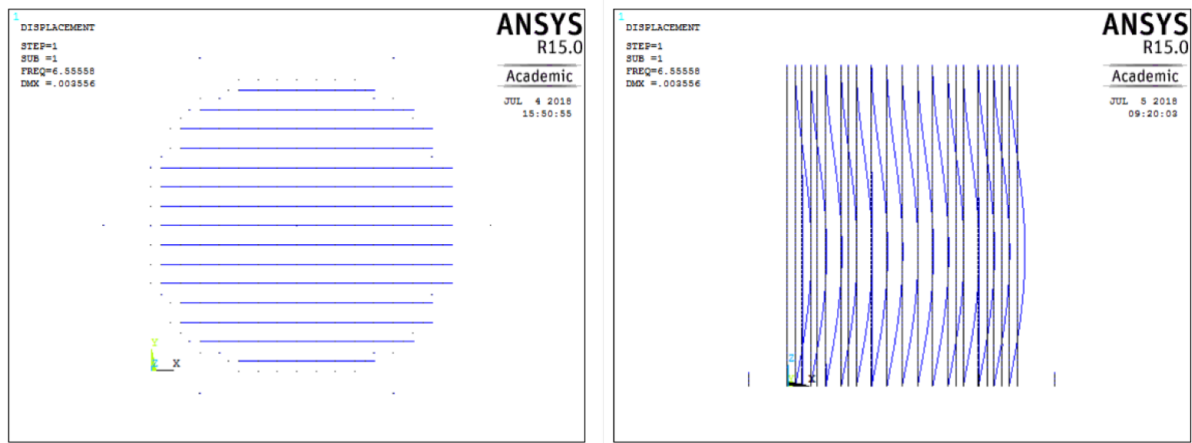
Figure 6-4: First mode

Regarding the second mode, the affected elements move in the positive y direction as can be seen in the top view, which means 90 degrees of difference regarding the first mode due to the symmetry of the model. That is why it is now necessary to represent the other side view of the structure in order to see the elongation that occurs in this case. As can be seen in this view, apart from the direction of the elongation there is no difference between the first and the second mode. So, the elongation in this mode is equivalent as in the first one explained above.
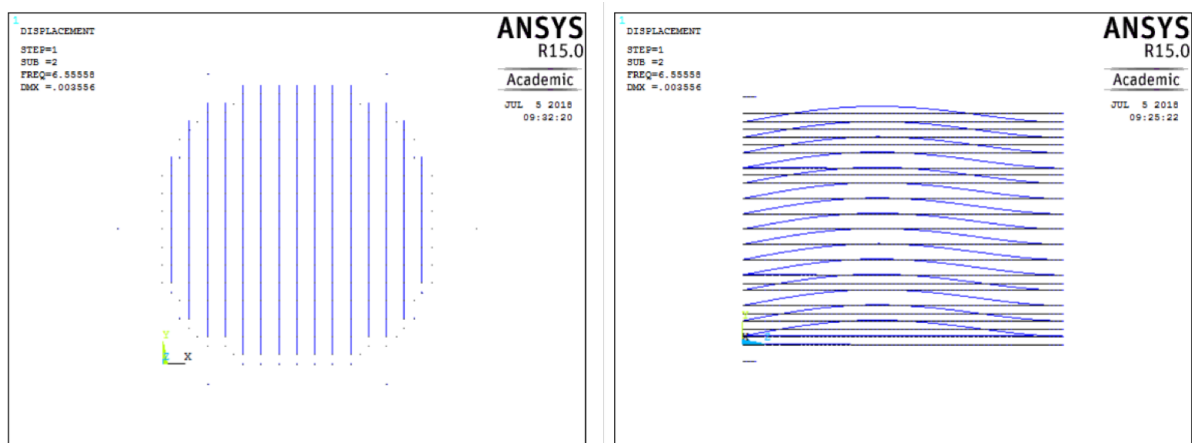
Figure 6-5: Second mode

In the third mode an unexpected phenomenon is observed. All the fuel assemblies move in the same direction in such a way that looking the trajectory of its displacement, a circle is observed from the top view.
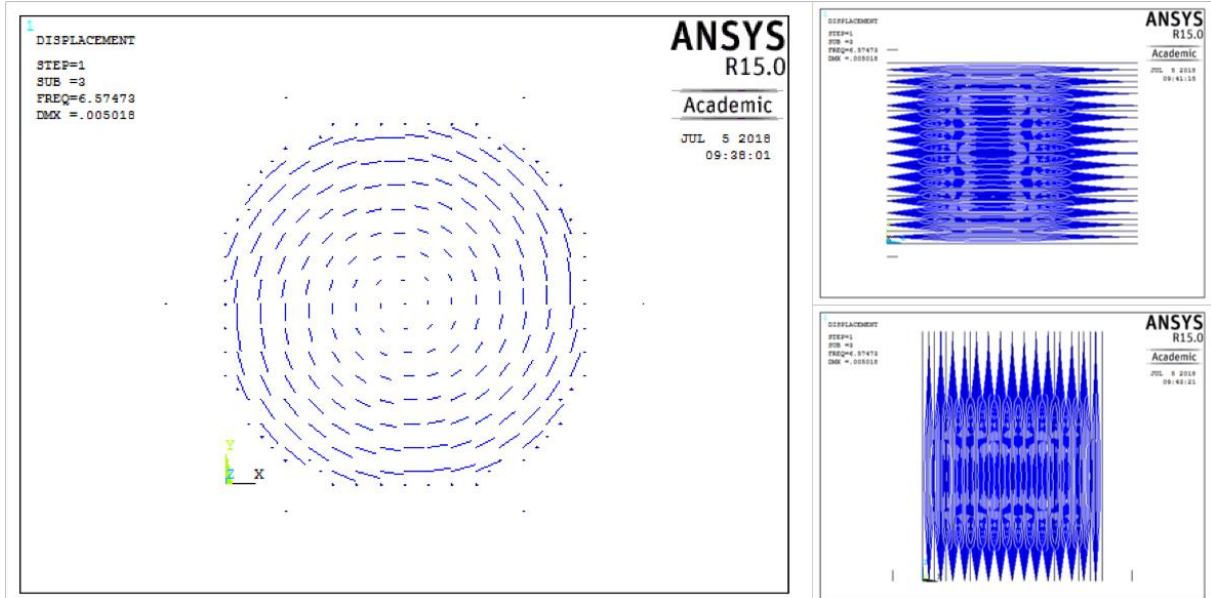
Figure 6-6: Third mode

The following image shows the fourth and fifth modes. As can be seen, in both modes the deformation only occurs in some fuel assemblies. This is due to the fact that only some sets of elements are in phase so they deform in an equal way in one mode.
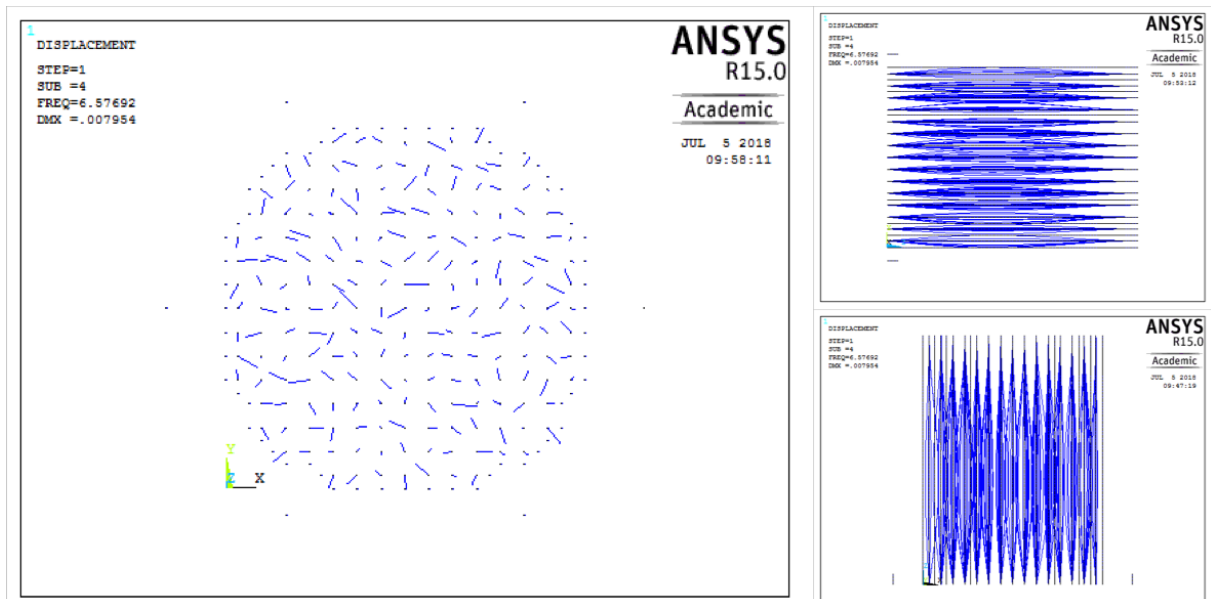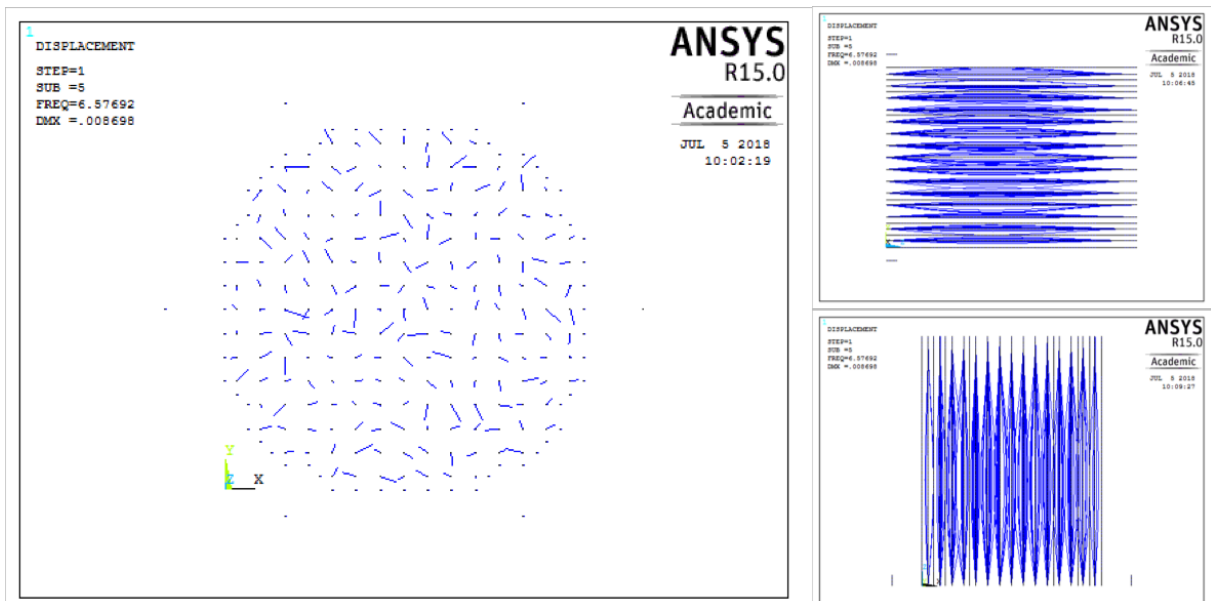
Figure 6-7: Fourth and fifth mode

The data obtained from the natural frequencies are shown in the following table,**Table 6-5**: Natural frequencies. It is observed that the natural frequencies of the first two modes are equal and from the third mode onwards the frequency changes regarding the first two modes but remains constant throughout the following modes. The reason why the first two modes have the same value is because it is a symmetric model and as it could be seen in the previous images, the first mode corresponds to the displacement in one direction and the second mode in another direction. Regarding the remaining modes, the natural frequency remains constant and this is due to the fact that, as has been observed before, displacement only occurs in some elements, these being different in each mode, which means that in each mode there is a different phase combination of the elements.

The value of the natural frequency is practically the same as in the case of the frequency of the first mode of the analyzed beam in the previous section which is completely normal as it has the same height and very similar boundary conditions. However, the value of this natural frequency is quite high for this type and dimensions of structures. The high value is due to the boundary conditions defined in the model, more specifically to the restriction of all the degrees of freedom in the upper part of the core barrel. This restriction taken in the model is a strong approximation since that part of the reactor is not totally clamped and can be affected by some rotational movements. Therefore, in order to obtain more precise results, another type of boundary condition should be implemented in this part of the model. A possible solution is to change the restriction of all the degrees of freedom by COMBIN14 element that considers the torsional spring constant. By making this change, the frequency values

would be significantly reduced and would be closer to the value observed in the neutron flux measurements (0.8 Hz) which is not definitely confirmed whether this value is due to the fuel assemblies. [35]

Table 6-5: Natural frequencies

Mode	Units	Natural frequency
1	Hz	6.5556
2	Hz	6.5556
3	Hz	6.5747
4	Hz	6.5769
5	Hz	6.5769
6	Hz	6.5769
7	Hz	6.5769
8	Hz	6.5769
9	Hz	6.5769
10	Hz	6.5769

In conclusion, the results of the analysis, apart from showing the total deformation for the four modes discussed above, show the frequencies at which there is a considerable amount of stress and deformation at determinate parts of the structure. In addition, it is observed that in all the modes obtained from the analysis, the only affected components of the whole model are the fuel assemblies. This is because the Young's module of the material that makes up those components is quite smaller than the one of the steel, there is a difference of 2 orders of magnitude, so that allows to have more elasticity and therefore more possibility of deformation to these components.

7 HARMONIC ANALYSIS

In this section, the performed harmonic analysis is discussed in order to determine the steady-state response of the structure when applying a load that varies with time. For this purpose, force with 100.000 N amplitude is applied in a frequency range of 0.1 to 10 Hz. The point of application of force

is the first node of the core barrel, that is, the one corresponding to its lowest height part. Then the graphs that represent displacements versus frequency are analyzed applying different stiffness damping values in order to choose the most appropriate value for the subsequent transient analysis, as it is a very important parameter to define in all the types of analysis. The choice of this parameter is made based on the data provided from the neutron flux fluctuations analyzes. [35]

As the elongations are the same in all the fuel assemblies due to the only one point of application of the static force and all the defined boundary conditions, only one of them is chosen to perform this analysis. The fuel assembly chosen for the analysis is located at the coordinates i=8, j=12, as can be seen in the following image:
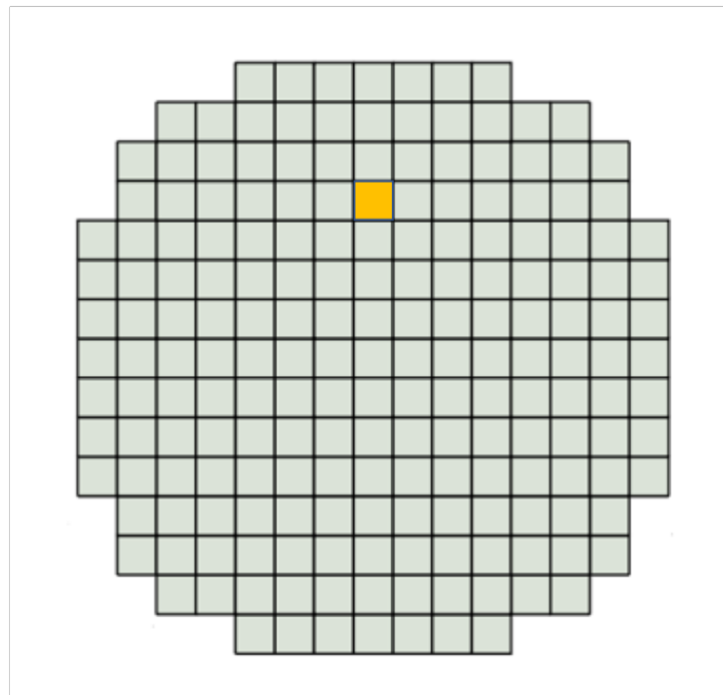
Figure 7-1: Position of the analyzed fuel assembly which is highlighted with orange color

7.1 Results

The analysis is done applying a force of 100.000 N at the point specified above in the introduction. To perform the analysis of the choice of the stiffness damping value the point of the fuel assembly that is analyzed is the one located in its middle height, that is at the height of 2.198 m. Below, the graphs obtained from the harmonic analysis for different values of stiffness damping are shown. The damping values from 0.1 to 1% are simulated and also the case that does not consider this parameter.

In the x axis of each graph the value of the amplitude of the frequency is represented and in the y axis the value of the elongation in the x direction in logarithmic scale.

- Stiffness damping = 0%
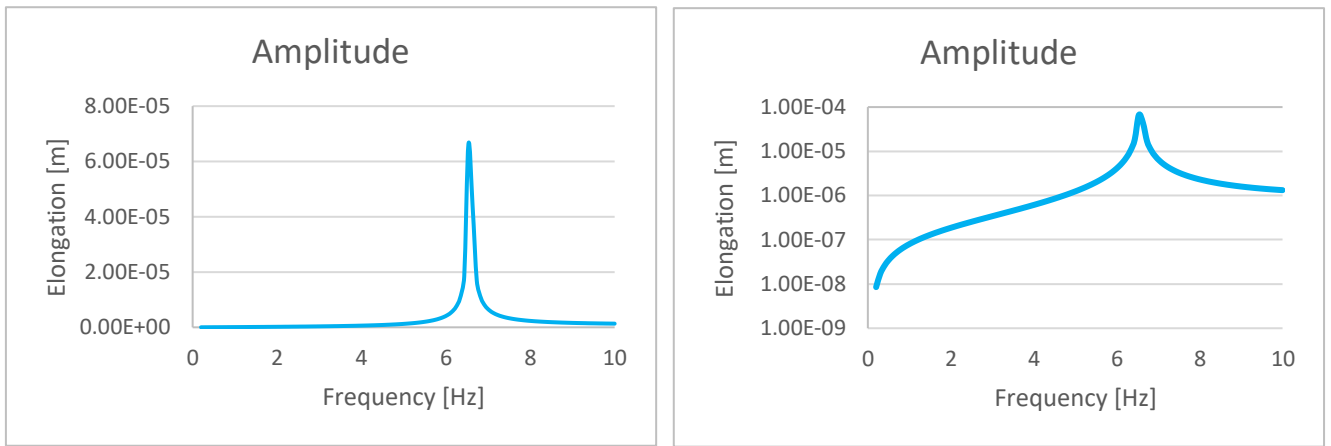
Figure 7-2: Frequency response, stiffness damping=0%, left normal scale, right logarithmic scale

- Stiffness damping = 0.1%
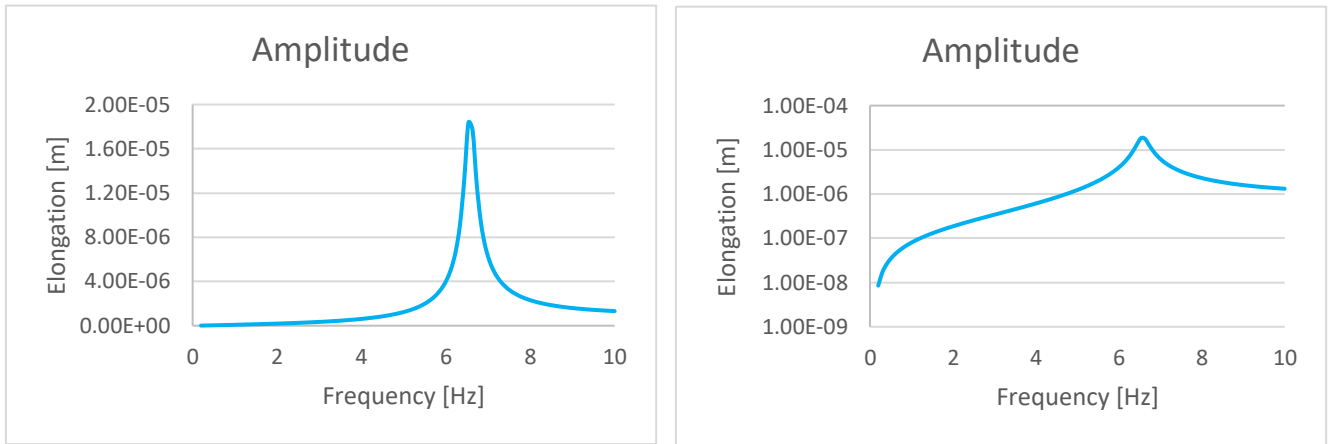
Figure 7-3: Frequency response, stiffness damping=0.1%, left normal scale, right logarithmic scale
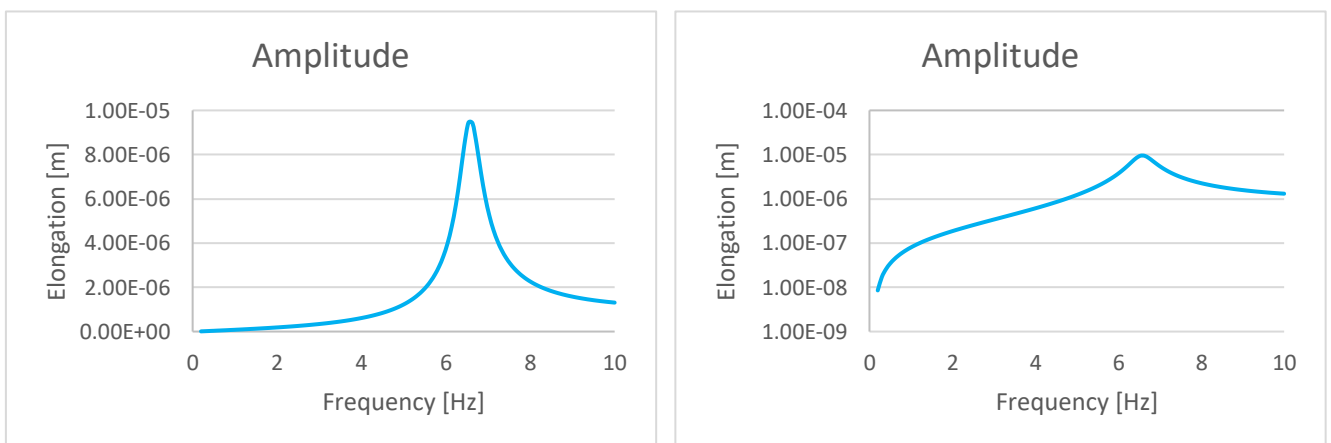
- Stiffness damping = 0.2%

Figure 7-4: Frequency response, stiffness damping=0.2%, left normal scale, right logarithmic scale

- Stiffness damping = 0.3%
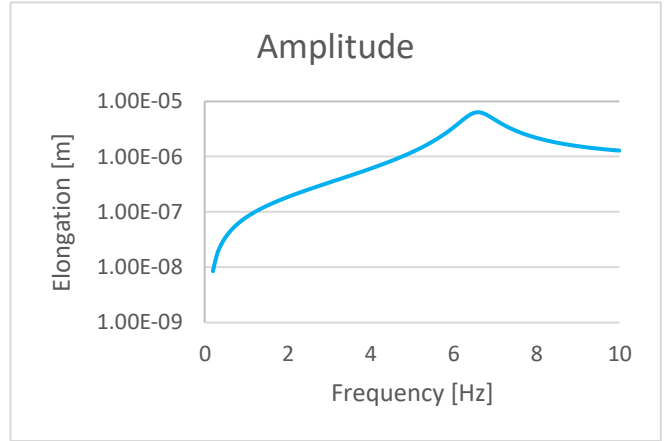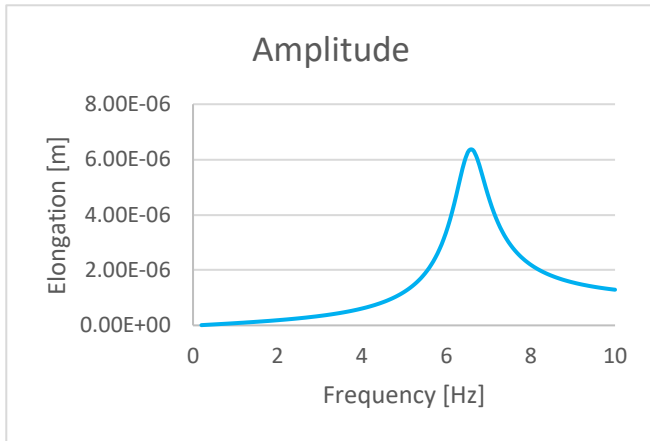
Figure 7-5: Frequency response, stiffness damping=0.3%, left normal scale, right logarithmic scale

- Stiffness damping = 0.4%
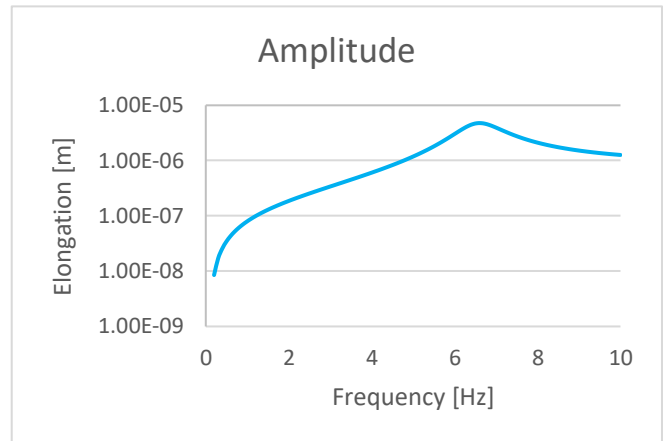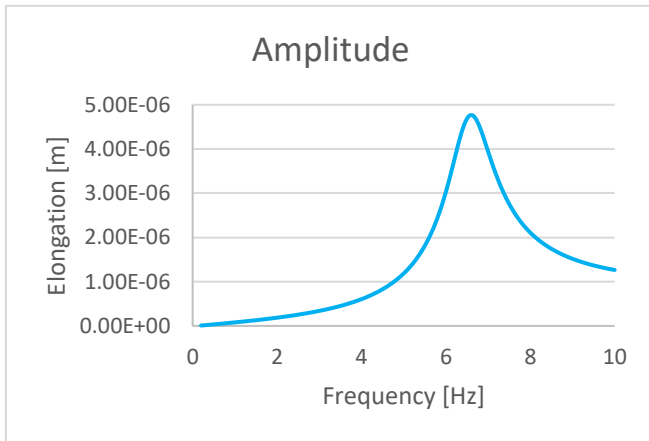
Figure 7-6: Frequency response, stiffness damping=0.4%, left normal scale, right logarithmic scale

- Stiffness damping = 0.5%
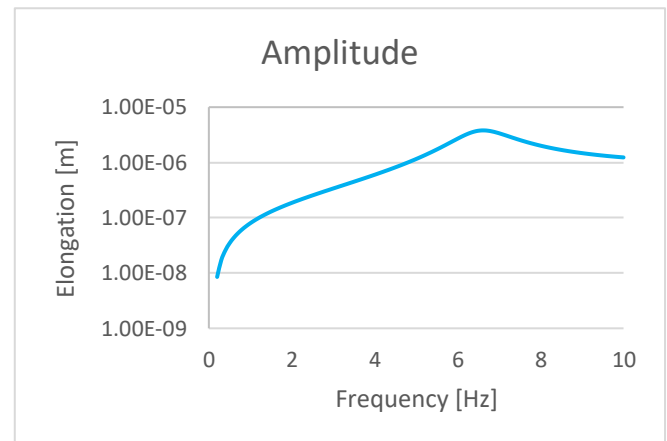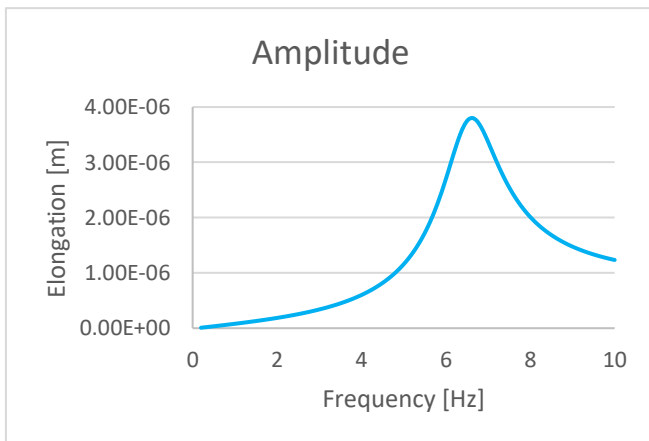
Figure 7-7: Frequency response, stiffness damping=0.5%, left normal scale, right logarithmic scale

- Stiffness damping = 1%
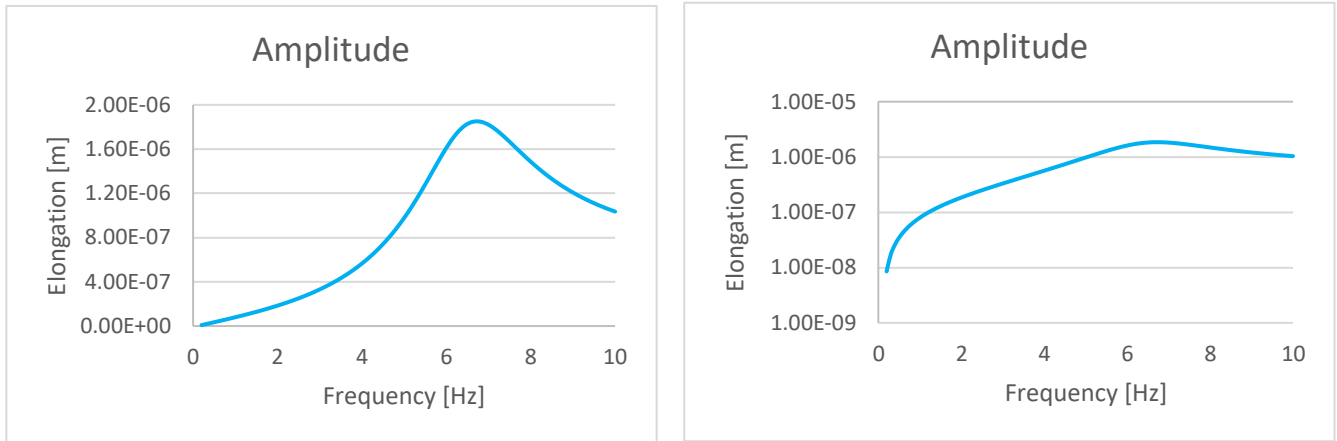
Figure 7-8: Frequency response, stiffness damping=1%, left normal scale, right logarithmic scale

It is observed that at very low frequency the amplitude is practically the same as if the force were static. When the frequency increases, the amplitude also reaches a maximum when the excitation frequency is equal to the system's own frequency, this is so-called resonance frequency. As is logical, when having zero damping the amplitude of the vibration is very large but as the damping increases, the phenomenon of resonance becomes less noticeable. As it has been seen in the modal analysis, the resonance frequency of the system is 6.5556 Hz, which is confirmed after carrying out the harmonic analysis and checking that the peaks actually appear at that frequency value.

To choose the right value of the damping, as already said above, the data obtained from the neutron flux fluctuations analysis is used. For this purpose, the following graph that represents the auto power spectral density of the nodal power density versus frequency is used.
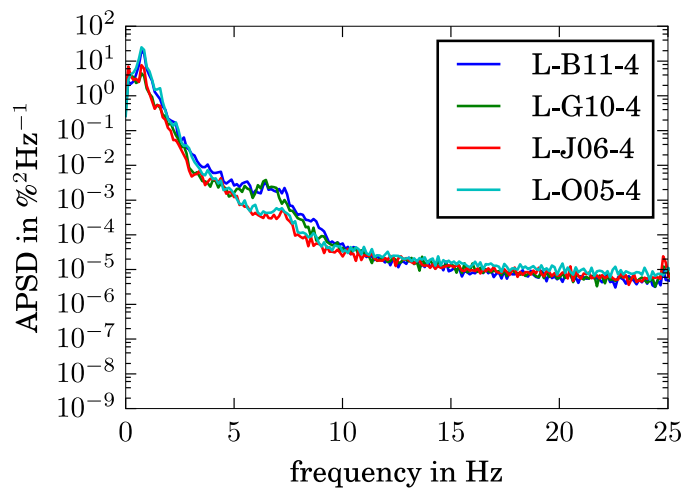
Figure 7-9: APSD of the nodal power density simulated with DYN3D as a radial comparison [35]

It is supposed that the first observed peak is due to the vibration of the fuel assembly. It is observed that the peak height is one order of magnitude. The comparison of this data with the amplitudes of vibration obtained in the performed harmonic analysis consists of checking with which value of damping the difference between the peak and the stability are of the same order of magnitude that the vibration observed in the peak corresponds to the vibration of the fuel assemblies in the neutron flux fluctuations analysis. Looking at the results obtained from the harmonic analysis in logarithmic scale it can be seen that the graph that approaches at most to this order of magnitude is the one corresponding to the value of stiffness damping of 0.2 % (see **Figure 7-4**: Frequency response, stiffness damping=0.2%, left normal scale, right logarithmic scale) and that is why this value is chosen.

8 TRANSIENT ANALYSIS

The main objective of this project is to perform an analysis under the action of time-dependent loads. Thanks to this type of analysis the dynamic response of the structure, such a time varying displacement can be determinated. In the first part of this section, the structure is analyzed under the action of a sinusoidal force. Then the analysis is done applying a white noise forces on the core barrel and on the fuel assemblies.

8.1 Sinusoidal force

To carry out the transient analysis with this type of force, it is necessary to define an input that is the function of the sinusoidal force for a defined amplitude. The equation that is used is the following:

$$F(t) = F_o \cdot \sin(\omega \cdot t)$$

Where F_o is the force amplitude and has a value of 100.000 N, and ω is the angular frequency and has a value of 0.125 Hz that is equivalent to $\frac{\pi}{4}$ rad/s. The load is applied as a ramped load, that means that its value increases gradually at each substep with the full value at the end of the step. As well as in the harmonic analysis, the point of application of the force is the node located in the lower part of the core barrel. The time chosen for the end of the load step is 20 s with an integration time step of 1 s, that is, the analysis is done for a time duration of 20 s. The equation used as input is as follows:

$$F = 100000 \cdot \sin\frac{\pi}{4} \cdot t$$

8.1.1 Results

The fuel assembly that is chosen to carry out this analysis is the same as in the harmonic analysis because the nodes number of this element are already known and since the load is applied in a single point of the core barrel, it does not matter which fuel assembly will be analyzed because the elongations are the same in all the fuel assemblies due to the boundary conditions defined in the model. It is recalled that the position of the analyzed element is i=8, j=12 as it is shown in the **Figure 7-1**: Position of the analyzed fuel assembl.

As expected, for each analyzed point, both a minimum and a maximum displacement are obtained since the load that acts on the structure is a sinusoidal force. The following table (**Figure 8-1**: Elongation with sinusoidal force) shows the minimum and maximum values of the elongations in the x direction in the nodes located at different heights of the analyzed element.

Table 8-1: Results of the elongations

Height [m]	Minimum elongation [μm]	Maximum elongation [μm]
0,01	-4.083	4.082
0,57	-3.385	3.369
1,11	-2.736	2.728
1,78	-1.941	1.953
2,19	-1.523	1.524
2,74	-1.008	1.010
3,28	-0.579	0.581
3,83	-0.255	0.255
4,37	-0.056	0.056

It is observed that the displacements obtained are of the order of micro meters. The largest elongations occur at the lowest points of the element since it is the closest point to the point where the load is applied. The higher is the height, the greater the decrease of the elongations since the point where the load is applied is farther away and has less effect.

To see the graphical representation of the load, one of the nodes located in one of the heights that appear in the previous table is chosen. In this case, the node belonging to the height of 2,19 m is chosen. The following graphical representation is obtained from the data of the substeps of this point over 20 s.
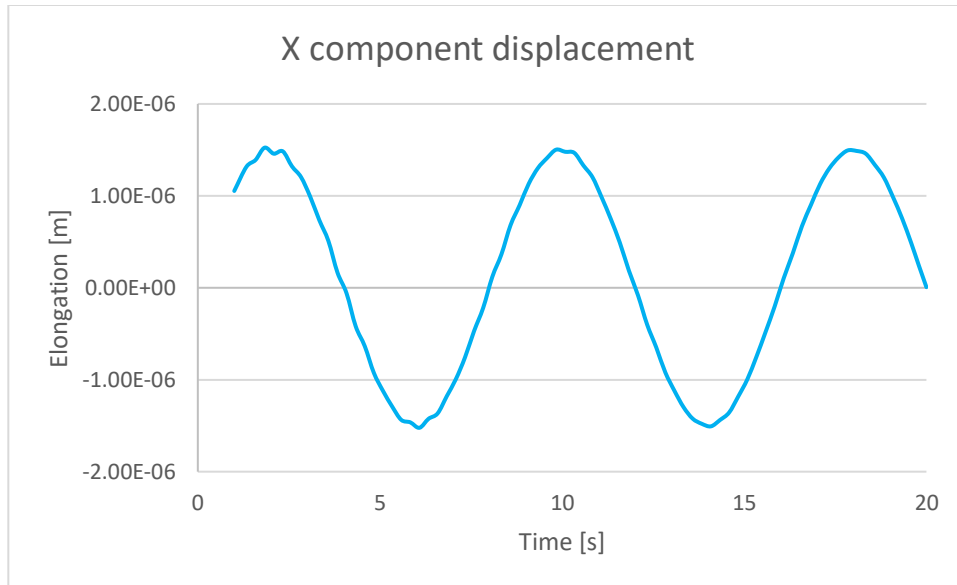
Figure 8-1: Elongation with sinusoidal force

As expected, the result of applying a sinusoidal force to the structure is to obtain a sinusoidal displacement as can be seen in the previous figure (**Figure 8-1**: Elongation with sinusoidal force). It is observed that the shape of the function is not perfect since the peaks have some imperfect lines, this may be due to the stiffness damping effect that has the purpose of reducing, restricting or preventing oscillations in an oscillatory system. [36] Its function is to receive, absorb and mitigate the force, either because it has been dispersed or the energy has been transformed so that the initial force has been reduced. In conclusion, as better the damping effect of the initial force, the lower the force received on the end point. Then, in the peaks where the imperfections are observed it means how the oscillation of the system has decayed.

8.2   White noise force

This second transient analysis is the main part of the project. It consists in analyzing the elongation that occur in certain fuel assemblies and compare them with the data published about the neutron fluctuations.

The forces act on the lower part of the core barrel and on the midpoint of each fuel assemblies in both, x and y direction. The values of the forces are obtained randomly using Gaussian distribution, it is so-called white noise force. To obtain it a Python program is used (see Appendix A). The amplitudes of the forces that act on the core barrel are the following: 1,000 N and 100,000 N. In the case of the fuel assemblies the force applied is 100 N since the coolant acts directly on the core barrel and does not on the fuel assemblies so the force on them is lower. The input file obtained from Python and used for the transient analysis contains a total of 2048 force values for each application point since this is the number of substeps.

The analysis time starts at 0.05 s and ends at 102.4 s with a time step of 0.05 s. With this a total of 2048 steps are obtained. It is convenient that the number of steps is a power of 2, as in this case 2048 = 2^{11} since the data can be utilized for Fast Fourier Transform best for powers of 2 domain. [37] Since the natural frequency has a value of 6.5556 Hz, the analysis is obtained for a total amplitude of 10 Hz. For this, it is necessary to define sample frequency of 20 Hz since the double value of the desired frequency amplitude ensure that the maximum frequency will show the complete oscillation, that is, its positive and negative variations in one period of time, as defined in the Nyquist theorem.

In this analysis, the points where the elongation in the x and y direction is analyzed are those corresponding to the fuel assembly where the detectors that measure the neutron flux are located, since the data of the elongations will be compared with the neutron flux data. [2] There are eight fuel assemblies in total where these detectors are located. As already specified in another section of this document, there is a total of six in-core detectors for each fuel assembly distributed at different heights. The following picture shows the positions where these detectors are located and, the table the approximate heights of them as estimated from the figure (**Figure 8-2**: Schematic **representation** of the detectors positions in a KWU **PWR [2]**).
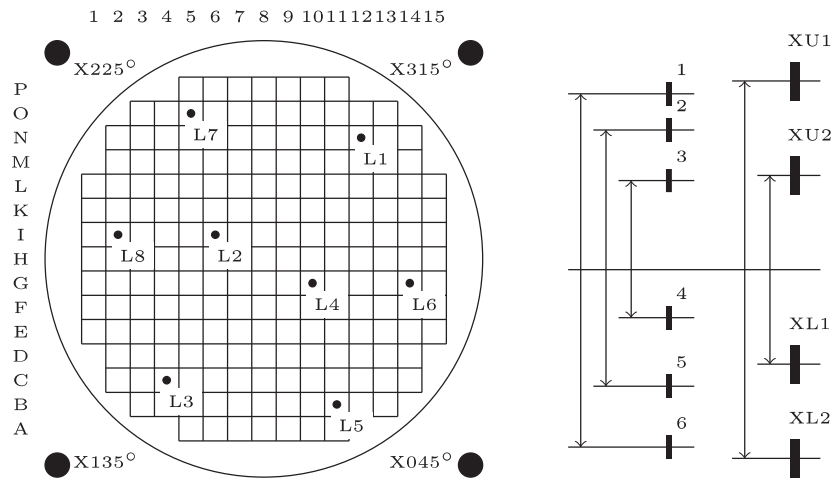
Figure 8-2: Schematic representation of the detectors positions in a KWU PWR [2]

Table 8-2: Heights of the in-core detectors

Detector	Units	Height
1	m	3.596
2	m	3.442
3	m	2.879
4	m	1.789
5	m	1.243
6	m	0.764

8.2.1 Results

The results obtained in the analysis through the ANSYS software are the elongations produced due to the applied forces in both directions, x and y, in the selected nodes. These results are processed in a Python program [38] in order to perform a frequency analysis (see Appendix B). Thus, data of auto power spectral density, coherence and phase are obtained as a function of frequency. [2] The auto power spectral density shows how the signal's power is distributed over different frequencies from which it is formed. Coherence can only take values between 0 and 1. When the coherence value is 0 for a considered frequency, it means that the signals compared at this frequency are uncorrelated. On the contrary, two signals are correlated at a considered frequency when the value of the coherence is

1. For values greater than 0 and less than 1, it means that the signals contents at this frequency have each a correlated fraction. The phase is the phase angle between the correlated fractions. [37]

In the first place, the results obtained for different fuel assemblies at points located at the same height each one of them, are shown applying the force amplitude indicated above. The height chosen to show the results is the one corresponding to the 4th detector, that is at 1.789 m (**Table 8-2**: Heights of the in-core detectors). The fuel assemblies from which data are taken are shown in the following image (**Figure 8-3**: Positions of the analyzed fuel assemblies) where the yellow fuel assembly is the reference one [2]:
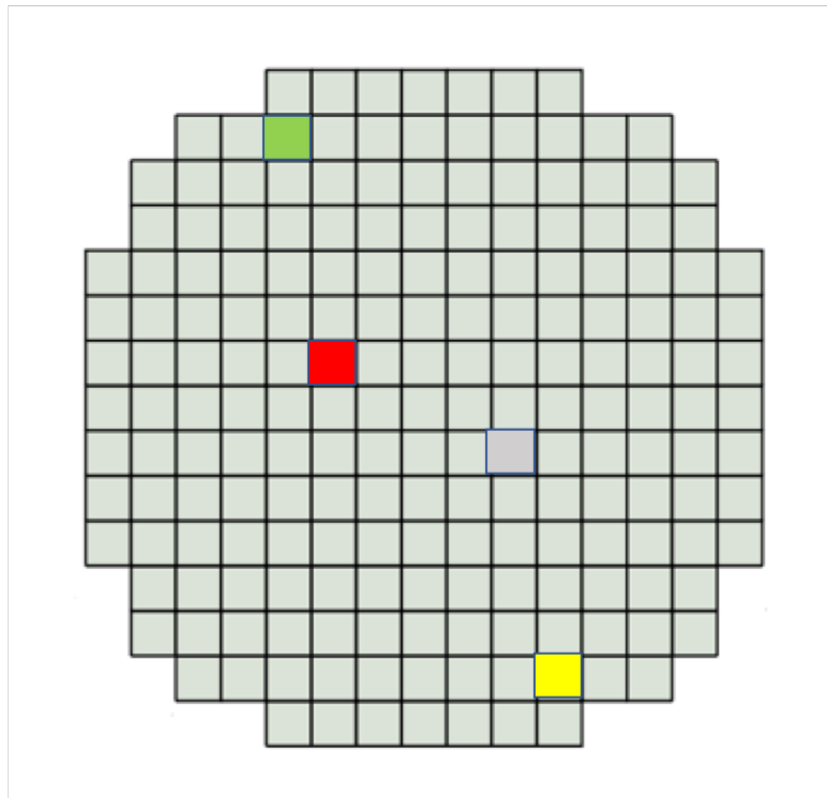
Figure 8-3: Positions of the analyzed fuel assemblies

Next, the results obtained by applying a force of 100,000 N on the core barrel and 100 N on the fuel assemblies are shown in both directions, x and y:
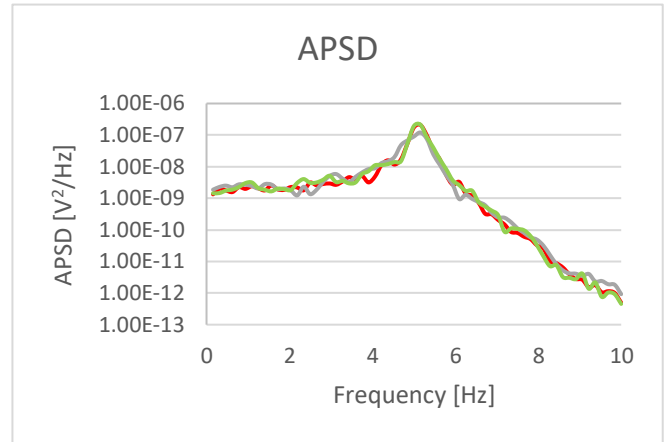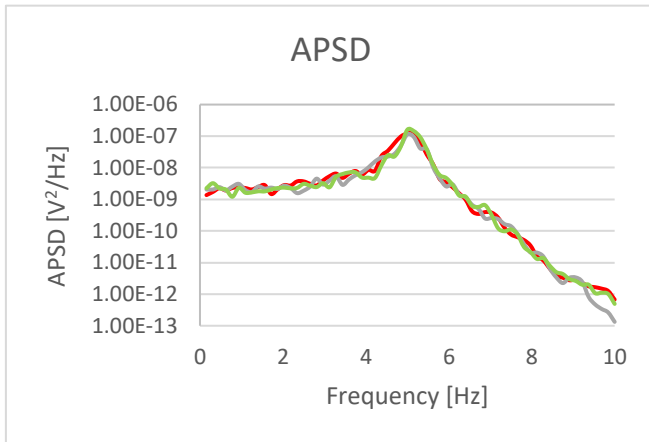
Figure 8-4: Auto power spectral density (100,000 N on CB, 100 N on FAs): left x direction, right y direction (radial)
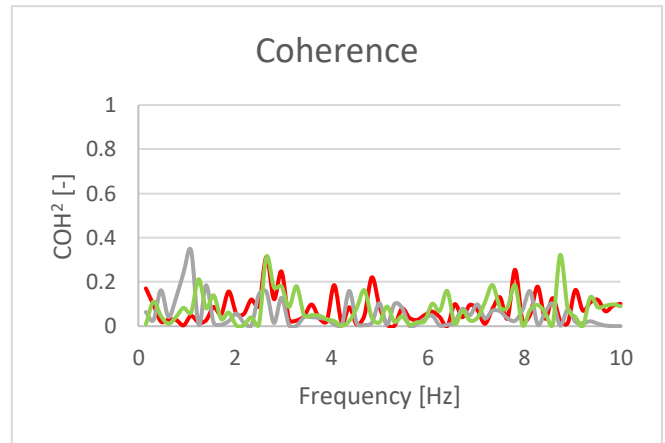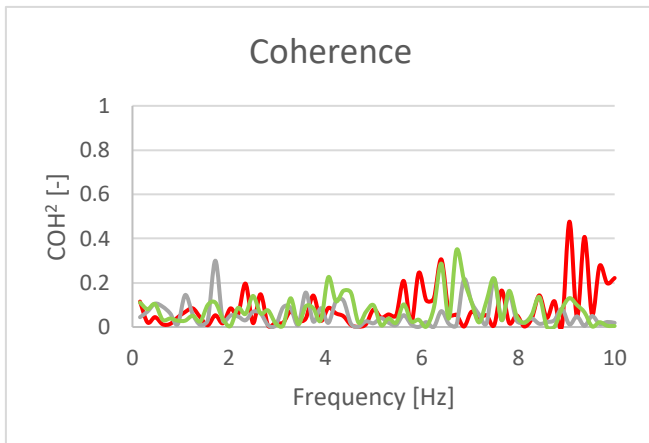
Figure 8-5: Coherence (100,000 N on CB, 100 N on FAs): left x direction, right y direction (radial)
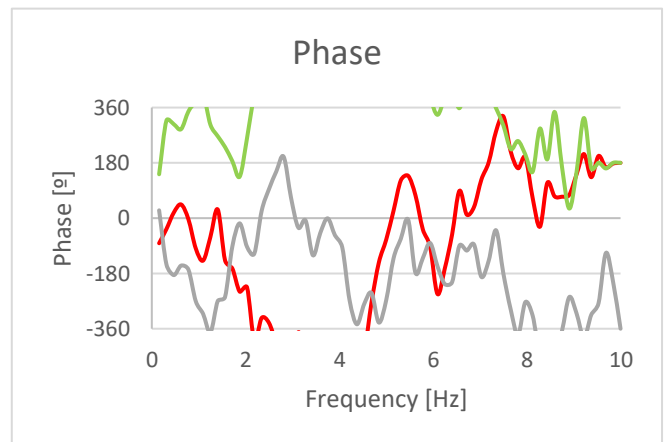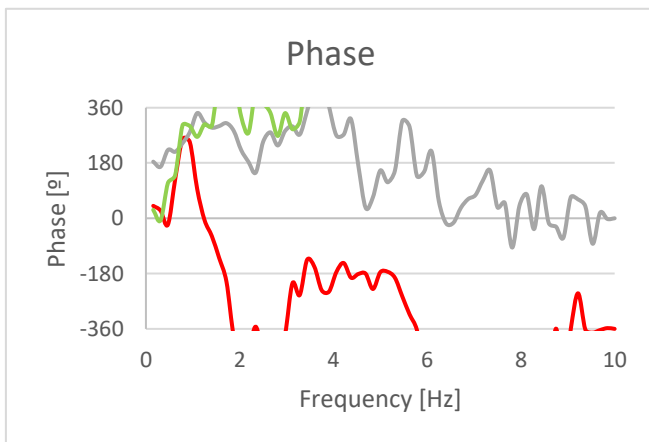
Figure 8-6: Phase (100,000 N on CB, 100 N on FAs): left x direction, right y direction (radial)

In general, the results for the forces in both directions are similar due to the boundary conditions defined in the model. In addition, the results for the different fuel assemblies also present certain similarity in terms of the behavior they experience.

The APSD shows the higher value for an approximate frequency of 5Hz. This means that for this frequency value more signal fluctuations occur. However, this frequency does not coincide with the resonance frequency of the model (6.2876 Hz) and this may be explained with further analyses.

Looking at the coherence graph, it is observed that the values of it are very low, almost zero. This means that the fuel assemblies at this position are uncorrelated with the one that is taken as a reference. Therefore, the graph that shows the phases is not relevant in this case because in the absence of coherence the phases will fluctuate independently.

In summary, after applying the force of this magnitude and checking the results, it can be said that the fuel assemblies show a chaotic behavior.

Next, the results obtained for the data for only one fuel assembly at different heights are shown. In this case, the fuel assembly that is analyzed is the same one that is taken as reference in the previous case (yellow square in **Figure 8-3**: Positions of the analyzed fuel assemblies). The heights where the results are analyzed are those corresponding to detectors 1, 4 and 6 (**Table 8-2:** Heights of the in-core detectors) taking as reference the number 1 (yellow color) located at a height of 3.596 m, as can be seen in the next image:

Figure 8-7: Positions of the analyzed detectors of one fuel assembly

Next, the results obtained by applying a force of 100,000 N on the core barrel and 100 N on the fuel assemblies are shown in both directions, x and y:
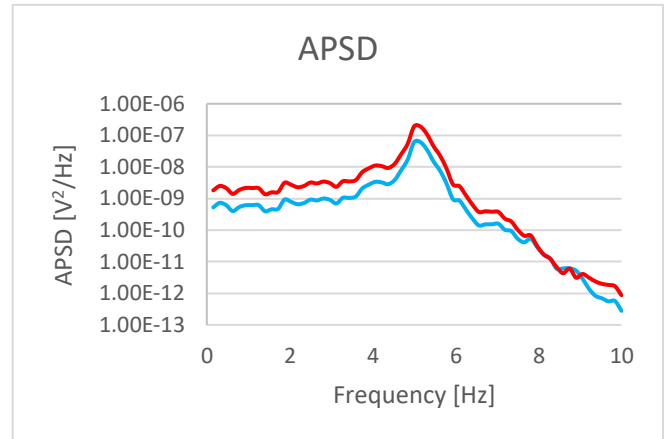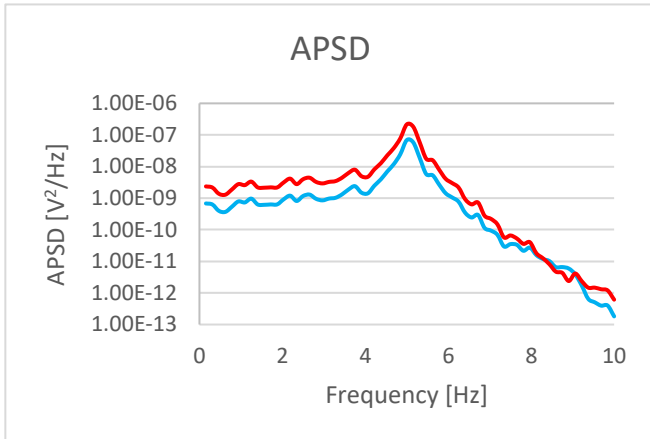
Figure 8-8: Auto power spectral density (100,000 N on CB, 100 N on FAs): left x direction, right y direction (axial)
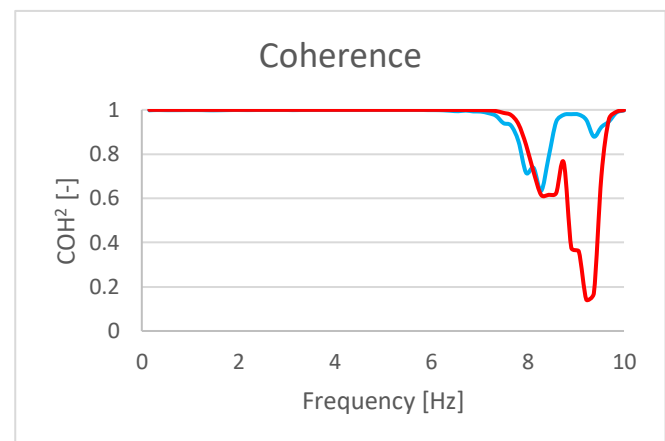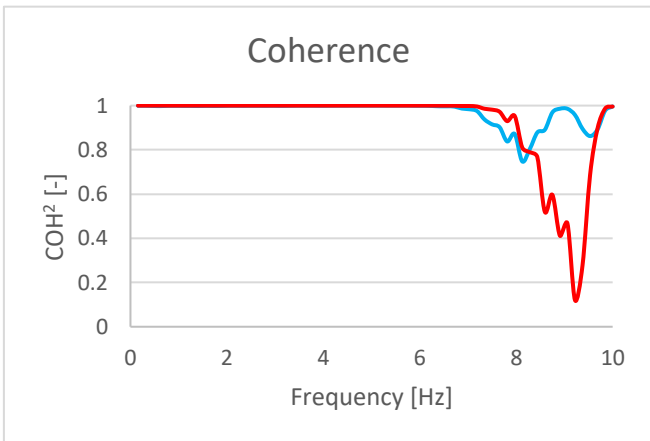
Figure 8-9: Coherence (100,000 N on CB, 100 N on FAs): left x direction, right y direction (axial)
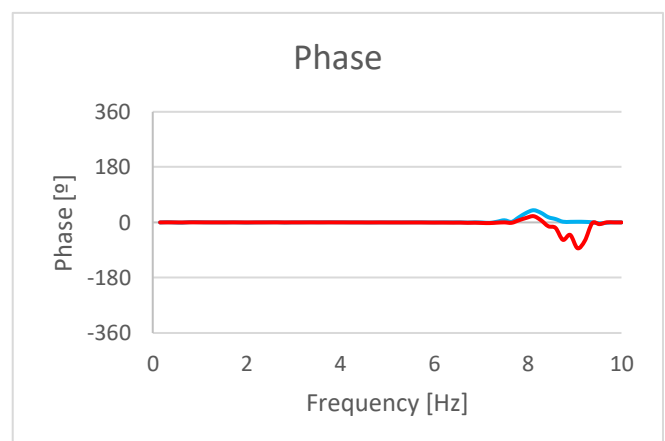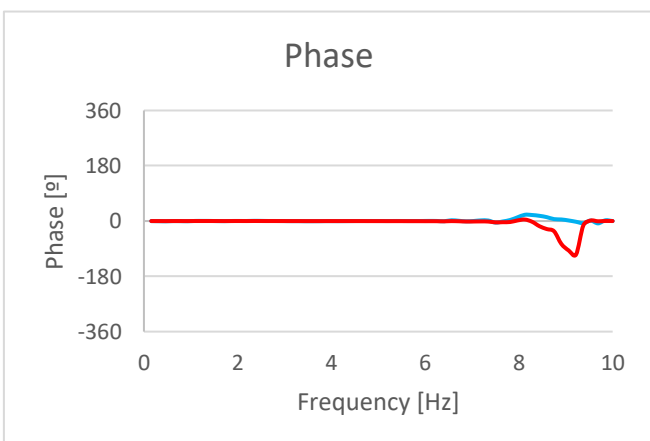
Figure 8-10: Phase (100,000 N on CB, 100 N on FAs): left x direction, right y direction (axial)

As in the previous case, the results in both directions, x and y, are very similar. However, in the results at the different analyzed heights, small differences can be observed.

Analyzing the results of the coherence, both points present a constant line in the range on 1 which means that the different points at different heights of one fuel assembly are correlated. However, the red line, which corresponds to the closest point to the point take as a reference (see **Figure 8-7**: Positions of the analyzed detectors of one fuel assembly), experiences an unexpected downward peak for an approximate value of frequency of 9 Hz. This peak means that the point at this frequency in uncorrelated.

The results of the graphs of the phases have value of 0 which means that the points belonging to the analyzed fuel assembly are in phase. As well as in the case of the coherence, at the frequency value of 9 Hz there is an unexpected downward peak that indicates that at this point has different behavior.

The same analysis has been made but for a force value of 1,000 N on the core barrel and 100 N of the fuel assemblies. The results of this combination of forces are practically the same as the analyzed above since the combination of forces is not enough to observe a big change. The results obtained for this case can be found attached in the appendix C.

After carrying out these two analyses, another one is performed applying the same force on the core barrel (100.000 N) but without applying any force to the fuel assemblies. This is made in order to see the effect that the applied force on the core barrel has on the fuel assemblies.

First, the results obtained for the points analyzed at different positions of the fuel assemblies at the same height are shown (see **Figure 8-3**: Positions of the analyzed fuel assemblies).
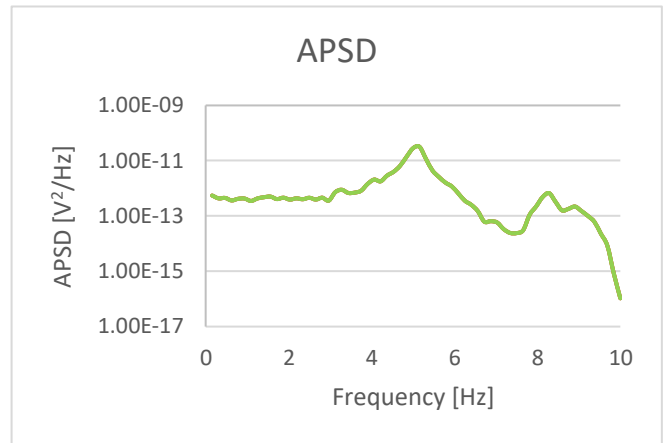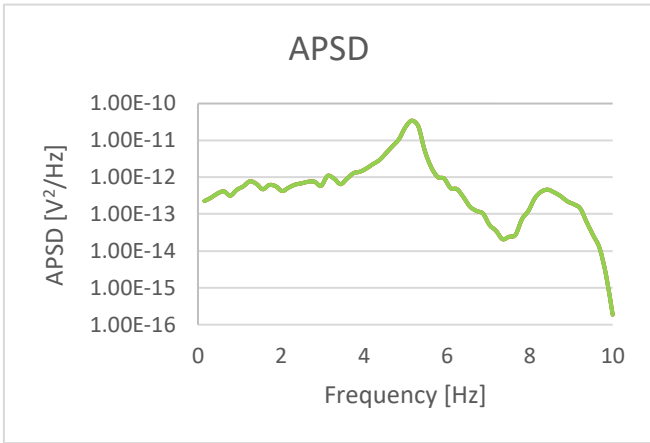
Figure 8-11: Auto power spectral density (100,000 N on CB, 0 N on FAs): left x direction, right y direction (radial)
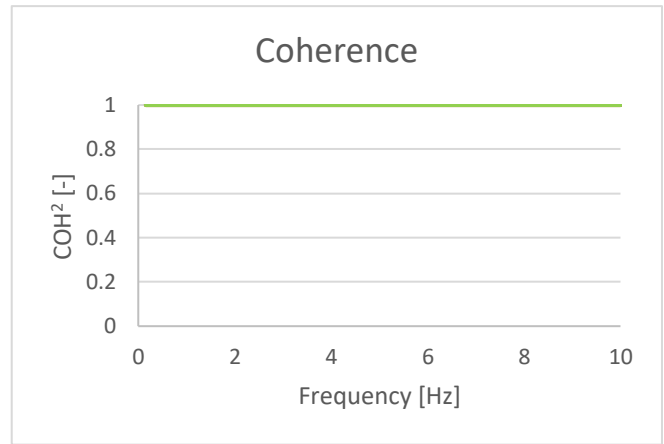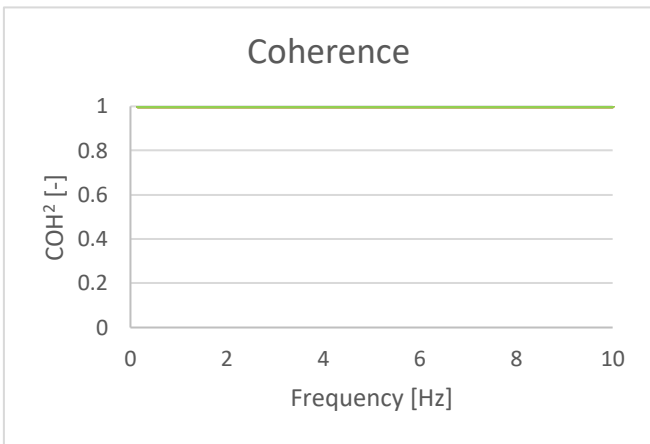
Figure 8-12: Coherence (100,000 N on CB, 0 N on FAs): left x direction, right y direction (radial)
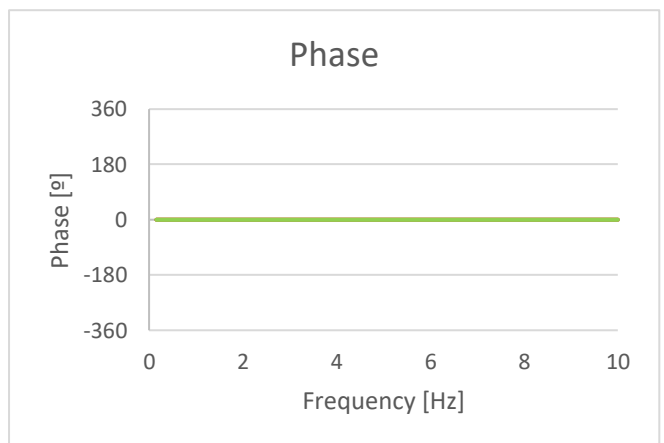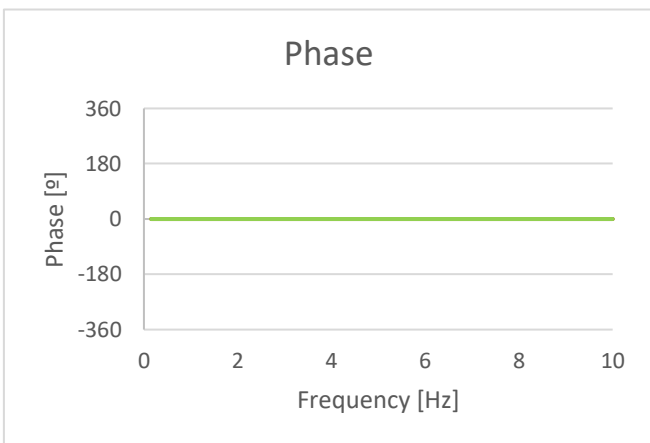
Figure 8-13: Phase (100,000 N on CB, 0 N on FAs): left x direction, right y direction (radial)

As in the previous cases, the results for both directions are very similar. Despite analyzing points of three different fuel assemblies, it is possible to see only one line of one color in all the graphics. This is because all the analyzed fuel assemblies behave in the same way regarding to the reference fuel assembly. A possible explanation to this behavior is that, as already mentioned in previous sections, the assumption of clamping the core barrel in its upper part is quite strong approximation. For this reason and because of the rigid region in its lower part, the core barrel is a fairly rigid element so it fails to transmit enough force to the fuel assemblies so that its behavior would be altered in different way.

Looking at the APSD graph, it shows the same result as in the previous cases, that is, the peak is at an approximate frequency of 5 Hz.

The coherence has a value of 1 during the 10 Hz of the analysis, which means that all the fuel assemblies are correlated.

After seeing that the phase is 0, that is, all the elements are in phase, it means that all the fuel assemblies act simultaneously in the same way. This behavior makes sense because, as previously mentioned, the force that acts on the core barrel is barely transmitted in different way to the rest of the elements of the model.

Below are the results obtained for the same forces as in the previous case but analyzing different points located at different heights of a single fuel assembly (see **Figure 8-7**: Positions of the analyzed detectors of one fuel assembly, **Table 8-2**: Heights of the in-core detectors)
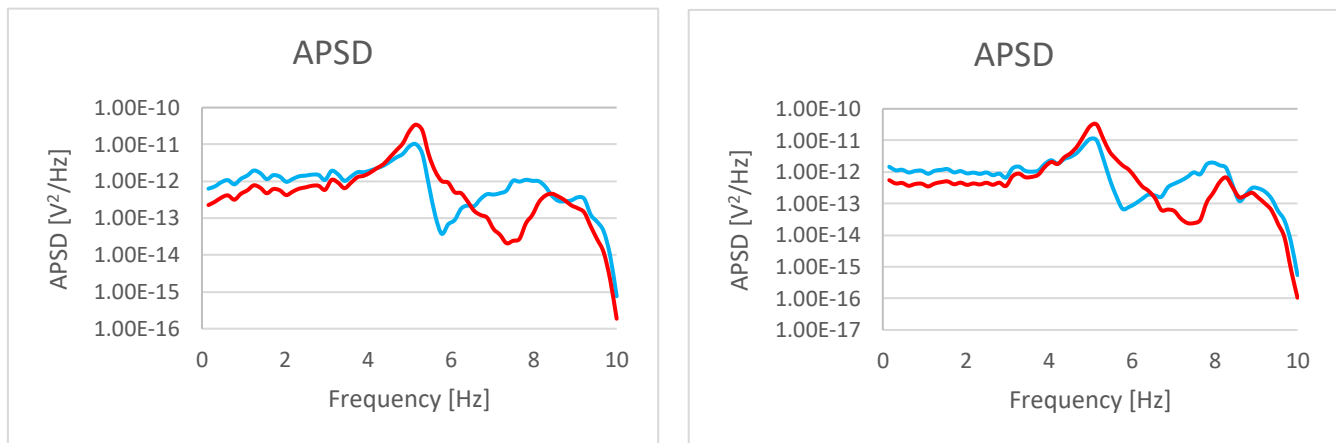
Figure 8-14: APSD (100,000 N on CB, 0 N on FAs): left x direction, right y direction (axial)
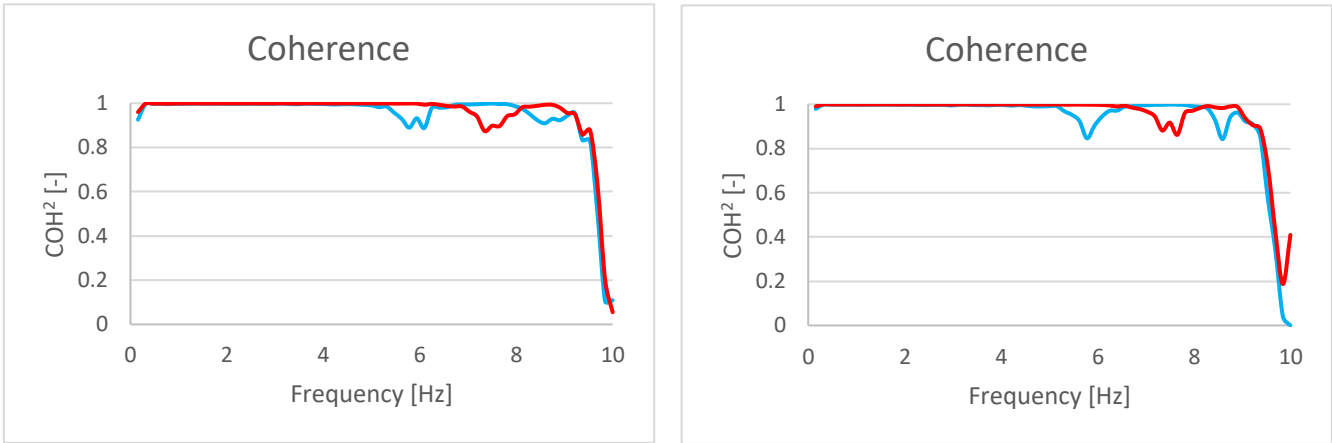
Figure 8-15: Coherence (100,000 N on CB, 0 N on FAs): left x direction, right y direction (axail)
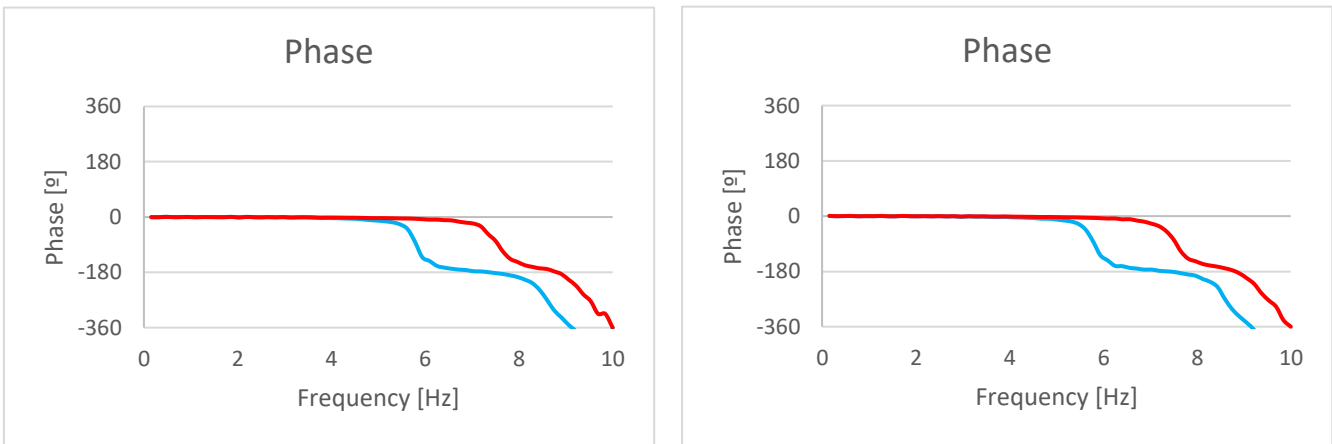
Figure 8-16: Phase (100,000 N on CB, 0 N on FAs): left x direction, right y direction (axial)

The situation where the same behavior for both directions is repeated as in all the previous cases. In general terms, the behavior obtained when analyzing different points of the same element is similar as when analyzing different fuel assemblies. However, the lines in the coherence and phase graph are not completely straight, which means that the fuel assembly does not act equally at different heights.

At first, all the points are correlated, that is, they are completely related with the reference point. As early as the resonance frequency of the system is reached, small fluctuations are observed that in the highest frequencies reach a value close to 0 which means that the points at that moment have no relation between each other.

The points analyzed are initially in phase, that is, they have the same behavior. As in the case of the coherence, when reaching the resonance frequency, those points ceases being in phase and there is one instant when they act in an opposite way.

9 COMPARISON WITH NEUTRON FLUX FLUCTUATIONS

In this section, the comparison of the results obtained from the transient analysis after applying random forces to the mechanical structure of the reactor core, with the data of a neutron flux fluctuations study is made. The results chosen to make the comparison are those corresponding to the following forces: 100,000 N on the core barrel and 100 N on the fuel assemblies. The reference data to make the comparison are obtained from the measurements of the in-core detectors in a KWU Vor-Konvoi PWR at the end of cycle. [35]

9.1 Different fuel assemblies at the same height

In order to make the comparison, the following data of neutron flux fluctuations are available. First, the data of the in-core detectors in radial position, which means points at the same height of different fuel assemblies, are discussed (see **Figure 9-1:** Coherence and phase of measured neutron flux fluctuations **[35] Figure 9-2:** Auto power spectral density of measured neutron flux fluctuations [35]).

The first graph (**Figure 9-2:** Auto power spectral density of measured neutron flux fluctuations [35]) shows the APSD data where a pronounced peak of approximately one order of magnitude at 0.8 Hz, which may correspond to the resonance frequency of the fuel assemblies, is observed. In the next picture (**Figure 9-1:** Coherence and phase of measured neutron flux fluctuations [35]), high value of coherence is observed at the same value of frequency as the peak in the APSD data.
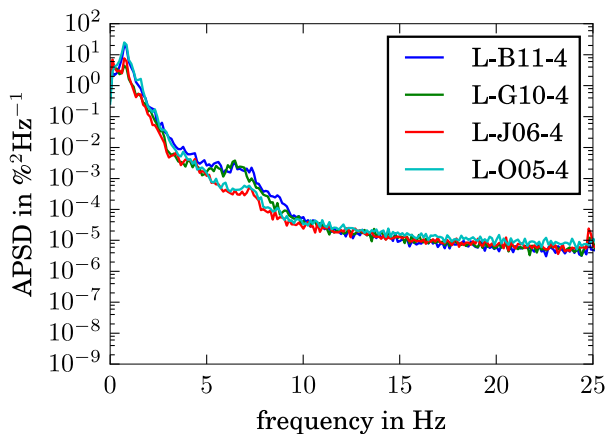
Figure 9-2: Auto power spectral density of measured neutron flux fluctuations [35]
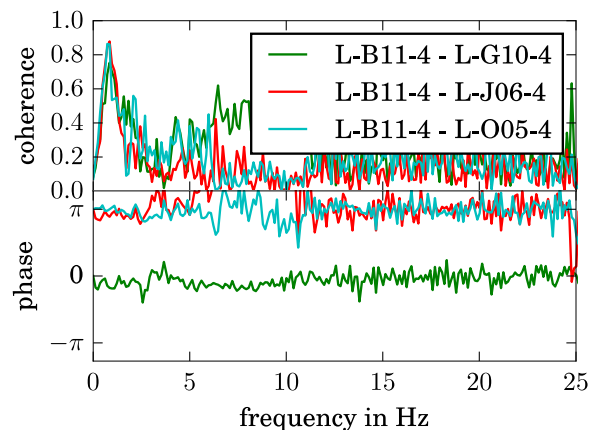
Figure 9-1: Coherence and phase of measured neutron flux fluctuations [35]

Comparing the first graph with the results obtained in the analyses carried out in this project, the peaks in the APSD do not coincide in the same frequency value. As can be seen in **Figure 8-4**: Auto power spectral density (100,000 N on CB, 100 N on FAs): left x direction, right y direction (radial), this peak

appears at higher frequency which may be due to the considered simplifications and defined boundary conditions.

Analysing the coherence values, it is observed that these do not coincide in both case since, as can be seen in **Figure 8-5**: Coherence (100,000 N on CB, 100 N on FAs): left x direction, right y direction (radial), the coherence values in the performed analysis are low, which is the opposite of the results of neutron flux fluctuations. The same applies to the phase comparison, looking at the results shown in **Figure 8-6**: Phase (100,000 N on CB, 100 N on FAs): left x direction, right y direction (radial), no similarities are observed between these results and de neutron flux fluctuation data. As specified above, this may be due to the simplifications considered in this model.

9.2 Same fuel assembly different heights

The following figures show the measurement data of the in-core detectors in axial position, that is, different points at different heights of the same fuel assembly (see **Figure 9-3:** Coherence and phase of measured neutron flux fluctuations [35] **Figure 9-4:** Auto power spectral density of measured neutron flux fluctuations [35]).

As well as in the previous section, the first graph (**Figure 9-4:** Auto power spectral density of measured neutron flux fluctuations [35])shows a pronounced peak of approximately one order of magnitude at 0.8 Hz. In the frequency range of 0-2 Hz the next graph shows a coherence of almost 1 and phase of 0. [34]
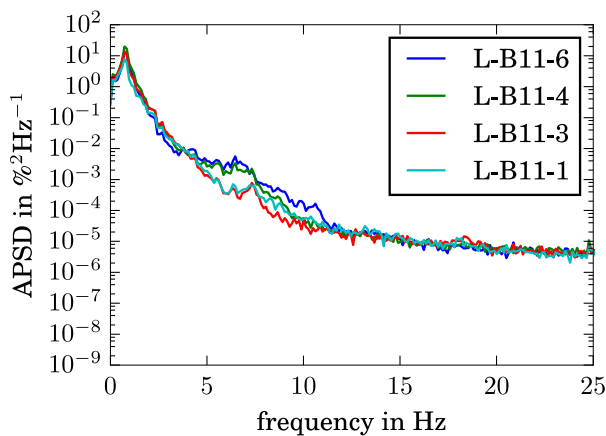
Figure 9-4: Auto power spectral density of measured neutron flux fluctuations [35]
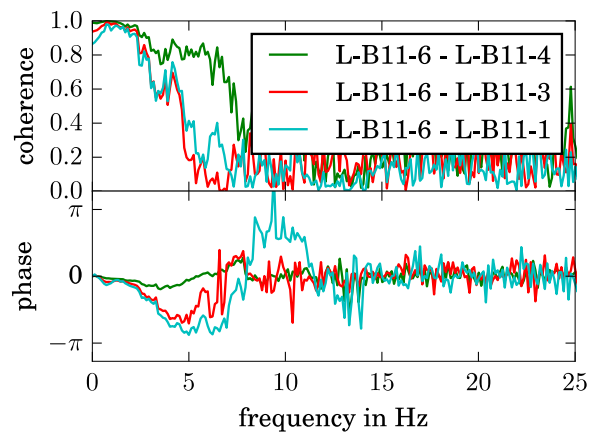
Figure 9-3: Coherence and phase of measured neutron flux fluctuations [35]

Comparing with the data obtained in this project (see **Figure 8-8**: Auto power spectral density (100,000 N on CB, 100 N on FAs): left x direction, right y direction), the pronounced peak in the APSD graph does not occur at the same frequency as in the neutron flux data but it has been already mentioned that this is due to the taken simplifications and the defined boundary conditions of this model, and further modifications and analyses may explain it.

However, the behaviour of the different points of one fuel assembly is equal in both, in the data obtained in the neutron flux measurements and in the analysis carried out with ANSYS. It is observed that the different points are initially correlated but after approximately 7 Hz the value of coherence decreases (see **Figure 8-9**: Coherence (100,000 N on CB, 100 N on FAs): left x direction, right y direction (axial)). In both cases, all the points located at different heights of the fuel assembly are initially in phase (see **Figure 8-10:** Phase (100,000 N on CB, 100 N on FAs): left x direction, right y direction (axial)).

10 CONCLUSION AND OUTLOOK

The objective of this work was to implement a geometrically simplified ANSYS model of the nuclear reactor core that could predict the dynamical behaviour of the fuel assembly collective. The reason is that a more accurate knowledge about the movement of the fuel assemblies can help explaining the phenomenon of the neutron flux fluctuations. The finite elements model designed in this project considers certain elements that are part of the reactor core, as core barrel, fuel assemblies, core shroud and core stops. In order to achieve the objective, different types of analyses have been carried out.

The first step was the implementation of the geometrical model of the structure. The fuel assemblies, with its corresponding core shroud, and the core stops were created as beam elements and the core barrel as a pipe element. Different boundary conditions have been defined. On the one hand, the restriction of degrees of freedom in the upper part of the structure and in the core stops has been applied. On the other hand, the rigid region between the shroud and the core barrel at the mid height, as well as, between the core barrel and the fuel assemblies at the bottom part of these elements, has been generated. In addition, the possibility of contact between different elements of the model has been created.

The second part of the project consists of performing complementary analyses to the main analysis that allow to know in more detail the designed model. In order to confirm the validity of the model, a comparison between static and transient analysis has been done. Secondly, a modal analysis of the complete model and of a single element that forms a fuel assembly has been carried out. The purpose of these analyses was to know the vibration modes and the natural frequencies of the structure. Then, a harmonic analysis that has allowed to know the value of the stiffness damping has been performed. Finally, two transient analyses, one with a sinusoidal force and the other with a white noise force, have been carried out. The results show the elongations produced in the fuel assemblies when subjected to the effect of a force acting on the core barrel.

Finally, the results of the last transient analysis have been performed in terms of auto power spectral density, coherence and phase in order to compare then with the results of the neutron flux fluctuations data. After the comparison of the results of the axial analyses, a certain similarity in the behaviour of the different points of the fuel assembly is observed in both data. However, in the case of the results of the radial points, a similar behaviour is not observed, which may be due to certain simplifications taken in the design of this model.

As future research lines it is proposed the inclusion of some additional elements in the design that are part of the nuclear reactor core, such as reactor pressure vessel or spacers. In general, it is also important to design the model with as less simplification and as much details as possible to resemble as much as possible to the real design of the reactor core. This includes the definition of more materials for the different elements that are part of the model since all of them have different material properties. It is interesting to try different type of contact conditions between the fuel assemblies which may ensure that all of them are coupled. Another interesting aspect would be to design the fuel assemblies in a more detailed way, including the fuel rods and the guide tubes that for part of them, as it is done in the detailed model of one fuel assembly which is available in the disposal of the chair (WKET). In order to simulate in a more realistic way the forces that act on the structure, it is recommended to calculate and apply vortex forces of the core barrel.

BIBLIOGRAPHY

[1] I. A. E. Agency, „Nuclear Power Reactors in the World," Vienna, 2006.

[2] M. Viebach, N. Bernt, C. Lange, D. Hennig und A. Hurtado, „On the influence of dynamicall fuel assembly deflections on the neutron noise level," 2017.

[3] ANSYS Inc., ANSYS Mechanical APDL Element Reference, 2013.

[4] European Nuclear Society, „European Nuclear Society," 28 11 2016. [Online]. Available: https://www.euronuclear.org/info/encyclopedia/n/npp-reactor-types.htm. [Zugriff am 10 5 2018].

[5] A. Ziegler und H.-J. Allelein, Reaktortechnik, Physikalisch-technische Grundlagen, Springer Vieweg, 2013.

[6] U. Rohde, M. Seidl, S. Kliem und Y. Bilodid, „Neutron noise observations in German KWU built PWRs and analyses with the reactor dynamics code DYN3D," 2018.

[7] „Wikipedia," Wikipedia, 6 7 2018. [Online]. Available: https://de.wikipedia.org/wiki/Kraftwerk_Union. [Zugriff am 8 7 2018].

[8] H. Union Iberduero, „Central Nuclear Trillo".

[9] „Nuclear Power," 2018. [Online]. Available: https://www.nuclear-power.net/nuclear-power-plant/nuclear-reactor/core-barrel/. [Zugriff am 10 5 2018].

[10] „Nuclear Power," 2018. [Online]. Available: https://www.nuclear-power.net/nuclear-power-plant/nuclear-fuel/. [Zugriff am 10 5 2018].

[11] D. Olander und A. Motta, Light Water Reactor Materials, Draft, 2009.

[12] „Wikipedia," 7 1 2015. [Online]. Available: https://en.wikipedia.org/wiki/Core_shroud. [Zugriff am 10 5 2018].

[13] E. Siwss Federal Nuclear Safety Inspectorate, „Swiss Federal Nuclear Safety Inspectorate ENSI," [Online]. Available: https://www.ensi.ch/en/. [Zugriff am 10 5 2018].

[14] M. Hubbell, The Fundamentals of Nuclear Power Generation, Author house, 2011.

[15] „Wikipedia,“ 5 6 2018. [Online]. Available: https://en.wikipedia.org/wiki/Noise_(signal_processing). [Zugriff am 14 5 2018].

[16] Universidad Central, „Ruido en comunicaciones,“ 2018. [Online]. Available: https://ruido.wikispaces.com/RUIDO+EN+COMUNICACIONES. [Zugriff am 14 6 2018].

[17] V. Torres, „5 Minutos de Matlab,“ 2011. [Online]. Available: http://5minutosdematlab.blogspot.com/. [Zugriff am 14 6 2018].

[18] A. Calle Gonzalez, „Problémática del ruido neutrónico,“ 2013.

[19] R. Altar und C. Dubi, „Modeling Zero Power Reactor Noise and Neutron Count Distribution: A Stochastic Differential Equations Approach,“ 2017.

[20] Y. Semchenkov, V. Mil'to, A. Pinegin und B. Shumskii, „Analysis of neutron flux noise due to coolant parameter fluctuations in a VVÉR core,“ 2007.

[21] RSK-Stellungnahme, „DWR-Neutronenflussschwankungen,“ 2013.

[22] Principios del método de análisis por elementos finitos.

[23] „Wikipedia,“ 30 June 2018. [Online]. Available: https://en.wikipedia.org/wiki/Finite_element_method. [Zugriff am 5 July 2018].

[24] O. Zienkiewicz, The finite elements method: its basis and fundamentals.

[25] *ANSYS Mechanical APDL Product Launcher 15.0.*

[26] Notepad++, 2016. [Online]. Available: https://notepad-plus-plus.org/.

[27] A. Wanninger, M. Seidl und R. Macian-Juan, „Mechanical analysis of the bow deformation of a row of fuel assemblies in a PWR core,“ 2017.

[28] W. Oldekop, Druckwasserreaktoren für Kernkraftwerke, Verlag Karl Thiemig.

[29] U. Gerhard, „Leichtwasser-Kernreaktor mit einer kühlwasserführenden Kernumfassung,“ 1985.

[30] „Arcelor Mittal,“ [Online]. Available: http://sections.arcelormittal.com/fileadmin/redaction/2-Products_Services/1_Product_Range/ES-EN-IT/Coefficients.pdf. [Zugriff am 30 5 2018].

[31] National Institute of Standards and Technology, „Libro del Web de Química del NIST, SRD 69,“ 2017. [Online]. Available: https://webbook.nist.gov/chemistry/. [Zugriff am 31 5 2018].

[32] ANSYS Inc., ANSYS Contact Technology Guide, 2014.

[33] E. Altstadt, G. Grunwald, M. Scheffler und F. Weiss, Analytische Modellierung mechanischer Schwingungen von Primärkreiskomponenten des Druckwasserreaktors WWER-440 mit Finiten Elementen, 1997.

[34] A. Tikhonov und A. Samarskii, Equations of Mathematical Physics, New York: Dover Publications, 1990.

[35] M. Viebach, C. Lange, N. Bernt, M. Seidl, D. Hennig und A. Hurtado, „Simulation of Low-Frequency PWR Neutron Flux Fluctuations".

[36] „Wikipedia," 9 5 2018. [Online]. Available: https://es.wikipedia.org/wiki/Amortiguamiento. [Zugriff am 11 7 2018].

[37] J. Bendat und A. Piersol, Random Data. Analysis and Measurement Procedures, Wiley, 2011.

[38] *Python Software Foundation. Python Language Reference, version3.0.*

LIST OF FIGURES

LIST OF TABLES

A PYTHON FILE TO GENERATE FORCES

```python
import numpy as np
import matplotlib.pyplot as plt

# arrays for loads
tsteps = 2048 # 10s with 10Hz + instant at 0s
nfa = 193 # 59 nodes

#delt = 0.01 # one hundredth of a second
delt = 0.1 # one tenth of a second

# gaussian noise
np.random.seed(1)
sigfa = 1.e2 # 100N
faxload = np.random.normal(0.0,sigfa,(tsteps,nfa))
fayload = np.random.normal(0.0,sigfa,(tsteps,nfa))
np.savetxt("faxload_%.1fN_%d.txt"%(sigfa,tsteps),faxload,delimiter='
',fmt='%15.7e')
np.savetxt("fayload_%.1fN_%d.txt"%(sigfa,tsteps),fayload,delimiter='
',fmt='%15.7e')

sigcb = 1.e3 # 1000N
#sigcb = 1.e5
cbxyload = np.random.normal(0.0,sigcb,(tsteps,2))
np.savetxt("cbxyload_%.1fN_%d.txt"%(sigcb,tsteps),cbxyload,delimiter='
',fmt='%15.7e')
```

B PYTHON FILE TO ANALYSE RESULTS

```python
import numpy as np
from scipy import signal

import matplotlib.pyplot as plt

"""frequency analysis preparation"""
fs= 20.0  # sample frequency
seqw = 128
seqo = 64
foup = 128
window = signal.get_window('hamming', seqw)

bfilt, afilt = signal.butter(3, .25, 'low')

"""specification of the displacement file, the signals of it to be
used, and the reference signal"""

# assuming that the displacement time-series are stored in seperate
files for each considered node and for X and Y
#!!!!!!!!! counting starts from ZERO == 0 !!!!!!!!!!!!!!!!
# first  position: node number
# second position: X, Y
signals = [ \
[4526,"X"],\
[4513,"X"],\
[4505,"X"],\
[14071,"X"],\
[4525,"X"],\
[4526,"X"]
\
]

refsignal = 0 # first one of signals is the reference for calculating
the coherence and phase

"""read all simulated data and
   calculate relative fluctuations about respective mean value in
percents"""
pname = "response" # project name
data=[]
meandata=[]
dataname=[]
for s in signals:
    dname="%d%s"%(s[0],s[1])
    dat = np.loadtxt("%s_%s.txt"%(pname,dname), skiprows=1,
usecols=[1])
    meandat=np.mean(dat)
    data.append(dat)
    meandata.append(meandat)
    dataname.append(dname)

"""frequency analysis and saving of results"""
```

```python
headerline = 'freq in Hz      APSD in %^2/Hz  COH^2 in -      Phase in
deg'# header

def freqanalysis(data1,data2):
    f,pxx  = signal.csd(data1,data1,fs,window,seqw,seqo,foup) # signal
with itself
    _, coh = signal.coherence(data1,data2,fs,window,seqw,seqo,foup) #
signal with reference
    _, pxy = signal.csd(data1,data2,fs,window,seqw,seqo,foup) # signal
with reference
    pha = np.unwrap(np.angle(pxy))*180.0/np.pi
    return np.transpose(np.array([f[1:], pxx[1:], coh[1:], pha[1:]]))

datafreq=[]
for i in np.arange(len(signals)):
    datafreqi = freqanalysis(data[i],data[refsignal])

np.savetxt("%s_freqana_signal%s_refsignal%s.txt"%(pname,dataname[i],dat
aname[refsignal]),\
                datafreqi, fmt='%15.7e', delimiter=' ',
header=headerline)
    datafreq.append(datafreqi)

plt.figure()
for i in np.arange(len(datafreq)):
    plt.plot(datafreq[i][:,0],datafreq[i][:,1])
plt.yscale("log")
plt.figure()
for i in np.arange(len(datafreq)):
    plt.plot(datafreq[i][:,0],datafreq[i][:,2])
plt.figure()
for i in np.arange(len(datafreq)):
    plt.plot(datafreq[i][:,0],datafreq[i][:,3])
plt.show()
```

C RESULTS TRANSIENT ANALYSIS, FORCES: 1,000 N ON CB, 100 N ON FA

Different FAs at the same height for each one:
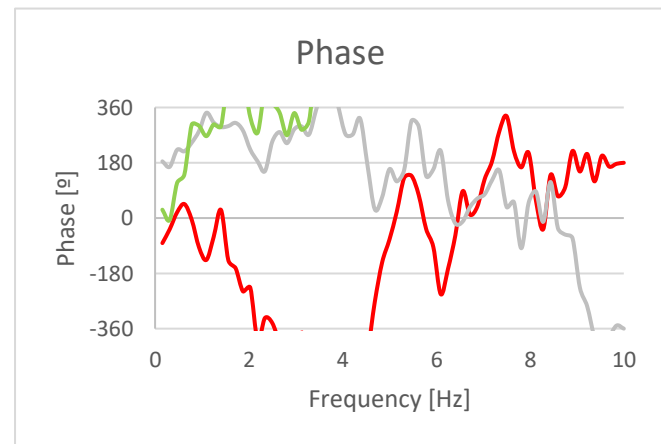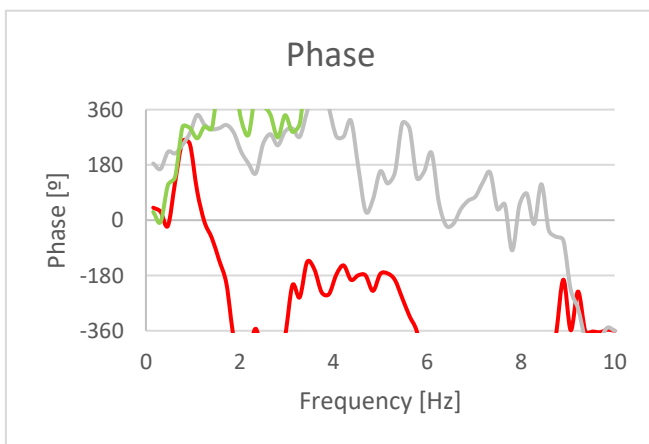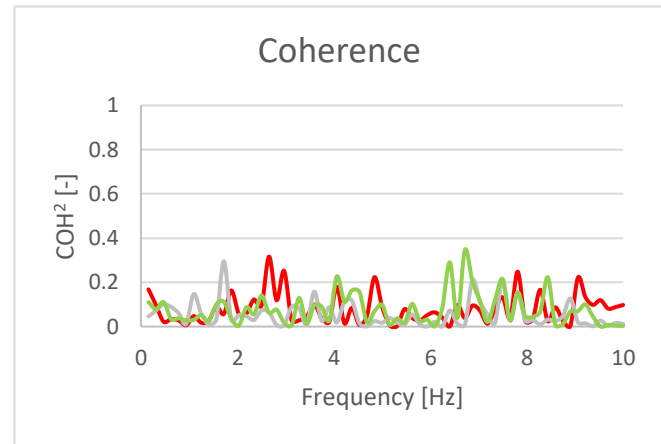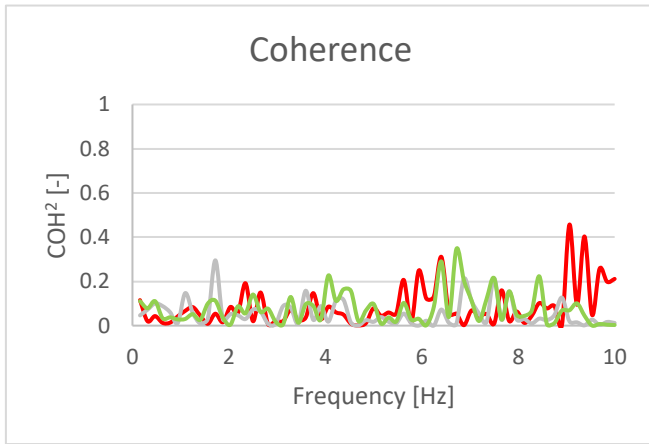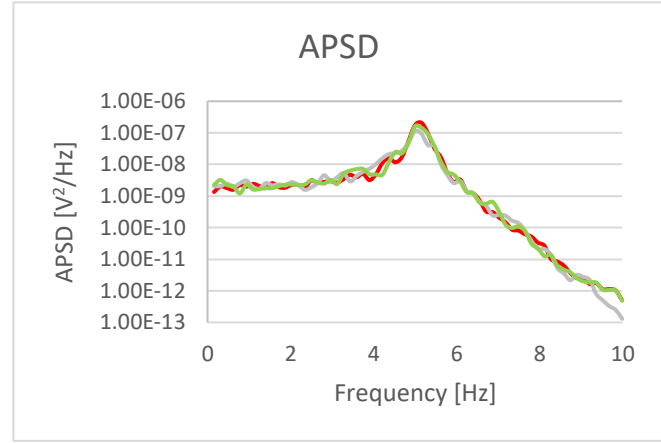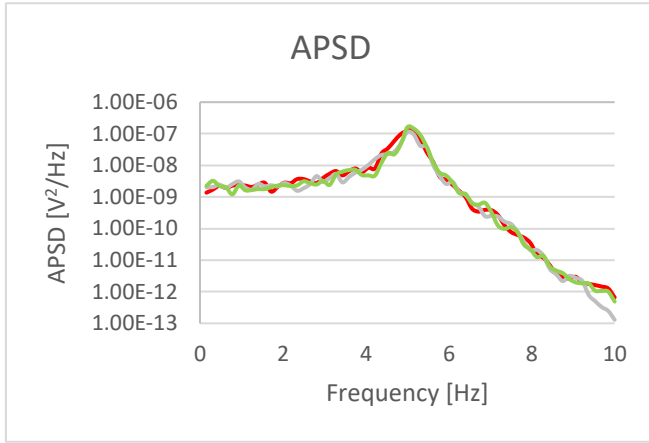
Same FA at different heights:
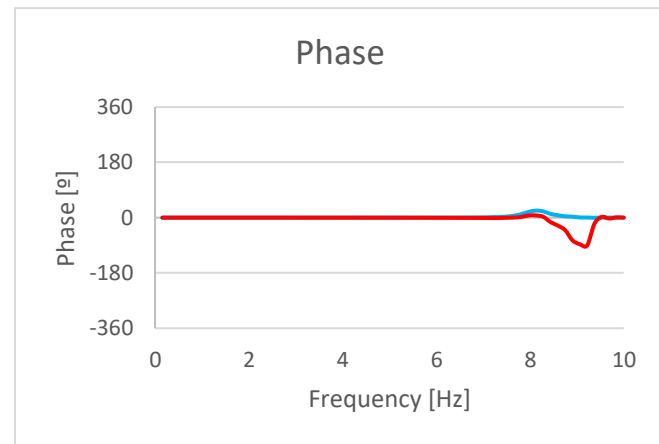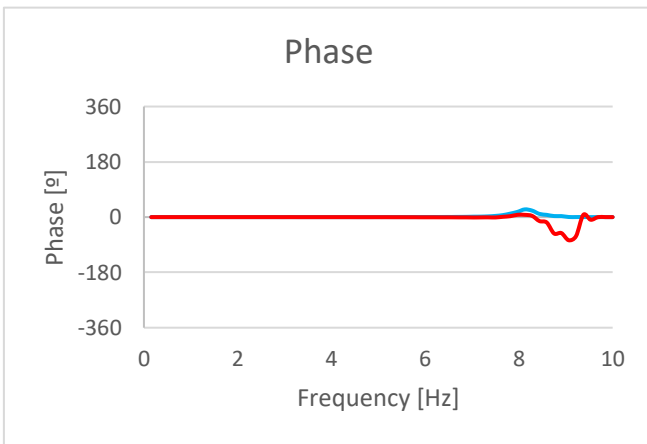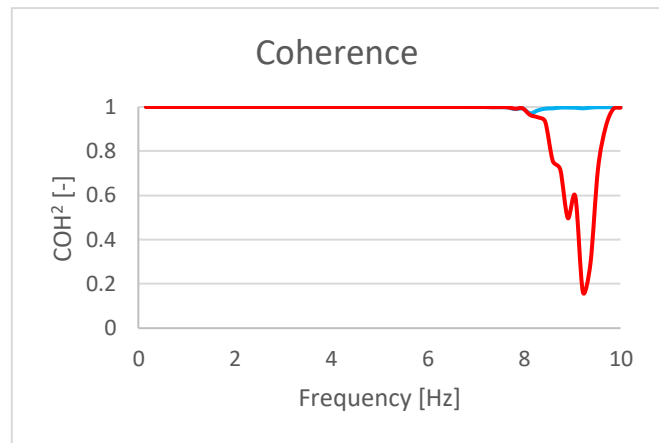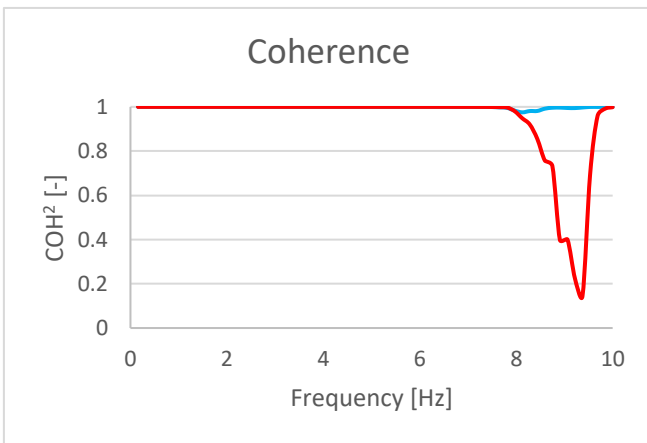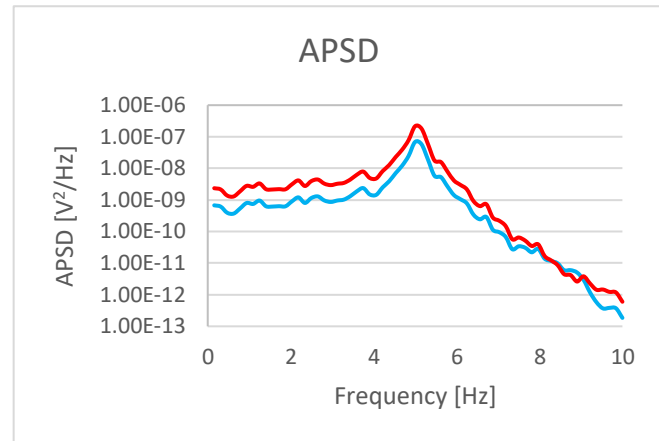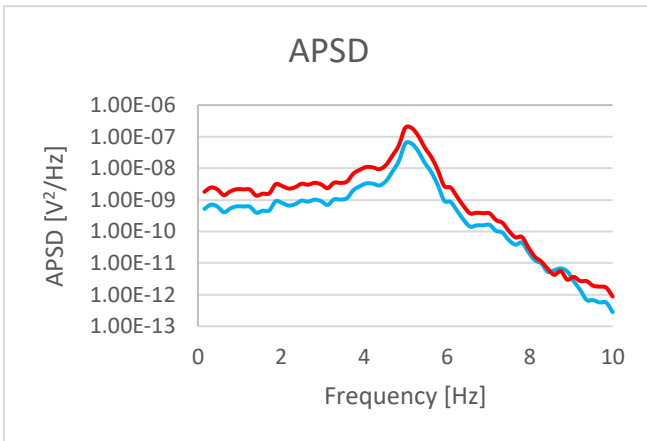
D DIFFERENT BOUNDARY CONDITION ON THE CORE BARREL

In this part of the document, addition analyses with different boundary conditions are attached.

As already specified throughout the document, some assumptions are strong approximations that can be modified and thus be closer to the reality. This is the case of the core barrel that has been considered as a clamped element that is totally fixed in its upper part without any possibility of movement or rotation in any direction. This is not totally true since this element can experience some movements like rotations.

As mentioned in the document, the restriction that is applied in the model can be substituted with another boundary conditions such as COMBIN14 element or by modifying the restricted degrees of freedom. In this section all the analyses are performed changing the boundary condition of the core barrel that up to the moment had all the degreed of freedom restricted, by the restriction only in the displacements and releasing the rotations. With this, the structure is not as rigid as in the previous case. The rest of the boundary conditions remain the same.

D.1 Modal analysis

The first analysis that is done with these new boundary conditions is the modal analysis of the whole model in order to see the different modes and the natural frequencies. This section references to the section corresponding to the modal analysis with the initial boundary conditions of the model (Full structure model).

The values of the obtained frequencies are shown in the next table (**Table D-1:** Natural frequencies different boundary conditions on the core barrel). It is observed that the natural frequency with the new conditions decreases considerably, as expected, to the value of 1.5670 Hz.

Table D-1: Natural frequencies different boundary conditions on the core barrel

Mode	Units	Natural frequency
1	Hz	1.5670
2	Hz	1.5670
3	Hz	2.6285
4	Hz	6.5769
5	Hz	6.5769
6	Hz	6.5769
7	Hz	6.5769
8	Hz	6.5769
9	Hz	6.5769
10	Hz	6.5769

The first two modes, as in the analysis with the initial boundary conditions, correspond to the elongation in x and y direction. The difference observed in this new case is that the elements only remain fixed in the upper part of the structure, producing an increasingly larger displacement in the lower part of the elements.
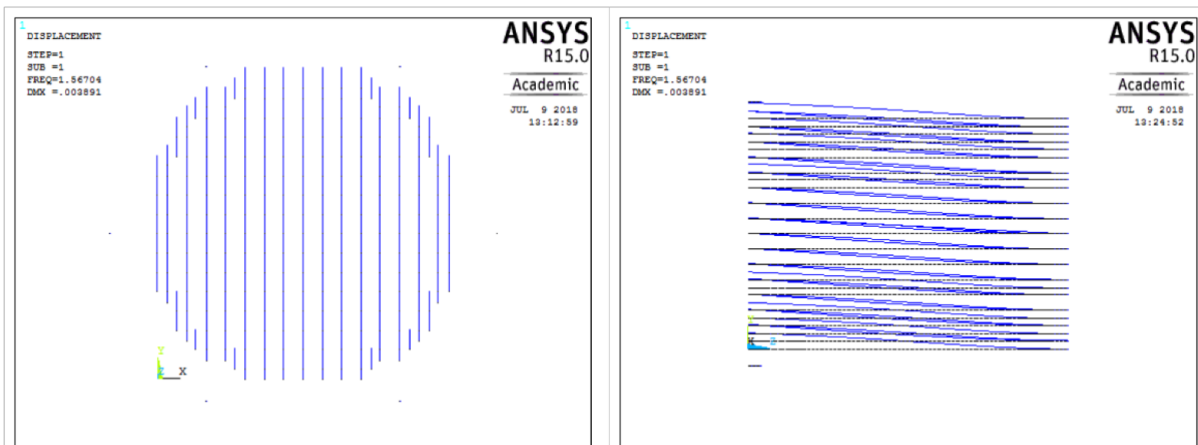
Figure D-1: First mode, model with new boundary conditions
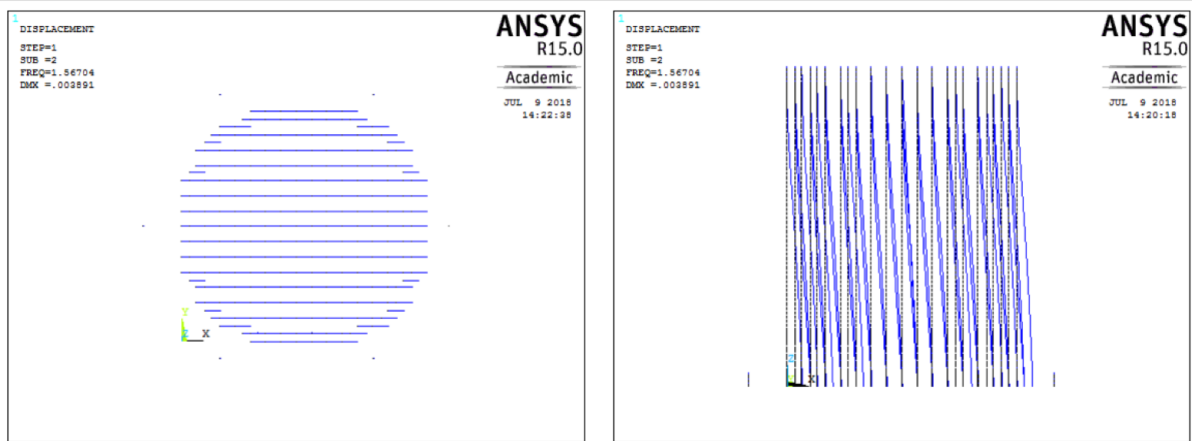
Figure D-2: Second mode, model with new boundary conditions

The third mode shows an unexpected phenomenon where all the elements move in the same direction in such a way that looking the trajectory of its displacements, a circle is observed from the top view. As in the first two modes, the elements remain fixed only in the upper part of the model.
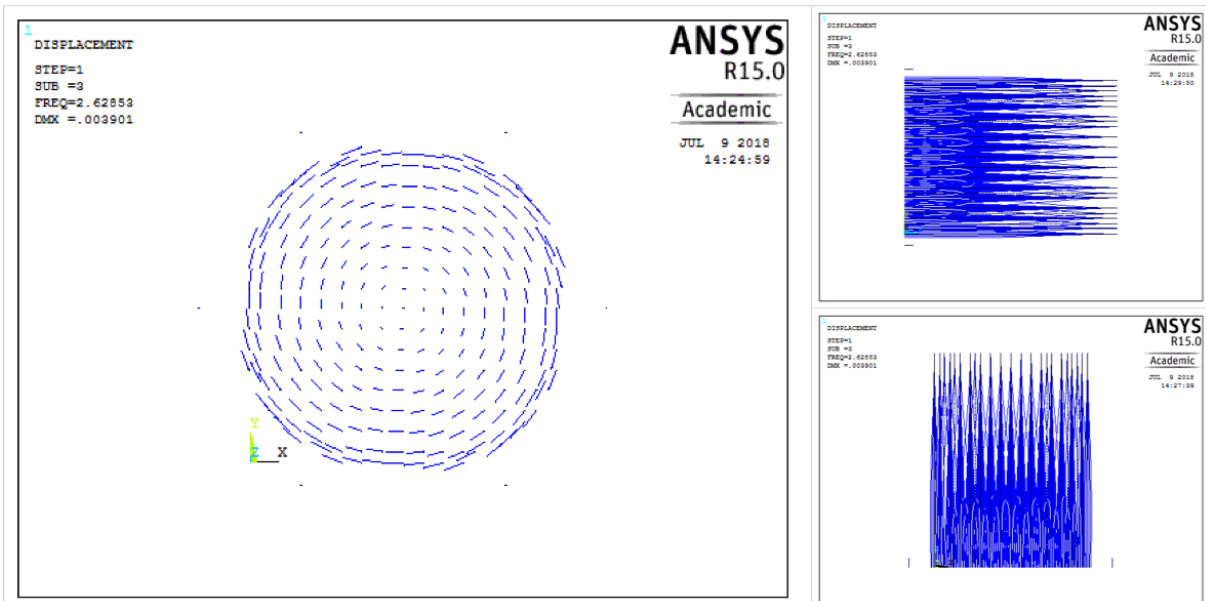
Figure D-3: Third mode, model with new boundary conditions

In the fourth and fifth modes, as well as in the following ones, the deformation only occurs in some elements which is due to the fact that only some sets of elements are in phase so they deform in an equal way in one mode.
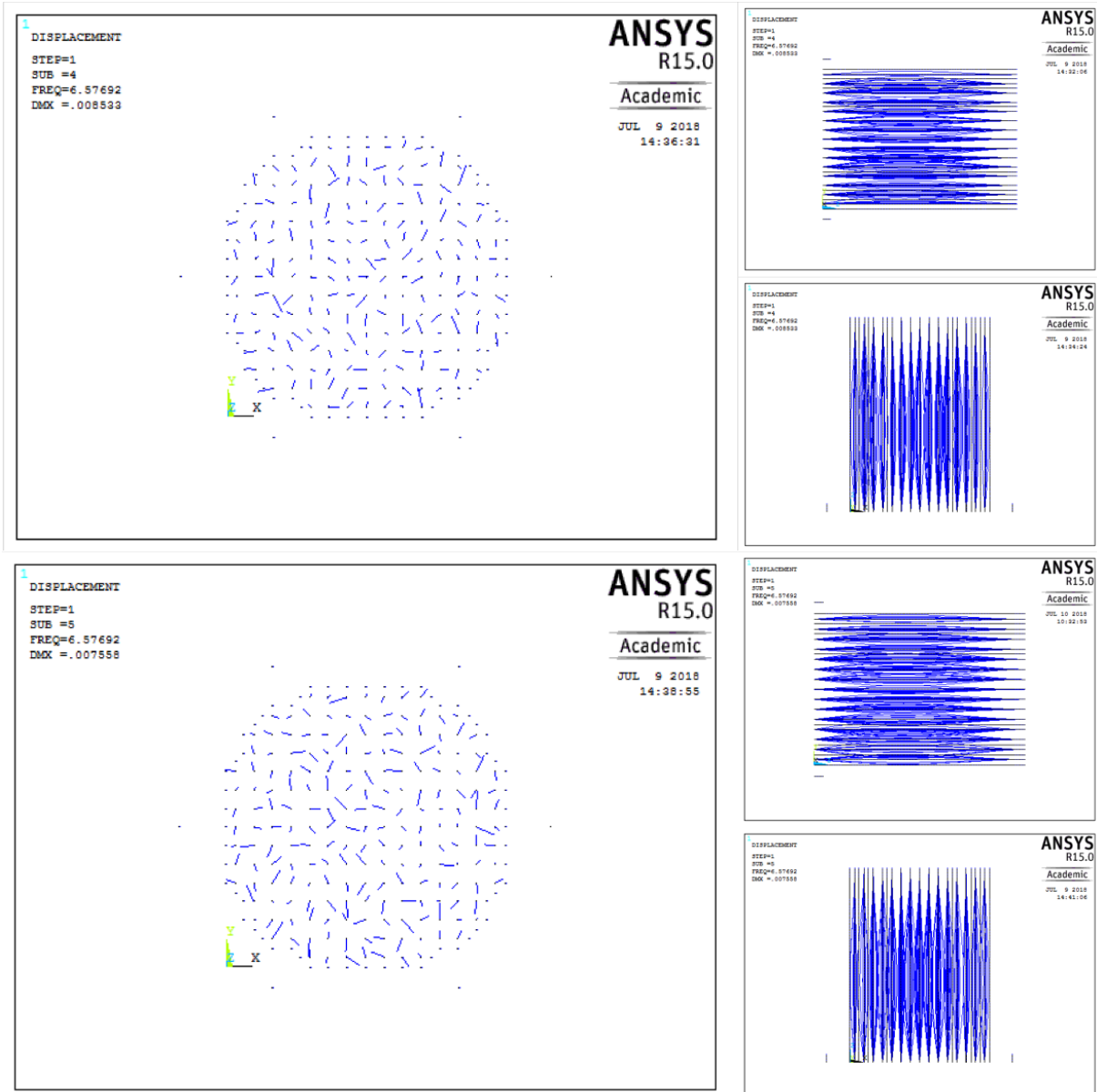
Figure D-4: Fourth and fifth mode, model with new boundary conditions

The main difference observed when comparing this analysis with the analysis of the initial boundary conditions is that the elongations do not occur only in the fuel assemblies but also in the shroud and the core barrel.

D.2 Transient analysis sinusoidal force

In the transient analysis applying a sinusoidal force with the new boundary conditions on the core barrel, the same equation is applied as in the first transient analysis executed (Sinusoidal force).

That is a force amplitude of 100,000 N, applied as a ramped load on the node located in the lower part of the core barrel, with an angular frequency of 0.125 Hz which is equivalent to $\frac{\pi}{4}$ rad/s. The time duration of the analysis is 20 s, that is, the load step of 20 s with an integration time step of 1 s. These conditions are summarized in the following equation that is used as input in the analysis:

$$F = 100000 \cdot \sin\frac{\pi}{4} \cdot t$$

The fuel assembly, where the elongations are evaluated, is the same one as in the previous transient analysis (see **Figure 7-1**: Position of the analyzed fuel assembly which is highlighted with orange color). The following table shows the results obtained for the elongations at different heights of the analyzed fuel assembly (**Table D-2:** Results of the elongations in x direction after applying sinusoidal force).

Table D-2: Results of the elongations in x direction after applying sinusoidal force

Height [m]	Minimum elongation [μm]	Maximum elongation [μm]
0,01	-5.347	5.344
0,57	-4.432	4.411
1,11	-3.582	3.571
1,78	-2.558	2.557
2,19	-1.994	1.995
2,74	-1.319	1.322
3,28	-0.758	0.759
3,83	-0.334	0.335
4,37	-0.074	0.074

Observing the values of the previous table (**Table D-2:** Results of the elongations in x direction after applying sinusoidal force) and those obtained in the analysis where the core barrel was totally fixed in its upper part (see **Table 8-1**: Results of the elongations), it can be seen that in the case where the core barrel is not clamped, the displacements of the fuel assembly are larger since the core barrel is not as rigid as in the previous case and has more possibility of transmitting forces that act on it. But the fact that the values of the elongations are of the order of micro meters in both cases, means that the

change in the elongations is minimal so it is deduced that this new boundary condition is not enough for the core barrel to be able to transmit the force that acts on it in greater magnitude.

D.3 Transient analysis white noise force

Similarly as it was done in the analysis of the model with the first boundary condition for the core barrel (see White noise force), this second transient analysis consists of applying white noise forces of different amplitudes on the core barrel and fuel assemblies and then evaluating the elongations in certain fuel assemblies.

The forces act on the lower part of the core barrel and on the midpoint of each fuel assembly in both, x and y direction. The amplitudes of the forces that act on the core barrel are the following: 1,000 N and 100,000 N. In the case of the fuel assemblies the force applied is 100 N, 0.1 N and 0 N in order to see different behaviour of the elements and the influence of the force applied on the core barrel. The analysis has the same configuration as the other case, which allows to obtain the results for a total amplitude of 10 Hz.

The fuel assemblies where the displacements are evaluated are the same as in the first transient analysis with white noise force.

In the first place, the results obtained for different fuel assemblies at points located at the same height each one of them, are shown. The positions and heights of the analysed points of the fuel assemblies can be seen in the **Figure 8-3**: Positions of the analyzed fuel assemblies and consulted in the White noise force section.

Next, the results obtained by applying a force of 100,000 N on the core barrel and 100 N on the fuel assemblies are shown in both directions, x and y:
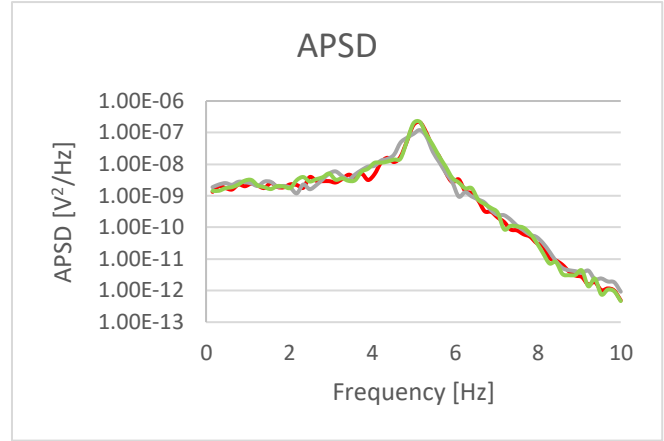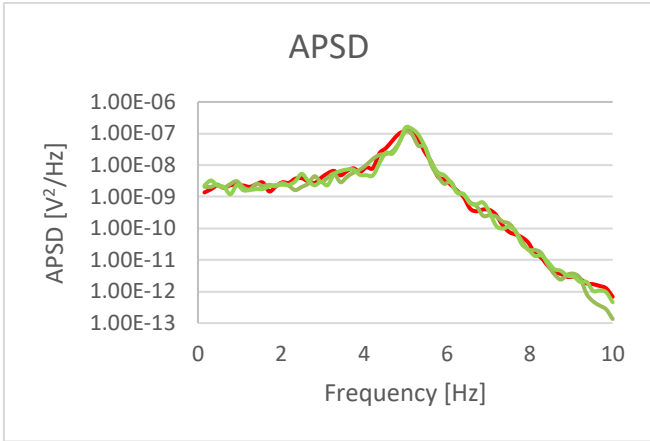
Figure D-5: APSD (100,000 N on CB, 100 N on FAs): left x direction, right y direction (radial)
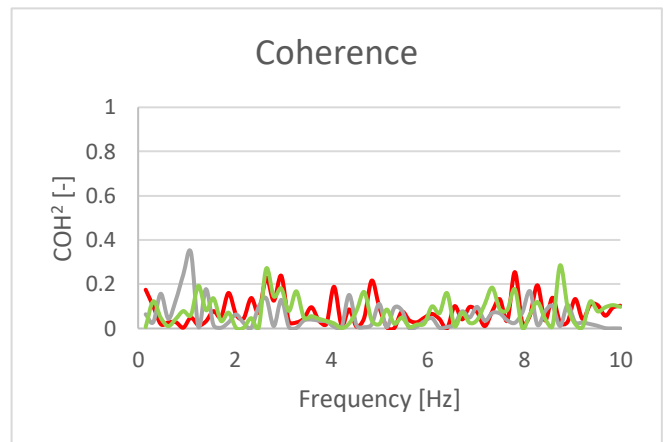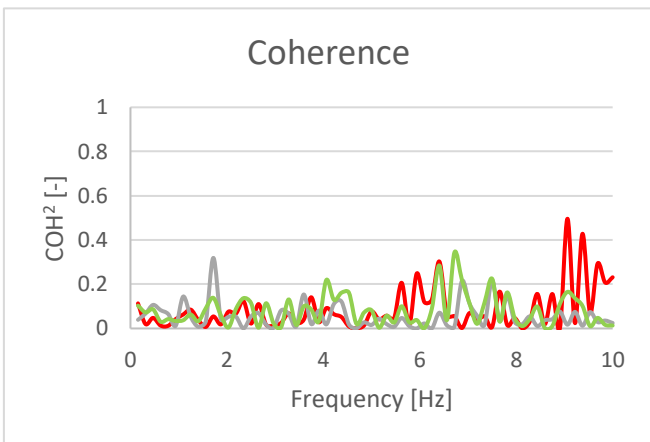
Figure D-6: Coherence (100,000 N on CB, 100 N on FAs): left x direction, right y direction (radial)
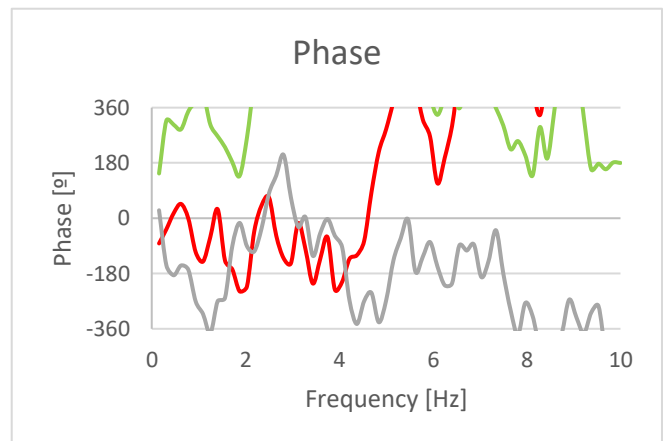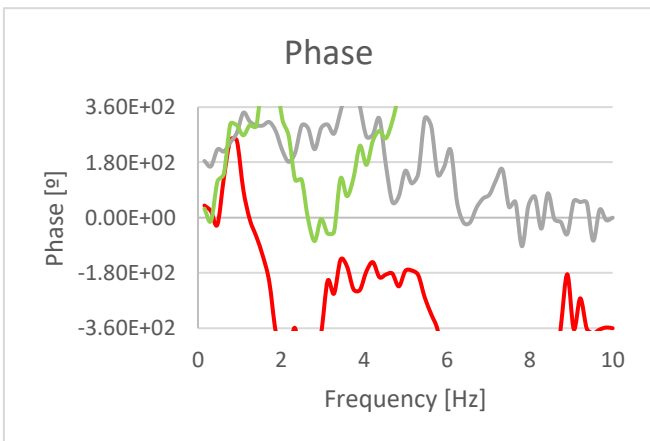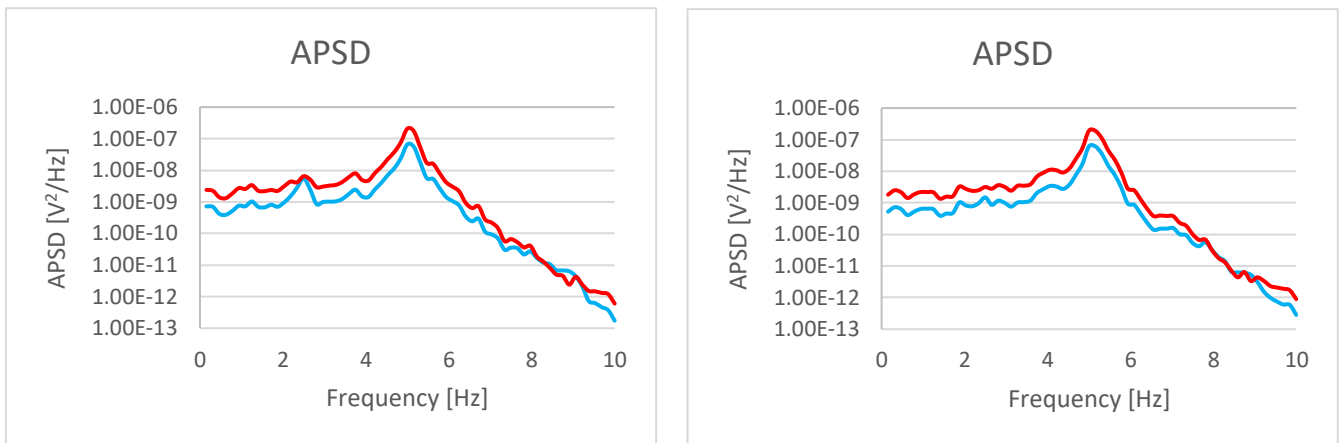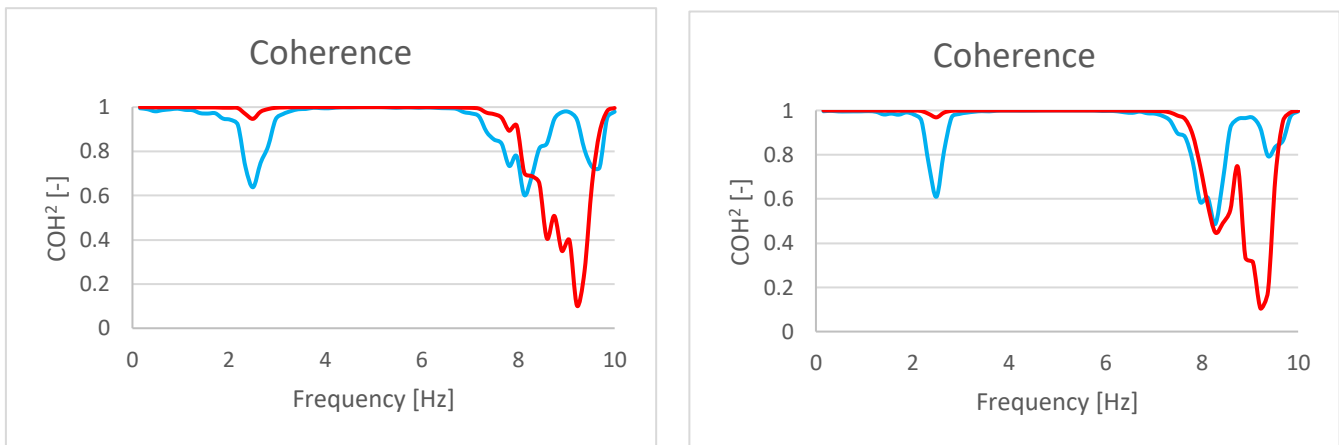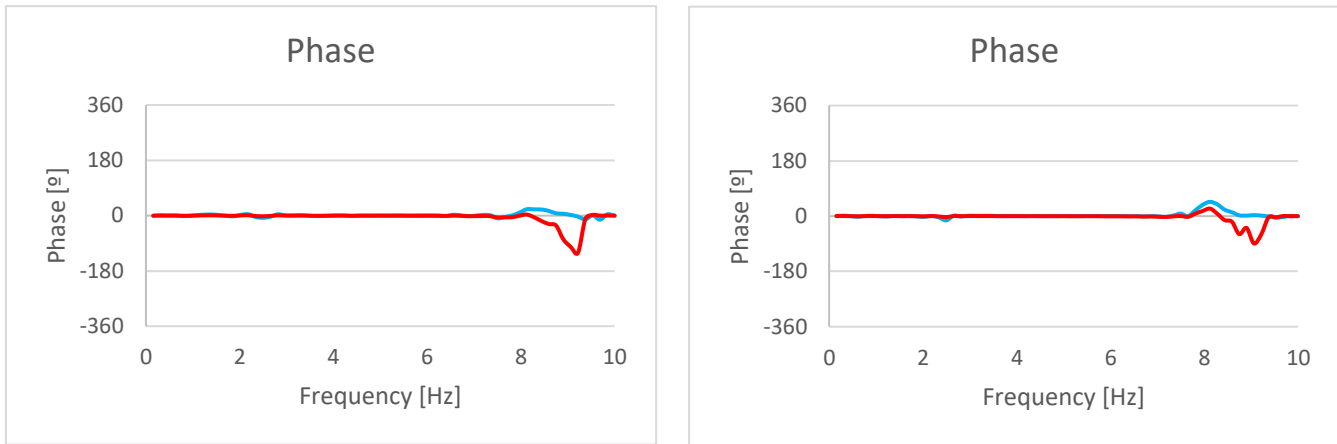

Figure D-7: Phase (100,000 N on CB, 100 N on FAs): left x direction, right y direction (radial)

In general, the results of the three graphs that shows the APSD, the coherence and the phase are similar than in the case of the first boundary conditions, that is, the behaviour of the different fuel assemblies is equivalent. The fuel assemblies are uncorrelated with the one that is taken as a

reference. The graph that shows the phases is not relevant because in the absence of coherence the phases will fluctuate independently. As well as in the first analysis, the fuel assemblies have a chaotic behaviour.

Next, the results obtained for the data for only one fuel assembly at different heights are shown. To see the exact positions and values of the evaluated heights, see **Figure 8-7:** Positions of the **analyzed** detectors of one fuel assembly and **Table 8-2**: Heights of the in-core detectors.
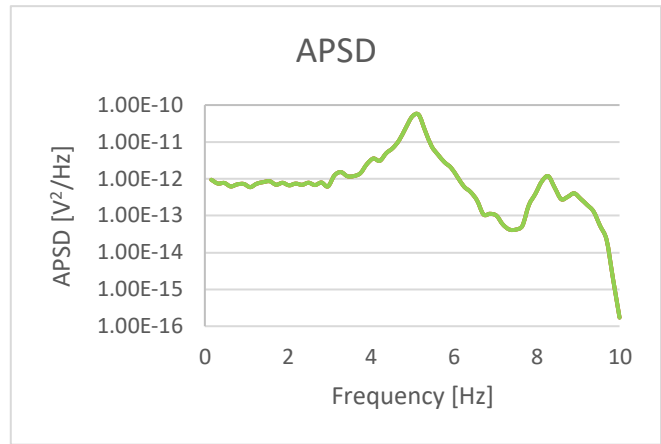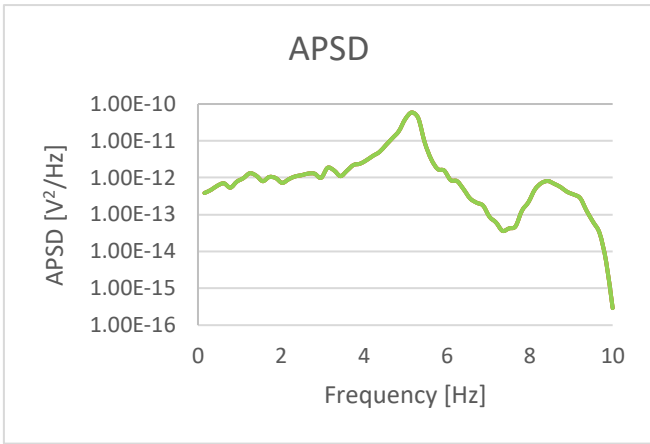

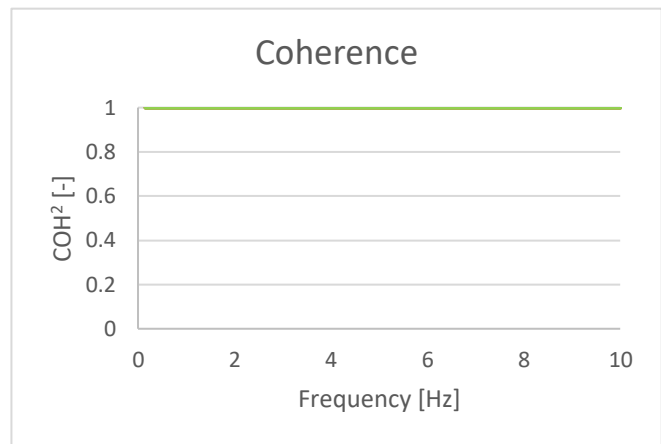**Figure D-8:** APSD (100,000 N on CB, 100 N on FAs): left x direction, right y direction (axial)
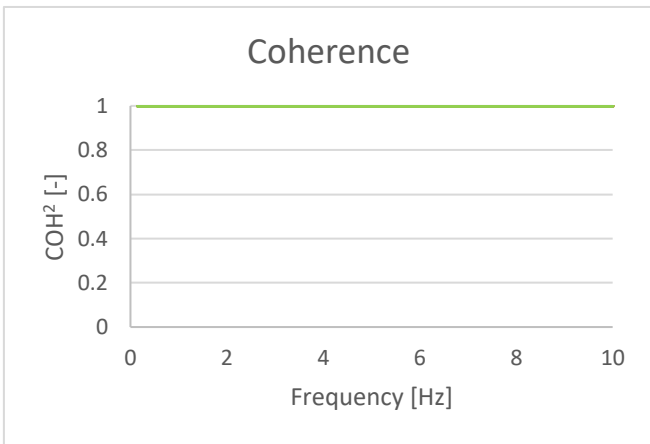

Figure D-9: Coherence (100,000 N on CB, 100 N on FAs): left x direction, right y direction (axial)

Figure D-10: Phase (100,000 N on CB, 100 N on FAs): left x direction, right y direction (axial)

As in the previous case, the results are similar than in the analysis with the first defined boundary conditions. Analysing the results of the coherence, it can be seen that the different point located at different heights of one fuel assembly are correlated. However, the blue line, which is the lowest analysed point (see **Figure 8-7**: Positions of the analyzed detectors of one fuel assembly), experiences an unexpected downward peak at the natural frequency value. Another unexpected downward peak occurs on the red line, which corresponds to the closest point to the point take as a reference (see **Figure 8-7**: Positions of the analyzed detectors of one fuel assembly), that means that the point is uncorrelated at this frequency. All the analysed points are in phase.

The results after applying the same force on the core barrel (100,000 N) but without any force on the fuel assemblies are shown below.

First, the results obtained for the points analysed at different positions of the fuel assemblies at the same height are commented.

Figure D-11: APSD (100,000 N on CB, 0 N on FAs): left x direction, right y direction (radial)

Figure D-12: Coherence (100,000 N on CB, 0 N on FAs): left x direction, right y direction (radial)
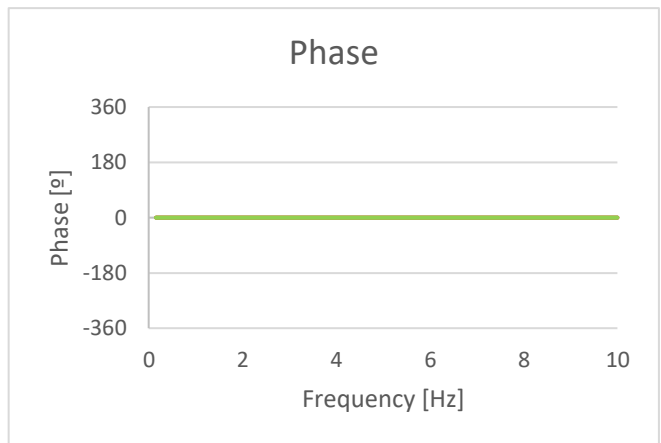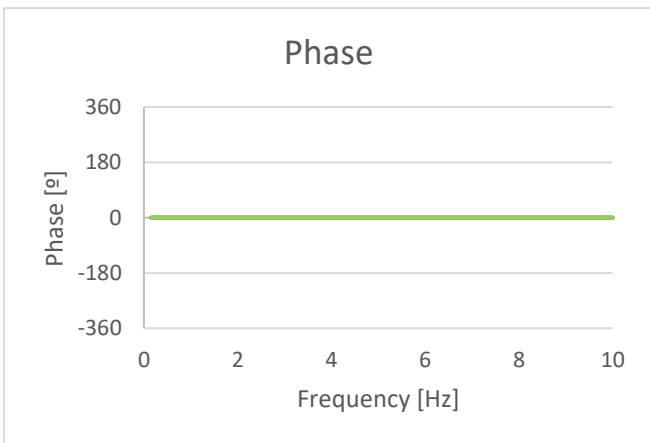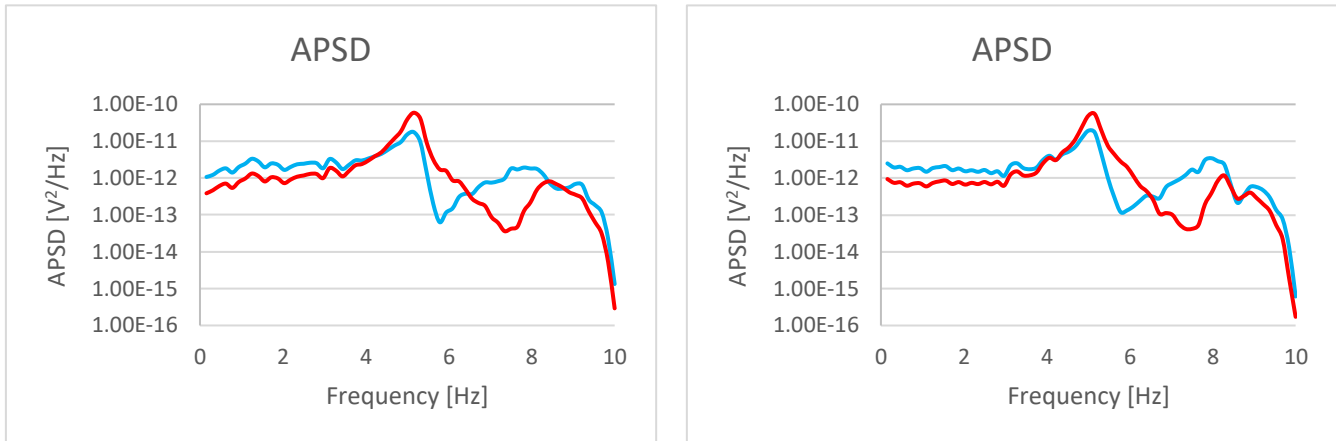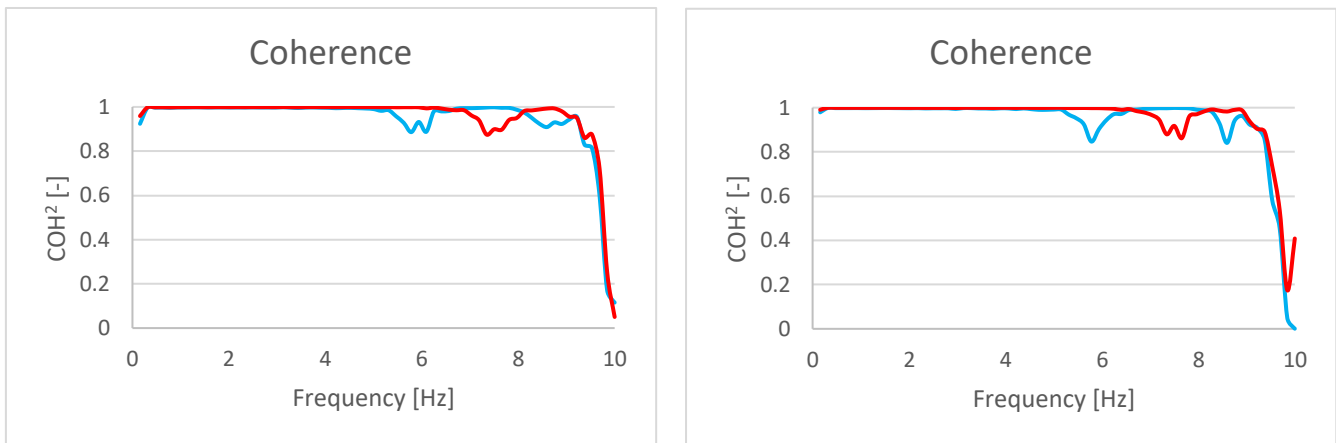

Figure D-13: Phase (100,000 N on CB, 0 N on FAs): left x direction, right y direction (radial)

As in the case of the first defined boundary conditions of the core barrel, it is observed that all the elements act equivalently, that is, there is only one line visible. The fuel assemblies are correlated since the coherence has a value of 1. Regarding the phase, it is seen that it has a value of 0 which means that

all the fuel assemblies act simultaneously in the same way. In contrast with the first analysis (see **Figure 8-13**: Phase (100,000 N on CB, 0 N on FAs): left x direction, right y direction), in this case the lines are not completely straight and this is where the small but negligible change in the behaviour of the fuel assemblies, after changing the boundary conditions, can be seen.

The results obtained for the same forces as in the previous graphs, but analysing different points located at different heights of a single fuel assembly, are shown below.

Figure D-14: APSD (100,000 N on CB, 0 N on FAs): left x direction, right y direction (axial)

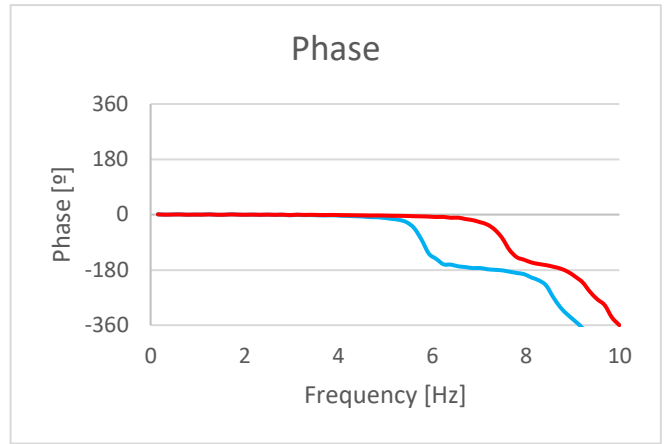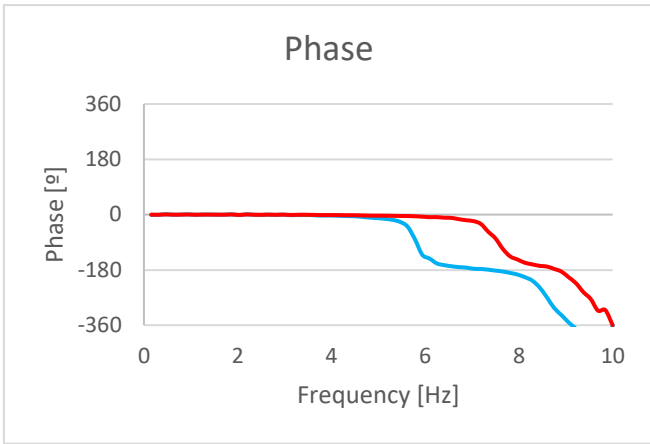**Figure D-15:** Coherence (100,000 N on CB, 0 N on FAs): left x direction, right y direction (axial)

Figure D-16: Phase (100,000 N on CB, 0 N on FAs): left x direction, right y direction (axial)

It is observed that all the points are correlated, that is, they are completely related with the reference point. Also, it is seen that the analysed points are in phase that means that they behave equal.

Finally, an additional analysis is performed where a force of 100,000 N is applied on the core barrel and 0.1 N on the fuel assemblies.

First, the results for points of different fuel assemblies at the same height (see **Figure 8-3**: Positions of the analyzed fuel assemblies) are presented:
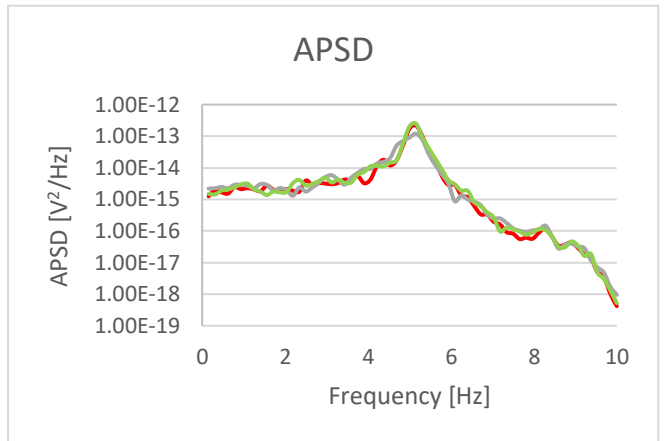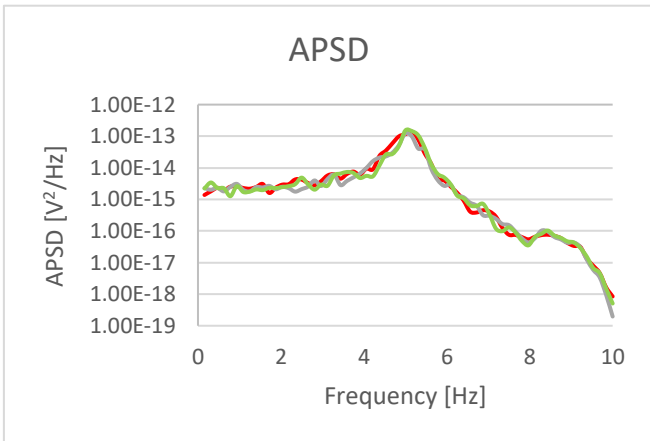

Figure D-17: APSD (100,000 N on CB, 0.1 N on FAs): left x direction, right y direction (radial)
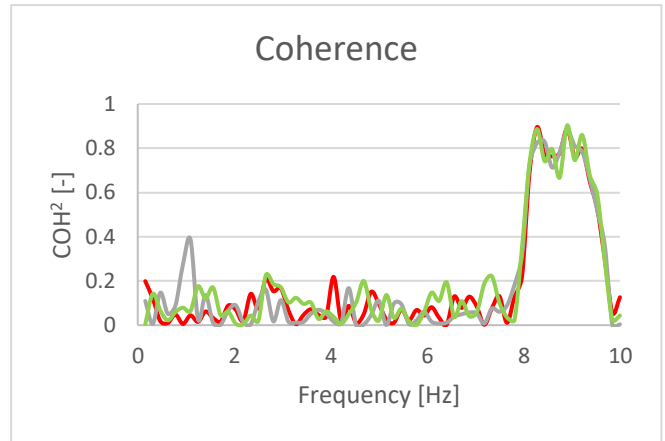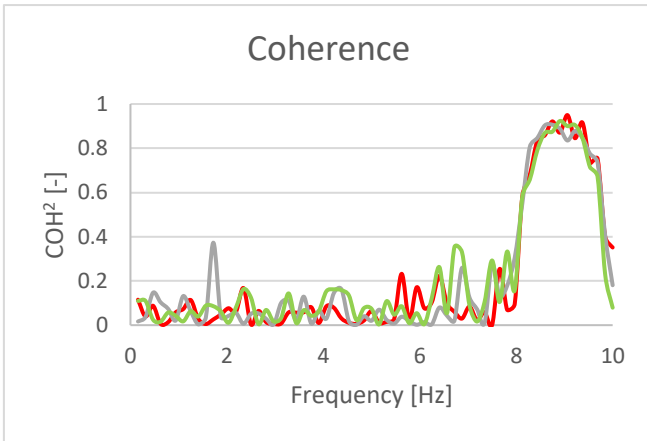
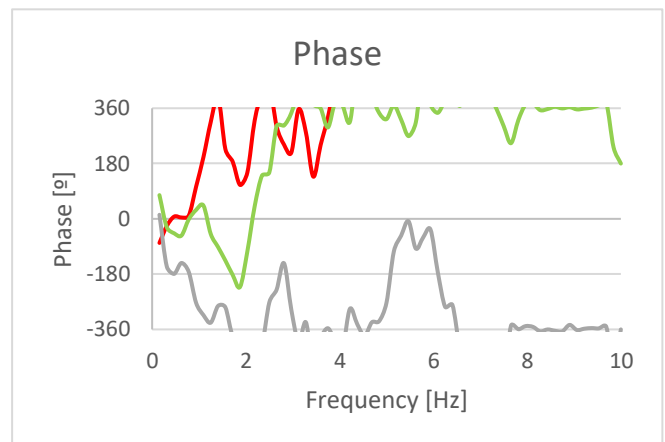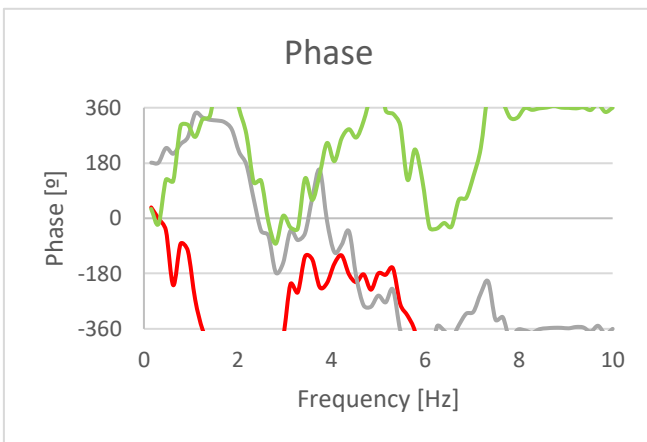**Figure D-18:** Coherence (100,000 N on CB, 0.1 N on FAs): left x direction, right y direction (radial)

Figure D-19: Phase (100,000 N on CB, 0.1 N on FAs): left x direction, right y direction (radial)

In the APSD graph it is observed that the first peak appears at a frequency of approximately 5 Hz. However, another peak can be seen with less intensity that appears at 8 Hz, a value that can be associated with the frequency mode of the unrestricted beam (see **Table 6-1**: Values of the simulated natural frequencies).

At first, all the analysed points of the different fuel assemblies are uncorrelated. The grey line corresponding to the closest fuel assembly respecting the reference one (see **Figure 8-3**: Positions of the analyzed fuel assemblies), shows a peak at 1.7 Hz where the value of coherence increases. This frequency is very similar to the frequency of the first mode of the unrestricted beam (see **Table 6-1**: Values of the simulated natural frequencies). As of 7.5 Hz, value which can be associated with the frequency of the second mode (see **Table 6-1**: Values of the simulated natural frequencies), there is an increase in coherence of all the fuel assemblies, where all of them are correlated.

Observing the graph of the phase, it can be seen that the closest fuel assembly to the reference one is in phase at the same frequency at which the coherence value increases. From the frequency value where the fuel assemblies start to be correlated, they also begin to be in phase.

Now the results for the axial positions applying the same force are shown:
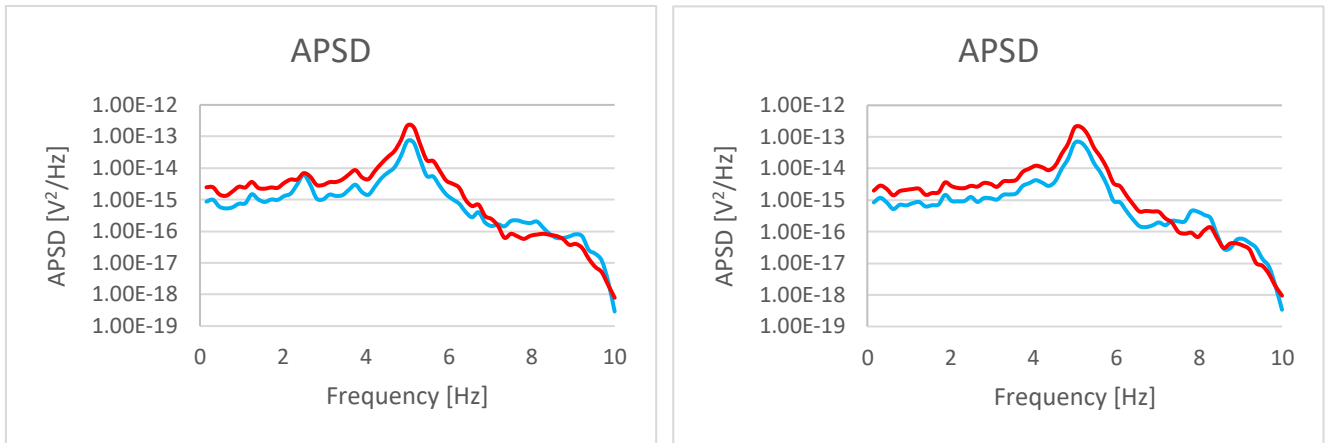

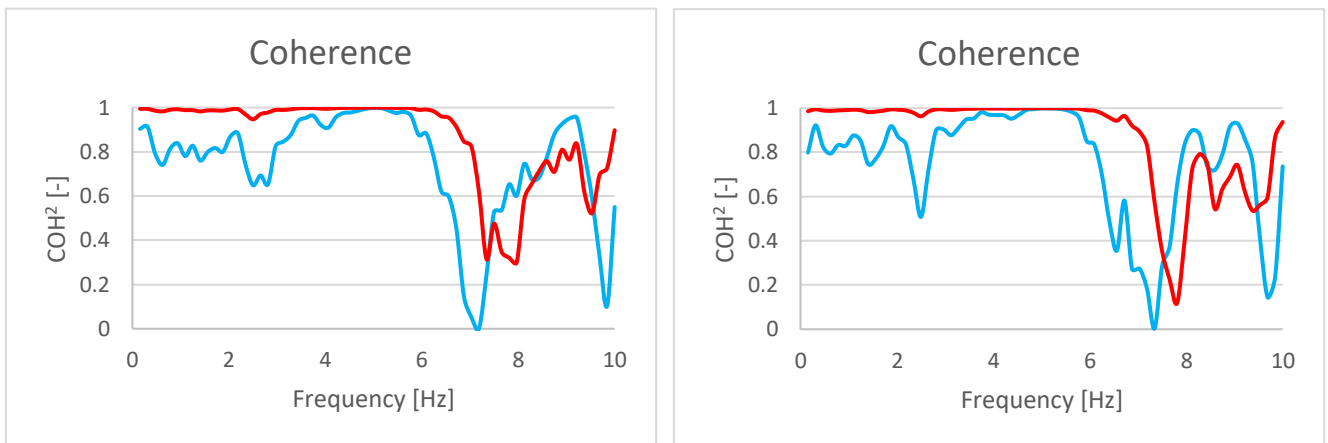**Figure D-20:** APSD (100,000 N on CB, 0.1 N on FAs): left x direction, right y direction (axial)

Figure D-21: Coherence (100,000 N on CB, 0.1 N on FAs): left x direction, right y direction (axial)
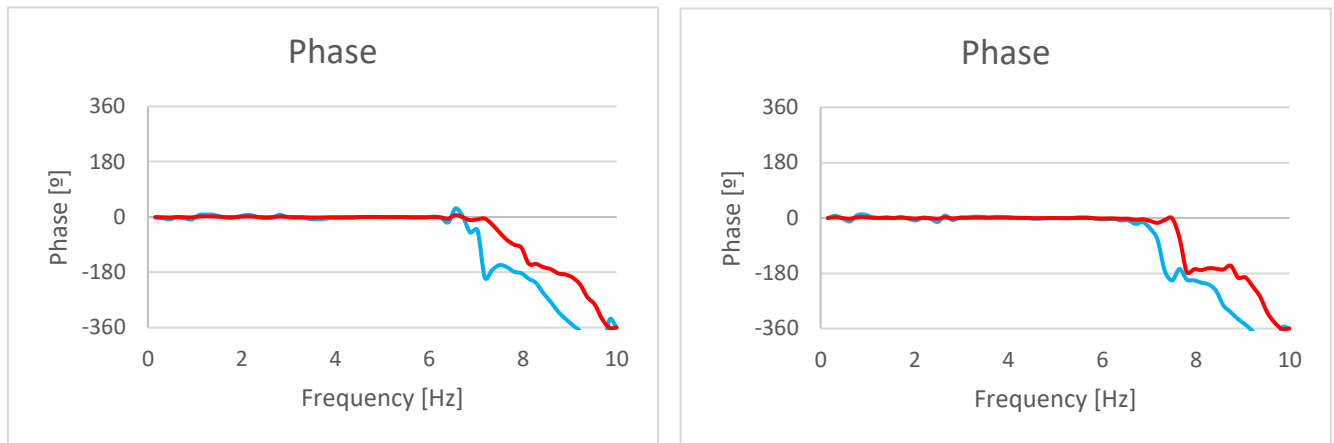
Figure D-22: Phase (100,000 N on CB, 0.1 N on FAs): left x direction, right y direction (axial)

A high coherence is observed for the two points of the analysed fuel assembly. However, the red line that represents the point closest to the reference point (see **Figure 8-7**: Positions of the analyzed detectors of one fuel assembly), has higher values of coherence. From 7 Hz the coherence decreases unexpectedly but returns to high values as long as it is nearer to 10 Hz.

All the points are initially in phase but as in the case of coherence, when reaching 7 Hz a different behaviour of each point is observed since the value of the phase reaches 360º.

After performing these three analyses, as in the case of applying a sinusoidal force, the structure undergoes some changes, comparing with the initial boundary conditions, but these are minimal.

Another possible improvement of the model, as already mentioned in the conclusion of this document, is the application of another type of contact between the elements that make up the structure. For this, two additional macros are included in the DVD where two alternatives to the created contact in the main model are suggested. The first option is to reduce the distance between two fuel assemblies (fuel assembly gap) using the same type of contact but with the purpose that after applying the forces, this contact will occur. This involves the modification of some parameters such as the section of the fuel assembly, and the density and the Young's modulus of the material. The second option consists of changing the created contact by the COMBIN14 element, which consists of coupling two or more elements. With this change, it is guaranteed that all the fuel assemblies are always coupled. In this case it is necessary to define the value of the stiffness.

EIDESSTATTLICHE ERKLÄRUNG

Hiermit versichere ich, *Sarah Nalewajski*, die vorliegende Arbeit selbständig, ohne fremde Hilfe und ohne Benutzung anderer als der von mir angegebenen Quellen angefertigt zu haben. Alle aus fremden Quellen direkt oder indirekt übernommenen Gedanken sind als solche gekennzeichnet.

Die Arbeit wurde noch keiner Prüfungsbehörde in gleicher oder ähnlicher Form vorgelegt.

Dresden, *23.07.2018*

....

Vorname und Name des Studenten

DIGITAL DATA MEDIUM